JOURNAL OF APPLIED PHYSICS

Vol. 10, No. 12 DECEMBER, 1939

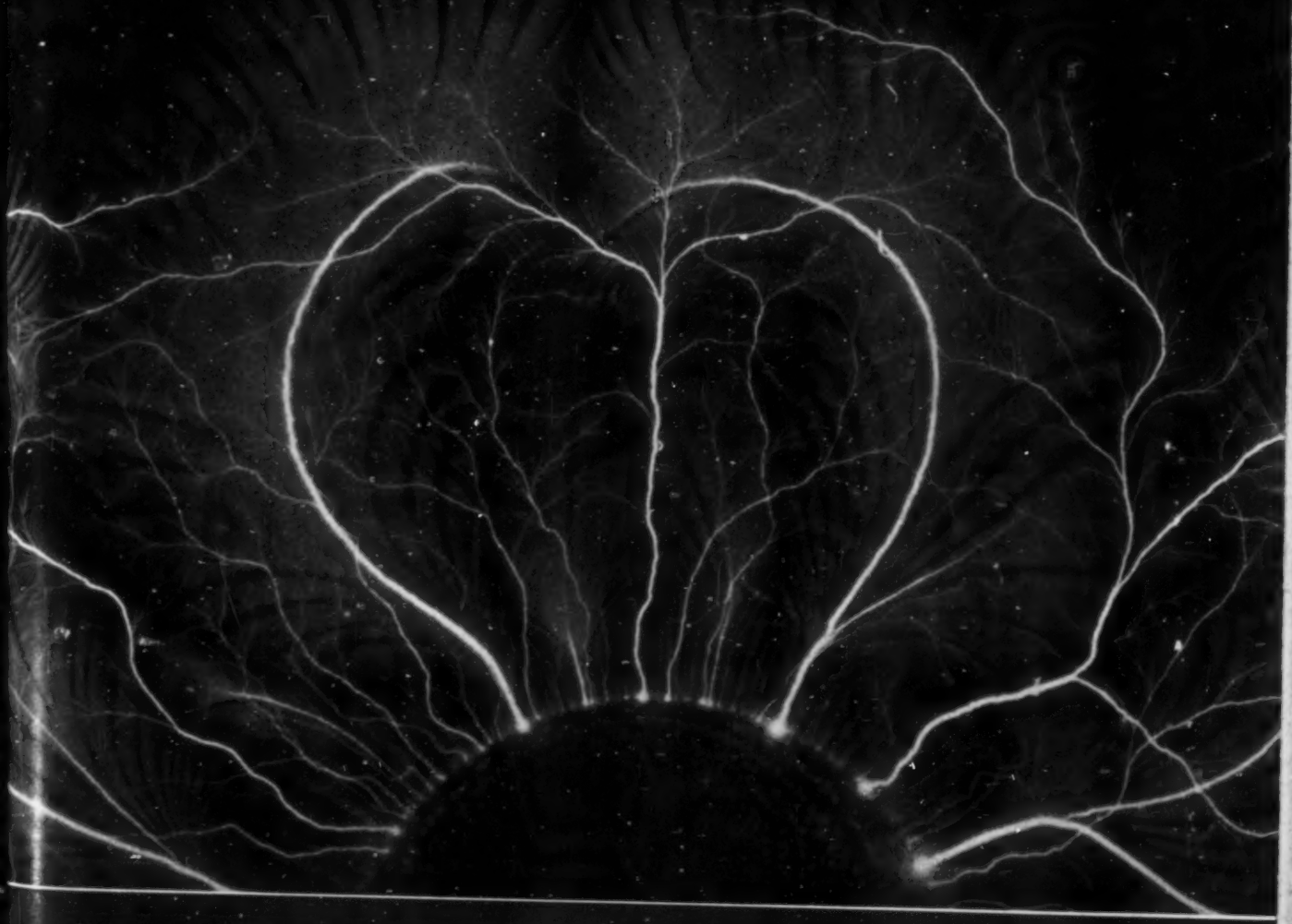

Lichtenberg Figures. J. H. Merrill and A. von Hippel

JOURNAL OF APPLIED
PHYSICS

DECEMBER, 1939 Vol. 10, No. 12

In This Issue

Page

The Symposium on Temperature 819

X-Ray Diffraction Applied to Chemical Analysis WHEELER P. DAVEY 820

Properties of Oxide-Coated Cathodes. II JOHN P. BLEWETT 831

Contributed Original Research

Matrix Theory of Oscillatory Networks LOUIS A. PIPES 849

Increase of Torsional Stiffness of a Prismatical Bar Due to Axial Tension M. A. BIOT 860

Theory of Klystron Oscillations DAVID L. WEBSTER 864

Atomphysical Interpretation of Lichtenberg Figures and Their Application to the Study of Gas Discharge Phenomena F. H. MERRILL AND A. VON HIPPEL 873

Note on the Elastic Properties of Vinyl Sheeting S. BATESON 887

Piezoelectric *Versus* Mechanical Spring Pressure Gauge R. ALDEN WEBSTER 890

Indexes

Author 894

Subject 897

Volume Table of Contents iii

In Every Issue

Here and There 892

Contributors to This Issue 893

Index to Advertisers x

BOARD OF EDITORS

ELMER HUTCHISSON, *Editor*

Associate Editors

F. BITTER
W. E. FORSYTHE
L. A. JONES
W. F. MEGGERS
B. E. WARREN
J. B. WHITEHEAD
V. K. ZWORYKIN

Publication of the American Institute of Physics

ADMINISTRATIVE STAFF

HENRY A. BARTON, *Director*

MADELINE M. MITCHELL, *Publications Manager*

F. K. RICHTMYER *Chairman, Advertising Committee*

GOVERNING BOARD

JOHN T. TATE, *Chairman*
KARL T. COMPTON
E. C. CRITTENDEN
WHEELER P. DAVEY
FLOYD A. FIRESTONE
HARVEY FLETCHER
ARTHUR C. HARDY
PAUL E. KLOPSTEG
MELVIN MOONEY
FREDERIC PALMER, JR.
R. L. PEEK, JR.
GEORGE B. PEGRAM
W. B. RAYTON
F. K. RICHTMYER
WALLACE WATERFALL

THE JOURNAL OF APPLIED PHYSICS, published monthly at Prince and Lemon Sts., Lancaster, Pa., is devoted to physics in its role as the science basic to other natural sciences and to the arts and industries. Previous to 1937 this publication was known as PHYSICS. It aims to be of service not only in physical laboratories, but also in the laboratories of industrial, chemical, geological, geophysical, meteorological, radio, and similar concerns. THE JOURNAL OF APPLIED PHYSICS publishes editorials, news of physicists and reviews, as well as technical papers of applied physics.

SUBSCRIPTION PRICE

	U. S., POSS. AND CANADA	FOREIGN
To members of scientific societies	$5.00	$5.70
To all others	7.00	7.70

Manuscripts should be submitted to Elmer Hutchisson, Editor, University of Pittsburgh, Pittsburgh, Pennsylvania.

Changes of address and proofs should be addressed to the Publications Manager.

Subscriptions and orders for back numbers should be addressed to Prince and Lemon Streets, Lancaster, Pa. or to the American Institute of Physics, 175 Fifth Avenue, New York, N. Y.

Advertising rates supplied on request. Orders, advertising copy and cuts should be sent to the American Institute of Physics.

Entered as second class matter at the Post Office at Lancaster, Pennsylvania, under the Act of March 3, 1897. Accepted for mailing at the special rate of postage provided for in the Act of February 28, 1925, authorized May 2, 1932.

Copyright 1939, by the American Institute of Physics.

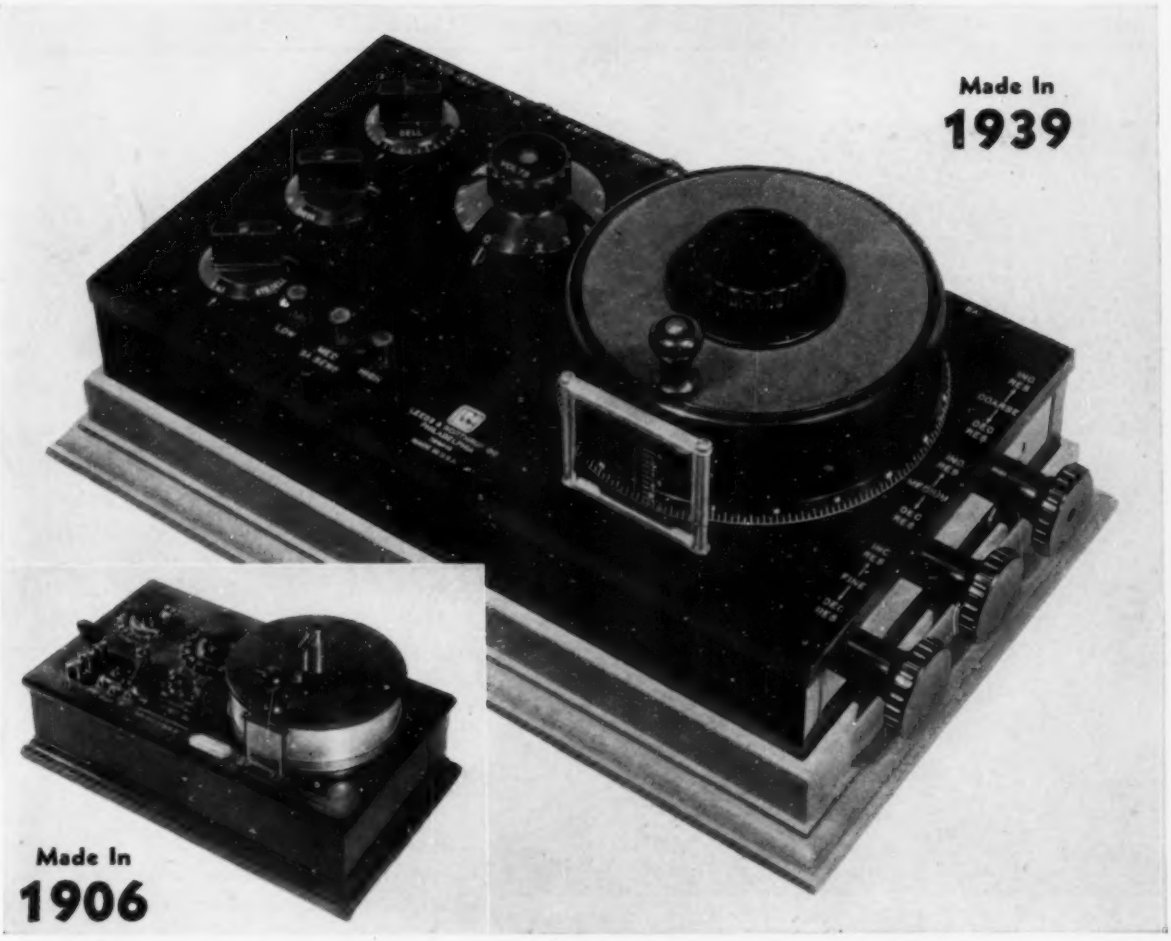

Time Favors the TYPE K

The old Type K Potentiometer (shown in the insert) at the Moore School of Electrical Engineering, University of Pennsylvania, is half again as old as the students who use it . . . and yet, it's as useful today as it was a third of a century ago . . . for the underlying principles of the original Type K were so thoroughly worked out and were so far in advance of their time, that for a general purpose instrument, they have never been bettered. Put together to stay, early Type K's stood up under the hardest use, and today's instruments are built in the same way.

A low resistance potentiometer of high accuracy, the Type K eliminates moving contacts between the measuring resistors by permanently connecting an eleven turn slidewire to fifteen dial resistors. This gives ample range and places the two moving contacts in the galvanometer circuit where contact-resistance changes have no effect. With only two measuring dials, operation is easy and fast. The standard cell is connected simply by throwing a switch, the range changed by moving a plug, protective galvanometer resistors connected by operating keys.

Incorporating the latest materials and mechanical designs, today's Type K-2 is even stronger, faster, and more convenient than the original model. Yet the features to which it owes its unique reputation for accuracy, sensitivity and versatility of application are the original ones . . . ones which time and experience have been unable to improve.

Write for Further Information

LEEDS & NORTHRUP COMPANY, 4978 STENTON AVE., PHILA., PA.

LEEDS & NORTHRUP

MEASURING INSTRUMENTS · TELEMETERS · AUTOMATIC CONTROLS · HEAT-TREATING FURNACES

Jrl Ad E-50B(1)

PRECISION INSTRUMENTS FOR MEASUREMENT AND CONTROL

Portable D'Arsonval Galvanometers

You are sure of close accuracy plus ruggedness when you choose a G-M designed taut-suspension galvanometer.

High angular sensitivity is combined with a large scale-angle to allow close accuracy both in measuring current and voltage, and for null point indicating in bridge and potentiometer circuits. The coil is sufficiently damped to give minimum reading time. It is also well balanced to give uniform scale accuracy. No special care is needed in leveling the instrument.

Mirror Type Shown at left is the G-M mirror type galvanometer. It is equipped with a mirror on the moving coil, plus a 6 volt lamp and lens system. A sharp black index line in an illuminated field is projected on the translucent scale. One model requires an extra power source. Another has an enclosed transformer. Both models have removable bottoms. Sensitivity ranges available run from 0.02 to 0.20 microampere per millimeter scale-division.

Pointer Type Shown at lower left is the G-M pointer type. The design of the magnetic circuit provides uniform flux density over the entire scale range. Sensitivity ranges available run from 0.10 to 1.00 microamperes per millimeter scale-division.

Write for the G-M Catalog giving specifications and prices on these galvanometers, as well as the complete line of G-M instruments.

Pointer Type This galvanometer is rugged enough to withstand severe handling in portable use.

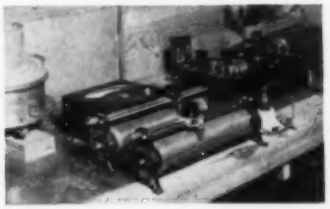

At Missouri This pair of G-M slide wire rheostats is representative of the G-M equipment being used at the University of Missouri. Other G-M instruments available for laboratory work are: suspended coil galvanometers, electric thermometers, photoelectric cells, demonstration photoelectric relays.

G-M LABORATORIES INC.

DEPT. B. 1731 BELMONT — CHICAGO, U. S. A.

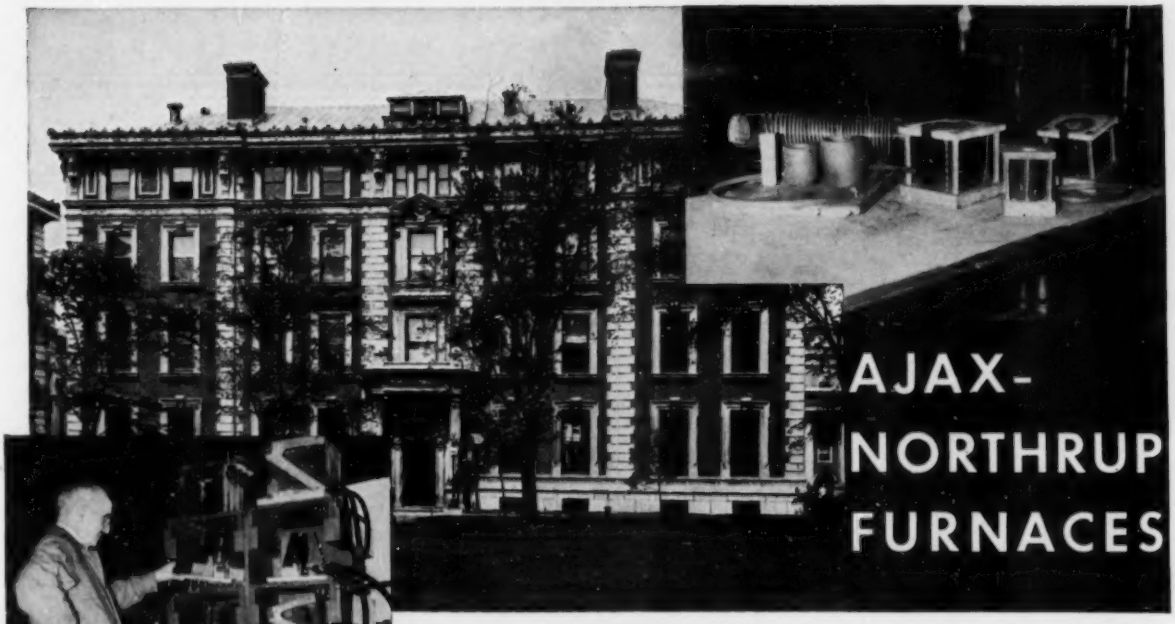

AT COLUMBIA UNIVERSITY

The Mines Building at Columbia and some of the melting units used in connection with Ajax-Northrup Furnaces.

The Departments of Mining Engineering and Metallurgy have used Ajax-Northrup Furnaces since 1928.

The extent of use is illustrated by the pyramid of Ajax-Northrup coils (at the left) of various types and sizes covering every conceivable requirement for thesis and sampling work.

In the laboratory for applied electrochemistry smaller Ajax-Northrup Furnaces are used. A detail view of the accessory equipment is shown at the top right.

AJAX-NORTHRUP MELTING FURNACE CAPACITIES: ONE OUNCE TO EIGHT TONS

AJAX ELECTROTHERMIC CORPORATION
•
AJAX PARK
TRENTON, N. J.

AJ-14-C

Announces

NELA SPECIALTY DIVISION

of the LAMP DEPARTMENT

GENERAL ELECTRIC COMPANY

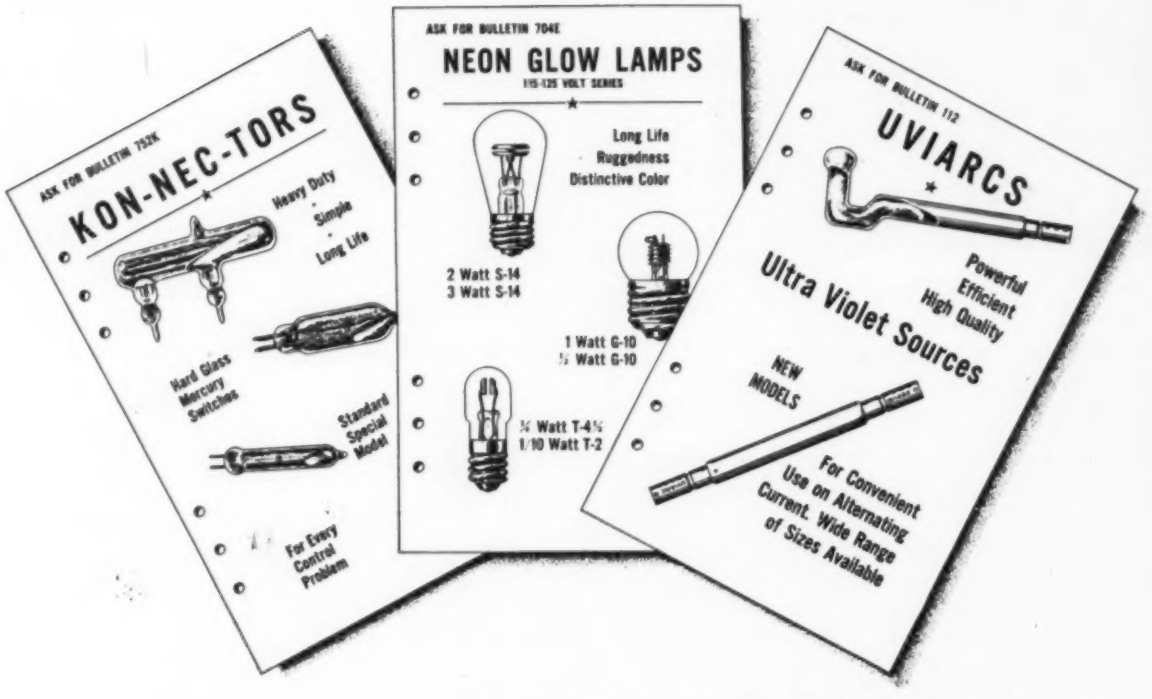

IN order to better serve you with an important line of specialty items — to give you better sales and design assistance — Nela Specialty Division has been organized, with headquarters at Hoboken, N. J. Here you may obtain the latest information on Mercury Switches, Glow Lamps, Quartz, Mercury Arcs and other specialty items.

Address: NELA SPECIALTY DIVISION, LAMP DEPT., GENERAL ELECTRIC CO.
416 EIGHTH ST., HOBOKEN, NEW JERSEY

HARVARD COLLEGE
DEC 16 1939
LIBRARY

Journal of Applied

Physics

Volume 10 December, 1939 Number 12

The Symposium on Temperature

LAST month the American Institute of Physics sponsored a symposium in New York on the definition, measurement and control of temperature in science and industry. Measured by the registered attendance of 615 people, the meeting was a grand success. Its success was, however, indicated in many other ways. For instance, fourteen national societies joined with the Institute in arranging the program. A total of 127 contributed papers formed the program which ranged in subject matter from the temperature of the human body to pyrometric methods in use in the blast furnace. The large number of papers necessitated the scheduling of several simultaneous sessions, and one's only regret was that it was impossible to be at more than one place at a time.

Particularly gratifying was the interest and large number of papers in the field of biophysics. Heat regulation in man is essentially a physical problem, yet it is one which the physicist himself is not competent to handle. Progress in this field and in many other biological fields requires cooperation between the research physician, the biologist and the physicist. No better way of bringing about this cooperation exists than to have joint meetings where each can discuss and criticize the work of the other.

Some permanent record should be made of the results of this symposium. Although arrangements are not yet complete, it is hoped that, in the near future, the American Institute of Physics will publish the entire group of papers in a well-edited volume. In the meantime some of the papers will be available in engineering publications. A special issue of the *Journal of Applied Physics* devoted to Temperature and its Applications is in preparation and will probably appear next March. As soon as final arrangements for the complete publication are made, notice will be given in these columns.

For January

Physics in 1939, by THOMAS H. OSGOOD

The Design of Wide-Aperture Photographic Objectives, by R. KINGSLAKE

Theory of the Photographic Latent Image Formation, by J. H. WEBB

Physics in Color Photography, by DAVID L. MACADAM

The Response of Photographic Materials to Atomic Particles, by T. R. WILKINS

Contributed Original Research Papers on

An Investigation into the Gettering Powers of Various Metals for the Gases Hydrogen, Oxygen, Nitrogen, Carbon Dioxide and Air

Pressure and Temperature Effects on the Viscosity of Liquids

X-Ray Diffraction Applied to Chemical Analysis

By Wheeler P. Davey

The Pennsylvania State College, State College, Pennsylvania

IT is a well-known experimental fact that crystalline solids act like three-dimensional diffraction gratings toward x-rays. No two chemically distinct crystalline materials have ever been found which show identical diffraction patterns. All the evidence in the literature shows, without exception, that the interplanar spacings of a crystal, taken as a group, are as characteristic of that chemical entity as fingerprints are of a given human individual. The diffraction pattern of a crystalline solid (or its interpretation in terms of a systematic statement of interplanar spacings), offers, therefore, a convenient method of chemical analysis, and is so accepted in the patent courts of the United States. This method is quick, relatively inexpensive when used on a large scale, usually requires only about a milligram of material, is nondestructive of the specimen, and in the case of compounds reveals the state of chemical combination. Any method of chemical identification which claims so many outstanding advantages is obviously worth careful attention.

If the x-ray diffraction pattern is recorded photographically, the apparatus required for general chemical analysis is relatively simple, and can be bought for a total cost of less than $5000.00. This includes the necessary switches, controls, transformer, x-ray tube, tube holders, x-ray protection, multiple optical bench, slits of various types, specimen holders, x-ray cameras, complete darkroom equipment, viewing screens, scale, etc. The simplest satisfactory form of such equipment has already been adequately described elsewhere.[1, 2] More highly specialized equipment for more limited purposes has also been adequately described.[3]

Chemical analysis by x-ray diffraction methods will be taken up under three heads: (1) The identification of a one-component material; (2) The identification of a multi-component material; (3) The identification of a crystalline material which contains a second material dissolved in it in solid solution.

The Identification of a One-Component Material

The identification by x-ray diffraction methods of an unknown pure crystalline solid consists of two steps: (a) obtaining a systematic list of the interplanar spacings of the "unknown"; (b) finding some chemically known material which gives identically the same diffraction pattern. It is not enough to determine the type of crystal structure from (a), in fact, the crystal structure need not be known at all. All that is needed is to find some chemically identified "standard material" whose list of interplanar spacings is identical to that found under (a) for the "unknown." It is not sufficient to guess the chemical identity of the standard material nor to guess what its diffraction pattern "ought" to be; the chemical identity of the standard and its list of interplanar spacings must be the result of definite experimental study.

The situation is much like that of a fingerprint expert trying to identify a bank robber. He must start with the fingerprints on the bank safe. Then he must hunt through his files until he finds a set of prints, *made by a person whose identity is known*, which match exactly the prints from the bank safe. It does no good to find a set of prints which match if the identity of the man who made the "standard" set is unknown; that merely tells that the two men are the same, but it does not name the burglar. It does no good to guess what kind of prints Public Enemy No. X "ought" to have and then claim that the bank robber is Mr. X. The only way for the fingerprint expert to identify the robber is to show an exact correspondence between the robber's prints and those made by a man whose name is definitely known. If such a

match cannot be found in the files, the only way by which the fingerprint expert can identify the robber is to take, systematically, fingerprints of every man, woman, and child in the world until he stumbles upon an exact match.

Corresponding to the fingerprint file, is the crystal analyst's file of interplanar spacings of known crystalline materials. Such a file can be made by calculation from the structure data and dimensions of unit-crystals to be found in the literature,[4–6] or the experimentably determined interplanar spacings of the "standards" can be tabulated directly. Tables of interplanar spacings found by the "powder" method for 1000 common chemicals have been published by Hanawalt, Rinne, and Frevel,[2] and form the most convenient source of this information. The Hanawalt tables give not only the interplanar spacings but also the relative intensities of the lines in the diffraction pattern. These relative intensities form the basis of Hanawalt's scheme of indexing his data. The Hanawalt system of classification is undoubtedly the outstanding contribution of the year (1938), to chemical analysis. It is so simple and so convenient that it is certain to be adopted by all those who do chemical analysis by x-ray diffraction methods.

Hanawalt divides the interplanar distances ordinarily met with in chemical analysis by x-ray diffraction methods into 77 groups each of which covers a spread of from 5 to 10 times the error in measurement of a photograph of a "powder" pattern taken with Mo K alpha-rays at a radius of 8 inches and corrected against a calibration standard.[7] These groups have a width all the way from 5.0A in the 20.00–15.00A range down to 0.05A in the 1.05–1.00A range. Imagine, now, a book of 77 pages with these groups tabulated in vertical columns on every page as shown in Fig. 1, and let the pages be headed with the successive ranges of the various groups. We must now imagine ourselves tabulating the diffraction data of some chemical individual in the classification book. For purposes of illustration let us choose SrO_2 whose interplanar spacings are given in Table I. The strongest line of SrO_2 (and therefore the most likely to be found even on the weakest photograph of the diffraction pattern), corresponds to an interplanar spacing of 2.52A, so we must turn to the page of our imaginary book headed "Group 2.55–2.50A." The second strongest line corresponds to an interplanar spacing of 3.13A. This corresponds to the subgroup interval 3.20–3.10A on the page of our imaginary book, so we shall insert the chemical symbol SrO_2 at this point. The next most intense lines on the diffraction pattern correspond to interplanar spacings of 2.00A and 1.87A. It just happens that these two lines are of equal intensity, so we shall follow the convention of considering the line of larger interplanar spacing as the more intense of the two. We therefore write the numbers 2.00 and 1.87 in the two subcolumns to the right of the chemical symbol (see Fig. 1). In similar fashion the interplanar spacings of all other common chemical substances are listed in the book. A crystalline "unknown" may now be identified by comparing its interplanar spacing with the recorded spacings in the book, starting with the strongest line in the diffraction pattern. After the first four lines in the pattern have been compared, further comparison may be made between the complete pattern of the "unknown" and that of the standard "known" substance. A complete match between the two patterns identifies the "unknown."

Our fictitious book of tabulated data corresponds to Hanawalt's actual book except that he requires more pages since he provides room for 15 substances in each of his sub-groups instead of the one which we have provided in our imaginary book. He would therefore have several pages in succession all headed "Group 2.55–2.50A" and it

TABLE I. *Diffraction data for* SrO_2.

INTERPLANAR SPACING $=d$	RELATIVE INTENSITY OF LINE $=I/I_1$
3.30	0.40
3.13	0.88
2.52	1.00
2.00	0.50
1.87	0.50
1.78	0.15
1.57	0.30
1.55	0.30
1.375	0.05
1.290	0.35
1.260	0.05
1.210	0.05
1.176	0.10
1.127	0.10
1.066	0.10
1.045	0.05
1.015	0.10

would be necessary to pick out the one of these which contains the sub-group 3.20–3.10A and then proceed as in our imaginary case.

Hanawalt listed, at the bottom of each page of his book of classified data, three additional tables. The first of these tabulates, for each compound listed on the classified form on that page, (1) his serial number for the compound, (2) the chemical symbol for the compound, (3) the interplanar spacings corresponding to the three most intense lines of the diffraction pattern of that compound. The second table lists those compounds which would have been found on that page of classified data if the intensities of the first and second lines had been reversed. The third table lists those compounds which would have been found on that page if the intensities of the first and third lines had been reversed. In these additional tables, the interplanar spacings of the three most intense lines of the diffraction pattern are recorded for easy reference.

So far, out of a total of over 1000 diffraction patterns of chemically known substances there are only 27 sub-groups which contain within their narrow range, lines of more than three patterns, and only one which contains lines of more than five patterns, so that probably a much smaller book would suffice instead of Hanawalt's book of 462 pages.

Out of over 1000 recorded diffraction patterns, Hanawalt finds only 11 sub-groups in which two patterns have, within twice the error of measurement, the same positions for the three most intense lines, and only four sub-groups in which three patterns have the same positions for the three most intense lines. In seven of these cases the fourth most intense line is sufficient to distinguish the patterns. It is evident, then, that the four most intense lines of a diffraction pattern either point definitely to a single definite composition for the "unknown" under investigation, or else narrow down the choice to not more than three substances. The whole diffraction pattern must now be compared line-by-line with the known standard pattern of the substance (or in rare case, substances), for which a match is to be expected. This comparison must show a complete match to within the precision of the data, both for the location (interpreted in terms of interplanar spacings), and for the relative intensities of all the lines on the diffraction pattern. Within the limits of visibility on the photographic film, no lines on the comparison standard must be missing from the pattern of the "unknown," and for one-component unknowns there must be none left unaccounted for. For one-component specimens there are only three instances known where the diffraction patterns can be so nearly alike that they cannot be distinguished at once by even a most cursory examination. In the case of these three pairs of substances, careful measurement of the diffraction patterns will remove the ambiguity, or the ambiguity may be removed by spectrographic analysis.

If the diffraction pattern of the "unknown" shows no match with any recorded diffraction pattern, the only way of identifying the "unknown" by x-ray diffraction methods is to record systematically the patterns of every possible crystalline chemical compound until we stumble on one which gives an exact match. The chance of having to do this is now extremely rare.

We have shown, then, using Hanawalt's scheme of tabulation, the parallel between the technique of the fingerprint expert and that of the crystal analyst while making an identification of a one-component "unknown." In the case of a multi-component "unknown," the crystal analyst has considerable advantage over the fingerprint expert.

The Identification of a Multi-Component Material

Let us assume at first for the sake of simplicity of presentation that we have an "unknown" compound of two chemical individuals such that no index lines from one are superimposed on index lines of the other, and let us assume that Table II gives the experimental data. In this table, the intensities of the lines are given in terms of units of blackness obtained from a calibrated comparison-strip of film. (The lines on the calibration strip are made by known exposures to x-rays at a rate of exposure corresponding that ordinarily need in taking diffraction patterns.) The greatest blackness recorded in Table II is 50 units. Three lines have this intensity, namely 2.93A, 2.52A, and 2.32A. We shall follow the convention of starting with the largest interplanar spacing of these three, taking each one in turn as a starting point if necessary.

TABLE II. *Diffraction data for a two-component "unknown" with no superimposed "index" lines. (Hanawalt.)*

"UNKNOWN"			$NaClO_3$		CuO	
d	*I*	I/I_1	*d*	I/I_1	*d*	I/I_1
4.65	6	0.12	4.65	0.20	—	—
3.79	12.5	0.25	3.79	0.33	—	—
3.28	30	0.60	3.28	0.67	—	—
2.93	50	1.00	2.94	1.00	—	—
2.67	20	0.40	2.68	0.40	—	—
2.52	50	1.00	—	—	2.51	1.00
2.32	50	1.00	2.32	0.01	2.31	1.00
2.18	15	0.30	2.18	0.33	—	—
2.07	2	0.04	2.07	0.07	—	—
1.97	6	0.12	1.98	0.13	—	—
—	—	—	1.89	0.01	—	—
1.86	10	0.20	—	—	1.85	0.20
1.82	4	0.08	1.83	0.07	—	—
1.75	30	0.60	1.76	0.67	—	—
1.71	2	0.04	—	—	1.70	0.08
1.63	1	0.02	1.64	0.01	—	—
1.58	10	0.20	1.59	0.11	1.57	0.08
1.54	1.5	0.03	1.55	0.03	—	—
1.50	15	0.30	1.51	0.11	1.50	0.15
1.465	1.5	0.03	1.470	0.03	—	—
1.430	6	0.12	1.434	0.13	—	—
1.406	10	0.20	—	—	1.408	0.20
1.373	10	0.20	—	—	1.370	0.20

Figure 2 shows the page in our simplified book of classified data corresponding to group 2.95–2.90. This range includes our 2.93 line. We next find sub-group 2.55–2.50 on this page only to discover that there is no known compound which has a third most intense line corresponding to any line in the first column of Table II. We next find sub-group 2.35–2.30 only to discover that again there is no match. Still keeping to group 2.95–2.90 until we have exhausted all its possibilities, we find the sub-group corresponding to the next most intense line of Table II. It is either 3.28A or 1.75A. Again following the convention of giving precedence to the larger of two spacings whose lines show equal intensity, we find sub-group 3.30–3.20 in our imaginary book, (Fig. 2), and discover that sodium chlorate, $NaClO_3$, belongs in this sub-group and that it has its third most intense line at 1.76A and its fourth most intense line at 2.68A. These match, within an assumed maximum error of $\frac{1}{2}$ percent for this range, the lines 1.75A and 2.67A of the unknown in the first column of Table II, so we turn at once to the standard tabulation of spacings for $NaClO_3$, (shown in the fourth column of Table II). We find that, with the exception of one line whose relative intensity is lower than any line recorded on the pattern of the "unknown," every line on the standard pattern of $NaClO_3$ checks in position some line from the "unknown." Except for two lines at 1.58A and 1.50A, all the matched lines from the "unknown" have either the same or lower intensity than those recorded for the standard pattern of $NaClO_3$.

We must now account for the lines of Table II which do not match those of $NaClO_3$, and see, too, whether the abnormally black lines at 1.58A and 1.50A do not represent coincident lines from both of the components. We start with the strongest of the remaining lines, which corresponds to a spacing of 2.52A. We turn to group 2.55–2.50 of our classification book (Fig. 1). The second most intense line, according to our convention for lines of equal intensity, is 2.32A, so we find sub-group 2.35–2.30. Our book, as illustrated by Fig. 1, shows that CuO belongs to this sub-group and has its third and fourth most intense lines at 1.85A and 1.408A, respectively. These match, within the experimental errors of 0.5 and 0.3 percent, respectively for these ranges, the lines 1.86A and 1.406A of the pattern of the "unknown," so we turn at once to the standard tabulation of spacings for CuO (shown in the sixth column of Table II). Within the range of the experimental data every line from CuO finds its counterpart in the pattern of the "unknown." We find lines at 1.57A and 1.50A superimposed on those for $NaClO_3$, and we see that their combined intensities account for the intensities of the two lines from the "unknown."

Every line from the "unknown" has been identified as belonging either to $NaClO_3$ or to CuO or to both. There are no lines of the "unknown" left unaccounted for. Within the limits of intensity shown by the lines on the pattern of the "unknown," every line of $NaClO_3$ and of CuO is accounted for. We may therefore say confidently that the crystalline portion of the "unknown" is a mixture of $NaClO_3$ and CuO and of nothing else. The reader has probably noticed by this time that the whole procedure of interpreting the diffraction pattern of the "unknown" could have been carried out just as well by using as "index" lines only the *three* most intense lines for each component instead of the first *four*. In actual practice, Hanawalt finds but little ad-

Group 2.55–2.50.

Compound	3rd line	4th line	Compound	3rd line	4th line	Compound	3rd line	4th line	Compound	3rd line	4th line
20.00–15.00			4.50–4.40			2.75–2.70			1.75–1.70		
15.00–12.00			4.40–4.30			2.70–2.65			1.70–1.65		
12.00–10.00			4.30–4.20			2.65–2.60			1.65–1.60		
10.00–9.00			4.20–4.10			2.60–2.55			1.60–1.55		
9.00–8.50			4.10–4.00			2.55–2.50			1.55–1.50		
8.50–8.00			4.00–3.90			2.50–2.45			SiC (Cubic)	1.31	2.17
8.00–7.50			3.90–3.80			2.45–2.40			1.50–1.45		
7.50–7.00			3.80–3.70			2.40–2.35			Fe_2O_4	1.61	2.10
7.00–6.50			3.70–3.60			2.35–2.30			$ZnFe_2O_4$	2.97	1.61
6.50–6.00			3.60–3.50			CuO	1.86	1.408	$MgFe_2O_4$	2.95	1.60
6.00–5.75			3.50–3.40			2.30–2.25			1.45–1.40		
5.75–5.50			3.40–3.30			2.25–2.20			1.40–1.35		
5.50–5.25			3.30–3.20			2.20–2.15			1.35–1.30		
5.25–5.00			3.20–3.10			2.15–2.10			1.30–1.25		
$Ba(NO_2)_2 \cdot H_2O$	3.48	3.01	SrO_2	2.00	1.87	2.10–2.05			1.25–1.20		
5.00–4.90			3.10–3.00			2.05–2.00			1.20–1.15		
4.90–4.80			3.00–2.95			2.00–1.95			1.15–1.10		
4.80–4.70			2.95–2.90			1.95–1.90			1.10–1.05		
$Na_2SnO_3 \cdot 3H_2O$	1.85	2.29	2.90–2.85			1.90–1.85			1.05–1.00		
4.70–4.60			2.85–2.80			1.85–1.80			1.00–.90		
4.60–4.50			2.80–2.75			1.80–1.75			.90–.80		
									.80–		

Supplementary Group Index 2.55–2.50.

Compound	1st line	2nd line	3rd line	Compound	2nd line	1st line	3rd line	Compound	3rd line	1st line	2nd line
$Ba(NO_2)_2 \cdot H_2O$	2.52	5.1	3.48	$BeSO_4 \cdot 4H_2O$	2.52	3.90	3.20	$Cu_2Fe(CN)_6 \cdot 7H_2O$	2.50	5.0	3.55
$Na_2SnO_3 \cdot 3H_2O$	2.51	4.75	1.85	$Ba_3(PO_4)_2$	2.51	3.58	4.45	$Na_2PbO_3 \cdot 3H_2O$	2.53	4.80	4.62
SrO_2	2.52	3.14	2.00	KI	2.50	3.53	4.08	$BaCl_2 \cdot 2H_2O$	2.54	4.48	2.91
CuO	2.51	2.31	1.86	KNO_2	2.50	3.31	2.20	$CdWO_4$	2.53	3.80	3.05
SiC	2.51	1.54	1.31	SbI_3	2.54	3.30	2.14	$Hg(CN)_2$	2.51	3.72	4.85
$ZnFe_2O_4$	2.53	1.48	2.97	$ZrSiO_4$	2.51	3.29	1.71	$(CdSO_4)_3 \cdot 8H_2O$	2.51	3.55	4.90
Fe_2O_4	2.53	1.48	1.61	Th	2.53	2.92	1.79	Ba	2.51	3.54	2.04
$MgFe_2O_4$	2.51	1.48	2.95	Ag_3AsO_4	2.50	2.74	1.63	$2CuCO_3 \cdot Cu(OH)_2$	2.51	3.51	5.1
				Fe_2O_3	2.51	2.69	1.84	$Ba(H_2PO_2)_2 \cdot H_2O$	2.54	3.34	7.8
								As_2O_3	2.53	3.18	6.3
								$K_2WO_4 \cdot 2H_2O$	2.51	3.09	3.92
								KCNS	2.51	2.97	2.79

FIG. 1. Sample page from imaginary classification book.

Group 2.95–2.90.

Compound	3rd line	4th line	Compound	3rd line	4th line	Compound	3rd line	4th line	Compound	3rd line	4th line
20.00–15.00			4.40–4.30			2.80–2.75			1.90–1.85		
						Sn	2.01	2.05			
15.00–12.00			4.30–4.20			CaC_2II	1.95	2.09	1.85–1.80		
			$NaIO_3$	3.19	1.66	2.75–2.70			NaN_3	2.42	2.18
12.00–10.00			4.20–4.10			Na_2CrO_4	4.09	3.88	1.80–1.75		
						2.70–2.65			In_2O_3	1.52	2.52
10.00–9.00			4.10–4.00						1.75–1.70		
			$Pb_3(PO_4)_2$	3.61	3.31	2.65–2.60					
9.00–8.50			4.00–3.90						1.70–1.65		
						2.60–2.55			CsCl	4.11	2.05
8.50–8.00			3.90–3.80			$NaHCO_3$	3.48	3.04	1.65–1.60		
						2.55–2.50					
8.00–7.50			3.80–3.70			Th	1.79	1.52	1.60–1.55		
			$CdCO_3$	1.83	2.46	2.50–2.45					
7.50–7.00			3.70–3.60			$K_2C_2O_4$	2.32	2.62	1.55–1.50		
			$Ba(ClO_4)_2 \cdot 3H_2O$	2.14	1.92	2.45–2.40					
7.00–6.50			3.60–3.50						1.50–1.45		
P_2S_5	4.90	4.05				2.40–2.35					
6.50–6.00			3.50–3.40						1.45–1.40		
$HgSO_4 \cdot 2HgO$	5.5	3.3				2.35–2.30					
6.00–5.75			3.40–3.30						1.40–1.35		
			$C_{16}H_9O_2N_2(SO_2K)_2$	3.00	2.22	2.30–2.25					
5.75–5.50			3.30–3.20						1.35–1.30		
			$NaClO_3$	1.76	2.68	2.25–2.20					
5.50–5.25			3.20–3.10						1.30–1.25		
$Na_2S_2O_3 \cdot 5H_2O$	2.84	2.76				2.20–2.15					
5.25–5.00			3.10–3.00			$Na_2B_4O_7 \cdot 5H_2O$	4.40	3.44	1.25–1.20		
						2.15–2.10					
5.00–4.90			3.00–2.95						1.20–1.15		
						2.10–2.05					
4.90–4.80			2.95–2.90						1.15–1.10		
						2.05–2.00					
4.80–4.70			2.90–2.85						1.10–1.05		
						2.00–1.95					
4.70–4.60			2.85–2.80						1.05–1.00		
						1.95–1.90					
4.60–4.50									1.00–.90		
4.50–4.40									.90–.80		
$(C_6H_4CO_2)_2BONa$	3.45	2.18							.80–		

Supplementary Group Index 2.95–2.90.

Compound	1st line	2nd line	3rd line	Compound	2nd line	1st line	3rd line	Compound	3rd line	1st line	2nd line
P_2S_5	2.90	6.7	4.90	$Mg_3(PO_4)_2 \cdot 8H_2O$	2.94	6.7	2.69	$C_6H_4(CO)_2NK$	2.90	14.5	6.4
$HgSO_4 \cdot 2HgO$	2.92	6.2	5.5	$MnCl_2 \cdot H_2O$	2.93	5.7	2.55	$Bi(C_2H_3O_2)_3$	2.90	13.5	3.35
$Na_2S_2O_3 \cdot 5H_2O$	2.93	5 4	2.84	$BaCl_2 \cdot 2H_2O$	2.91	4.48	2.54	$AgC_2H_3O_2$	2.91	10.0	3.04
$(C_6H_4CO_2)_2BONa$	2.94	4.40	3.45	$Mg(NO_3)_2 \cdot 6H_2O$	2.93	4.42	3.29	$Ba(CN)_2$	2.94	9.4	3.37
$NaIO_3$	2.93	4.25	3.19	$MgSO_4 \cdot 6H_2O$	2.92	4.40	4.04	$SnCl_4 \cdot 5H_2O$	2.94	6.2	5.3
$Pb_3(PO_4)_2$	2.91	4.03	3.61	KH_2PO_4	2.90	3.72	1.95	$CoCl_2 \cdot 6H_2O$	2.94	5.6	4.85
$CdCO_3$	2.94	3.77	1.83	α-ZnS	2.91	3.29	1.76	$CuOH \cdot CuPO_4$	2.91	4.81	2.63
$Ba(ClO_4)_2 \cdot 3H_2O$	2.90	3.65	2.14	PbO	2.93	3.06	2.72	$MgNH_4PO_4 \cdot 6H_2O$	2.93	4.28	2.69
$C_{16}H_9O_2N_2(SO_2K)_2$	2.90	3.35	3.00	CaC_2III	2.92	2.86	2.05	$HgCl_2 \cdot 3HgO$	2.92	3.95	2.70
$NaClO_3$	2.94	3.28	1.76	Hg_3PO_4	2.94	2.60	3.09	$PbHAsO_4$	2.93	3.39	3.17
Sn	2.91	2.79	2.01					$K_2S_2O_7$	2.90	3.23	3.07
CaC_2II	2.95	2.79	1.95					Ag_2CrO_4	2.92	3.14	3.02
Na_2CrO_4	2.91	2.73	4.09					K_2SeO_3	2.94	3.08	4.35
$NaHCO_3$	2.94	2.58	3.49					$(NH_4)HC_2O_4 \cdot H_2O$	2.90	3.00	6.2
Th	2.92	2.53	1.79					Li_2CO_3	2.91	2.80	4.16
$K_2C_2O_4$	2.92	2.46	2.32					$Na_2SiO_3 \cdot 9H_2O$	2.92	2.79	3.83
$Na_2B_4O_7 \cdot 5H_2O$	2.94	2.19	4.40								
NaN_3	2.91	1.82	2.42								
In_2O_3	2.91	1.78	1.52								
CsCl	2.90	1.68	4.11								

FIG. 2. Sample page from imaginary classification book.

vantage in using the fourth most intense line as an "index" line.

The technique of using the book of classified data requires a slight change in the case of "unknowns" in which two components have overlapping "index" lines. Let us assume that the diffraction data from our "unknown" are given by the first three columns of Table III. Since our most intense line is at 2.52A, we turn to the page in our classification book which contains group 2.55–2.50 (illustrated by Fig. 1). Our second most intense line is 2.69A, so we find sub-group 2.70–2.65 but find no compound listed with a third "index" line corresponding to any line listed for our "unknown." Our next most intense line is 1.48A, so we find sub-group 1.50–1.45. We find at once that Fig. 1 shows that Fe_3O_4 has a third "index" line at 1.61A. This matches one of the lines on the pattern of our "unknown." We therefore turn to Hanawalt's published standard pattern for Fe_3O_4 (see fourth and fifth columns of Table III), and find a reasonably good match for the location of many of the lines in the "unknown." Some of the lines match exactly, but a few of the lines are "off"

TABLE III. *Diffraction data for a two-component "unknown" with one superimposed "index" line. (Hanawalt.)*

"UNKNOWN"			Fe_3O_4		Fe_2O_3	
d	I	I/I_1	d	I/I_1	d	I/I_1
4.90	2	0.04	4.85	0.06	—	—
3.68	4	0.08	—	—	3.68	0.18
2.96	7	0.14	2.97	0.28	—	—
2.69	25	0.50	—	—	2.69	1.00
2.52	50	1.00	2.53	1.00	2.51	0.75
2.43	1	0.02	2.42	0.11	—	—
2.21	7	0.14	—	—	2.20	0.18
2.08	8	0.16	2.10	0.32	—	—
1.84	15	0.30	—	—	1.84	0.63
1.69	17.5	0.35	1.71	0.16	1.69	0.63
1.61	15	0.30	1.61	0.64	1.60	0.13
1.480	25	0.50	1.483	0.80	1.485	0.50
1.450	10	0.20	—	—	1.452	0.50
—	—	—	—	—	1.351	0.03
—	—	—	1.326	0.06	—	—
1.309	4	0.08	—	—	1.038	0.18
1.274	2	0.04	1.279	0.20	—	—
1.256	3	0.06	—	—	1.259	0.13
1.220	1	0.02	1.210	0.05	—	—
1.189	2	0.04	—	—	1.190	0.08
1.160	2	0.04	—	—	1.163	0.05
1.140	2	0.04	—	—	1.140	0.13
1.120	1	0.02	1.121	0.10	—	—
1.103	1	0.02	—	—	1.104	0.10
1.089	2	0.04	1.092	0.32	—	—
1.054	2	0.04	—	—	1.056	0.08
1.040	1	0.02	1.049	0.10	—	—

beyond the normal experimental error. This is characteristic of the noncubic oxides of some metals, especially iron, and is probably due to the presence of oxygen in solid solution (see next section of this article). Bearing this in mind, and noting that the classification book shows that the lines which match poorly are *not* index lines of some other component, we have accounted for all the lines of our standard pattern of Fe_3O_4 except for one very weak line at 1.326. There are several conditions, well recognized by crystal analysts, which might tend to *weaken* a line below the relative intensity listed in the standard pattern but there are no experimental conditions possible in the powder method by which the relative intensity can be markedly *increased*. It is, therefore, easily possible that 1.326 was present on the pattern of the "unknown" but was too weak to read. We, therefore, feel justified in assuming that our "unknown" contains Fe_3O_4.

We next examine the relative intensities of our lines, and find that I/I_1 for the first few Fe_3O_4 lines of our "unknown" is only about half that called for by the standard pattern. This discrepancy would be accounted for if the absolute intensity of the 2.52A line were only 25 or 30 instead of 50. If this explanation is correct, we must include the 2.52A line (with an intensity of roughly 25), as part of the pattern for which we must still find a match. This gives, in our remaining pattern, two lines one at 2.69A and one at 2.52A of nearly the same intensity. Our imaginary classification book (Fig. 1), shows at once that there is no match for group 2.55–2.50, sub-group 1.50–1.45. We turn, therefore, at once to group 2.70–2.65 and sub-group 2.55–2.50 (Fig. 3). We find there a listing for Fe_2O_3 with a third index line at 1.84A. So we look up the standard pattern of Fe_2O_3 (shown in columns six and seven of Table III), and find a good match, with three additional superimposed lines. The relative intensities of the four superimposed lines are now seen to be consistent with the sums of the contributions from Fe_2O_3 and Fe_3O_4 so that our pattern now matches up completely (except for the displacements noted above), both in positions and in intensities the combined patterns of Fe_2O_3 and Fe_3O_4. We have therefore arrived at a definite qualitative analysis of our "unknown." If we had failed to notice the extra intensity of

Group 270–2.65.

Compound	3rd line	4th line	Compound	3rd line	4th line	Compound	3rd line	4th line	Compound	3rd line	4th line
20.00–15.00			4.40–4.30			2.70–2.65			1.85–1.80		
15.00–12.00			4.30–4.20			2.65–2.60			1.80–1.75		
12.00–10.00			4.20–4.10			2.60–2.55			1.75–1.70		
10.00–9.00			4.10–4.00			2.55–2.50			1.70–1.65		
9.00–8.50			4.00–3.90			Fe_2O_3	1.84	1.69	1.65–1.60		
8.50–8.00			3.90–3.80			2.50–2.45			1.60–1.55		
8.00–7.50			3.80–3.70			Ag_3PO_4	1.66	1.73	1.55–1.50		
7.50–7.00			3.70–3.60			2.45–2.40			1.50–1.45		
7.00–6.50			3.60–3.50			2.40–2.35			1.45–1.40		
6.50–6.00			3.50–3.40			2.35–2.30			1.40–1.35		
6.00–5.75			3.40–3.30			2.30–2.25			1.35–1.30		
5.75–5.50			3.30–3.20			2.25–2.20			1.30–1.25		
5.50–5.25			3.20–3.10			2.20–2.15			1.25–1.20		
5.25–5.00			3.10–3.00			$ZnCrO_4$	9.50	4.67	1.20–1.15		
5.00–4.90			3.00–2.95			2.15–2.10			1.15–1.10		
$5CaO \cdot 3Al_2O_3$	2.44	2.19				2.10–2.05			1.10–1.05		
4.90–4.80			2.95–2.90			$FeCl_3$	5.90	3.86	1.05–1.00		
4.80–4.70			2.90–2.85			2.05–2.00			1.00–.90		
			Mg_2Ca	3.14	1.75	2.00–1.95			.90–.80		
4.70–4.60			2.85–2.80			KF	3.08	1.54	.80–		
4.60–4.50			2.80–2.75			$Na_2HPO_4 \cdot 5H_2O$	1.54	4.23			
4.50–4.40			2.75–2.70			$3CaO \cdot Al_2O_3$	1.54	4.05			
			Ag_2CO_3	2.27	4.77	1.95–1.90					
						1.90–1.85					

Supplementary Group Index 2.70–2.65.

Compound	1st line	2nd line	3rd line	Compound	2nd line	1st line	3rd line	Compound	3rd line	1st line	2nd line
$5CaO \cdot 3Al_2O_3$	2.68	4.90	2.44	$CuCl_2 \cdot 2NH_4Cl \cdot 2H_2O$	2.68	5.5	2.75	$BiO_2C_{10}H_7$	2.67	20.0	9.9
Mg_2Ca	2.65	2.87	3.14	$Cr_2(C_2O_4)_3 \cdot H_2O$	2.68	4.75	9.2	$Ba(CNS)_2 \cdot 2H_2O$	2.66	7.7	3.4
Ag_2CO_3	2.65	2.73	2.27	$MgSO_4 \cdot 7H_2O$	2.66	4.22	5.9	$Mg_3(PO_4)_2 \cdot 8H_2O$	2.69	6.7	2.94
Fe_2O_3	2.69	2.51	1.84	$MgNH_4PO_4 \cdot 6H_2O$	2.69	4.28	2.93	$MnC_2O_4 \cdot 2\frac{1}{2}H_2O$	2.67	4.80	3.00
Ag_3PO_4	2.68	2.45	1.66	$Pb_3(SbO_4)_2$	2.65	3.48	5.8	KNO_3	2.66	3.77	3.03
$ZnCrO_4$	2.67	2.14	9.5	BiOCl	2.67	3.45	7.4	K	2.65	3.75	2.16
$FeCl_3$	2.68	2.08	5.9	BaO_2	2.68	3.37	2.11	$NaHC_2O_4 \cdot H_2O$	2.67	2.97	2.45
$Na_2HPO_4 \cdot 5H_2O$	2.67	1.89	1.54	$TeCl_2$	2.69	3.24	4.29	$Na_2CO_3 \cdot H_2O$	2.67	2.76	2.37
$3CaO \cdot Al_2O_3$	2.68	1.90	1.55	$Na_2C_5H_7O_4N_4 \cdot H_2O$	2.66	3.17	4.72	LiOH	2.67	2.75	4.35
KF	2.66	1.88	3.08	$SnSO_4$	2.67	3.08	2.10	FeS	2.65	2.06	2.98
				$(NH_4)_2C_2O_4 \cdot H_2O$	2.67	3.06	3.81	Mg_3N_2	2.66	1.76	2.12
				$Na_2SO_3 \cdot 7H_2O$	2.66	2.87	4.26				
				Cr_2O_3	2.67	1.67	2.47				

FIG. 3. Sample page from imaginary classification book.

the 2.52 line we might not have found a match so easily. In such a case, the supplementary tables at the bottom of the pages of the classification book would have given us valuable clews.

So far our analysis has shown *what* crystalline materials are present, but has not determined their proportions. The safest way of turning our qualitative analysis into a quantitative analysis, is to make up synthetic, uniform, mixtures of powdered $NaClO_3$ and CuO in different proportions until a mixture is found which gives lines of the same relative intensities as the lines on the diffraction pattern of the "unknown."[8] The number of synthetic mixtures required to find a match may be greatly lessened by noting the absolute intensities, on the Hanawalt scale[2] of the three strongest lines (i.e. the first three "index" lines), on the pattern of the "unknown" and then comparing these intensities with Hanawalt's published intensities for his standard patterns.[2] The proportions of various constituents in a crystalline mixture cannot be told by merely photometering the diffraction pattern of the mixture and comparing the heights of the curves for the lines from the various components.[2] Such a procedure would be false if for no other reason than that when the components of the mixture have different crystal structures there is no criterion as to which lines to choose in estimating the ratio of intensities. But there is a still more weighty reason. The efficiency of diffraction will, in general, depend upon particle size, perfection of crystallization, chemical composition, crystal structure, etc. This is well illustrated by Hanawalt's published lists of standard diffraction patterns which represent for each substance the normal particle size obtained by the grinding technique ordinarily used in the "powder method" of crystal analysis,[7] the normal degree of perfection of crystallization for the given compound, etc. In Hanawalt's lists he records the absolute intensity of the three most intense lines (i.e. of the "index" lines), of each pattern in terms of the Hanawalt scale. A study of his data will show at once the advantage, in comparatively rough work, of dealing with the ratios between the normal intensities of the "index" lines in the standard pattern and the intensities of the same lines in the "unknown," provided, of course, that the "unknown" has been given a normal exposure. Such a study will show the fallacy of comparing only the lines of the components as they appear on the diffraction pattern of the "unknown."[9] We may repeat;—in making as accurate a quantitative analysis as possible by x-ray diffraction methods, the only safe method is to find a synthetic mixture whose composition is known which gives a diffraction pattern identical to that of the "unknown."

The Identification of a Crystalline Material Which Contains a Second Material in Solid Solution

When substance B is "dissolved" in a crystalline solute A, B may occupy positions between the atoms of the host crystal (interstitial solid solution), (e.g. C in gamma Fe), or B may replace atoms of the host crystal (substitutional solid solution), (e.g. Ag in Au). In general, the interstitial type of solution increases the density. The substitutional type may increase or decrease the density, depending upon the relative weights of atoms of A and atoms of B and on whether the lattice of A contracts or expands because of the presence of B. In any case, the crystals of A retain a close approximation to their original mean positions in the crystal so that the characteristic diffraction pattern of A can still be recognized.

If the addition of B to A gives a marked change in the diffraction pattern so that the pattern of A can no longer be recognized, a complete solution of the crystal structure will show a close relation between the positions of A atoms and of B atoms. The new crystal thus formed is considered to be an intermetallic compound, and falls within the scope of the first two sections of this article. If the atoms of B take up a regular spacing (so-called super-lattice) in the crystal of A as a means of keeping as far apart as possible from each other, they will alter the relative intensities of the lines in the diffraction pattern of A, and may even produce an additional pattern corresponding to their very large spacing. The geometry of such a configuration requires a definite ratio between the number of atoms of A and of B. Since the chemical law of definite proportions is obeyed the material must be called a compound. Since the compound owes its existence solely to geometrical requirements these

materials are called "geometrical compounds." When a super-lattice is found, the methods of the second section apply except the relative intensities of the lines must now be calculated on the basis of a super-lattice of B interpenetrating the normal lattice of A.

If the atoms of B are irregularly scattered through the body of A, then we have a typical "solid solution." The diffraction pattern may be regarded as a slightly distorted pattern of pure A. Two types of distortion present themselves, one for the case of a host-material A of cubic crystal structure, and one for the case of a host-material A of noncubic structure. The symmetry of the cubic system of crystallization is such that the distortions in different directions combine to maintain rigorously the cubic type of diffraction pattern, but with some little change in the dimensions of the unit-cube. Although the absolute intensities of the lines in the diffraction pattern may be altered slightly, the order of intensity of the lines is rarely changed. For instance, the sixth most intense line is still, in general, the sixth in order of intensity, and certainly is not changed to stronger than the fifth nor to weaker than the seventh. The change in the lattice parameter of Pb caused by an impurity (probably oxygen), in solid solution is illustrated in Table IV. When both A and B are solid and crystallize in the cubic system (e.g. Cu-Ni), the lattice parameter increases linearly or nearly linearly with the composition. Of course, the diffraction pattern itself identifies only the host, A. B must be found by other means, usually by spectrographic analysis. If spectrographic analysis shows the presence of only two cubic metals in the alloy, the proportions of B in A can be obtained to a first approximation by interpolation from the lattice parameters of A and B. In most cases, for really accurate work the diffraction pattern of the "unknown" must be matched against synthetic solid solutions of B in A of known concentration.

When the host-material, A, is noncubic, the presence of atoms of B will cause more distortion in some crystallographic directions than in others. Many lines in the pattern will hardly be shifted at all, but a few lines may be shifted considerably, even as much as ten times the experimental error of reading the line, and the relative intensities of the shifted lines may be considerably changed. The oxides of iron appear to be very likely to contain additional oxygen in solid solution, and the shift in position of individual lines is well illustrated by the patterns of Fe_2O_3 and of Fe_3O_4 in Table III. As before, after A has been identified from the diffraction pattern, and B has been identified by other means, the proportion of B in A must be determined by matching the pattern of the "unknown" against patterns of known synthetic solid solutions of B in A. For details as to suitable specialized equipment for work in solid solutions, precautions to be observed, and other highly technical details the reader is referred to the articles by C. S. Barrett, K. R. Van Horn, W. P. Davey, and J. T. Norton in the "Symposium on Radiography and X-Ray Diffraction Methods" published by the American Society for Testing Materials, Philadelphia, Pennsylvania (1937).

TABLE IV. *Effect of traces of impurity in solid solution in metallic* Pb.

Interplanar Spacings Found for a Sample of Pure Pb[a]	Standard Interplanar Spacings for Pure Pb, $a_0=4.920$A	Interplanar Spacings Found for Impure Pb[a]	Interplanar Spacings Calculated for $a_0=4.950$A
2.84	2.840	2.85	2.859
2.46	2.460	2.48	2.475
1.739	1.739	1.75	1.751
1.485	1.483	1.497	1.493
1.420	1.420	1.432	1.429
1.231	1.230	1.239	1.238
1.129	1.128	1.134	1.135
1.101	1.100	1.103	1.106
1.005	1.004	1.010	1.011
0.947	0.947	0.953	0.953
0.870	0.870	0.875	0.875

[a] Last significant figure in doubt by 0.01 for values down to 2.0; by 0.005 from 2.0 to 1.2; by 0.002 below 1.2.

Bibliography

1. W. P. Davey, Gen. Elec. Rev. **25**, 565 (1922).
2. J. D. Hanawalt, H. W. Rinne and L. K. Frevel, Ind. Eng. Chem. (Analytical Edition), **10**, 457–511 (1938).
3. C. S. Barrett, "Symposium on Radiography and X-Ray Diffraction," American Society for Testing Materials, Philadelphia (1937), pp. 193–229.
4. P. P. Ewald and C. Hermann, *Structurbericht* (Akad. Gesell., Leipsig, 1931).
5. R. W. G. Wyckoff, *Structure of Crystals* (Reinhold Pub. Co., New York, 1930–1934).
6. Zeitschrift f. Kristallographie, current structure abstracts.

7. W. P. Davey, *A Study of Crystal Structure* (McGraw-Hill, New York, 1934), pp. 112–118, 158–163.
8. W. P. Davey, "Chemical Analysis by X-Ray Diffraction," Symposium on Radiography and X-Ray Diffraction, American Society for Testing Materials, Philadelphia (1937).
9. Diffraction theory shows that it should be possible to calculate the proportions of two unknowns by taking into account: (1) the volume of the specimen exposed to x-rays, (2) the molecular weight, (3) the number of atoms (or molecules) per unit cell, (4) the scattering power of the unit cell, (5) the structure factors of the atomic planes used, (6) the Lorentz factor, (7) the polarization factor, (8) the absorption factor as it exists under the diffracting conditions, (9) the intensity of the primary beam, (10) the intensity of the diffracted beam, measured as the integral of the interference curve. In this connection see K. Schaefer, Zeits. f. Kristallographie, **99**, 142 (1938). It is difficult to determine some of these quantities to any degree of real precision. In the general case, the scheme is too cumbersome for routine commercial analysis, and too involved in the abstract theory of x-ray diffraction from crystals to be useful in patent work. The special cases in which most of the above ten quantities cancel out are too restricted to be of much practical value.

Advice to Authors

If you've got a thought that's happy—
Boil it down.
Make it short and crisp, and snappy—
Boil it down.
When your brain its coin has minted,
down the page your pen has sprinted,
If you want your effort printed,
Boil it down.

Take out every surplus letter—
Boil it down.
Fewer syllables the better—
Boil it down.
Make your meaning plain—express it,
So we'll know—not merely guess it,
Then, my friend, ere you address it,
Boil it down.

Skim it well—then skim the skimmings—
Boil it down.
When you're sure 'twould be a sin to
Cut another sentence in two,
Send it in, and we'll begin to—
Boil it down.

Quoted by Professor R. B. Dustman from Canadian Public Health Journal, 1936.

The Properties of Oxide-Coated Cathodes. II*

BY JOHN P. BLEWETT

General Electric Research Laboratory, Schenectady, New York

5. Chemical Properties of the Alkaline Earth Oxides

A THOROUGH treatment of the general chemical properties of the alkaline earth oxides will be found in Mellor's *Treatise on Inorganic Chemistry*.[3a] We shall consider only those reactions which are of interest in connection with the activation of oxide cathodes.

The most efficient reducing agent for (BaSrCa) oxides is probably aluminum which takes part in "thermite" type reactions with all three oxides. Mixed powders of (BaSrCa) oxide and aluminum when heated react violently with evolution of heat and volatilization of the liberated alkaline earth. Magnesium partly reduces CaO at high temperatures. The reaction of magnesium with SrO is more vigorous than with CaO, and with BaO it is still more effective.

Other reactions of the type:

$$(BaSrCa)O+\text{metal}\rightleftarrows\text{Metal oxide}+(BaSrCa)$$

reach equilibrium for the most part in the presence of a very low vapor pressure of (BaSrCa). If the reaction takes place in the open, as is usually the case when the alkaline earth resides on a cathode, the (BaSrCa) may escape by diffusion or evaporation, and the reaction will continue until the supply of one of the components is used up or until the reaction is stopped by a layer of metal oxide.

An investigation now in progress under the direction of Dr. H. A. Liebhafsky and the author (cf. Blewett[17]) of the endothermic reactions of BaO with Ti, Ta, Ni, Mo, and C indicates that around 1400°K mixed powders of Ti and BaO yield Ba at a rate initially about 10^3 times the rate of evaporation of BaO. Ta is less efficient by a factor of about 30, while Ni and Mo liberate Ba at a rate less than the rate of evaporation of BaO. With carbon, BaO reacts to form barium carbide in quantities comparable with the yield of Ba from BaO+Ti. The slopes of the log yield *vs.* $1/T$ curve give heats for these reactions as follows:

$BaO+Ti$	$\Delta Q=83$ kcal.
$BaO+Ta$	$\Delta Q=96$ kcal.
$BaO+3C\rightarrow CO+BaC_2$	$\Delta Q=80$ kcal.

The titanium reaction is probably responsible for the easy activation of "Konel" core oxide cathodes (Lowry[9]). The tantalum reaction is employed in the "Batalum" getter filaments of Lederer and Walmsley,[16] and in the barium source described by Benjamin and Jenkins.[17]

The reaction of BaO with Ni is treated at some length by Wagner,[9] who shows by a thermodynamic argument that the vapor pressure of Ba to be expected at 1273°K from the reaction

$$BaO+Ni\rightarrow NiO+Ba$$

is about 3×10^{-17} atmosphere, or about 10^{-7} times the vapor pressure of BaO at the same temperature. Consequently very little reduction of a BaO coating by a Ni core is to be expected. It should be noted in this connection, however, that Mg, which, as we noted above, is a very efficient reducing agent, is frequently to be found as an impurity in commercial nickel.

A slight revision to Mellor's discussion of the existence of a suboxide of barium Ba_2O is necessary in the light of the recent experiments of Schriel.[16] These experiments demonstrated that the substance considered by earlier authors to be Ba_2O is merely a mixture of BaO and Ba. The paper of Schriel includes a study of the mutual solubilities of Ba and BaO. At 1000°K BaO can be dissolved to the extent of 20 percent in Ba. At 1473°K a 45 percent solution can be attained. The solubility of Ba in BaO is of the order of 1 percent.

6. Physical Properties of Mixtures of Alkaline Earth Oxides

Benjamin and Rooksby[12] have shown by x-ray diffraction that BaO and SrO form a series of

* Part I appeared in J. App. Phys. **10**, 668 (1939). Parts II and III have been combined so that this part concludes the review of oxide-coated cathodes.

solid solutions. Burgers[12] arrived at the same conclusion and demonstrated that the lattice parameter of the solid solution is a linear function of the molecular composition. Gaertner[14] and Darbyshire[17] have studied the surface of a mixed oxide cathode by electron diffraction and agree that, after it has been heated, the surface is composed mainly of SrO, as is to be expected from the higher vapor pressure of BaO.

Claassen and Veenemans[12] measured the rates of evaporation from mixtures of BaO and SrO and of BaO and CaO and showed that BaO evaporates at a rate which is a continuous but not linear function of the molecular concentration. They conclude that solid solutions are formed of BaO and SrO and of BaO and CaO.

Benjamin and Rooksby[12] assert that the best electron emission from a 50–50 atomic percent mixture of BaO and SrO is somewhat higher than the emission from either oxide by itself.

7. *Properties of the Alkaline Earth Metals; Thin Films on Tungsten*

Table II (Part I, p. 671) summarizes some of the most important properties of the alkaline earth metals. We shall consider in particular the thermionic behavior of thin films of barium.

Becker,[8(2)] Ryde and Harris (Reimann, reference 13, p. 159, *et seq.*), Nelson,[10] and Eglin[7] have observed the variations in electron emission of a tungsten filament as barium is deposited upon it. Becker's curve is reproduced in Fig. 7, in which the logarithm of the electron emission is plotted against f, the ratio of the time of deposition of barium to the time required to achieve the maximum of electron emission. Since barium was distilled at a uniform rate, f may be taken as a measure of the fraction of the tungsten surface covered by barium. Until recently the assumption has frequently been made that the maximum emission, i.e., $f=1$, corresponded to a monolayer of barium. Taylor and Langmuir[12] showed, however, that this assumption is untrue for the qualitatively similar case of caesium on tungsten, since in this case the maximum emission is achieved when 0.67 of a monolayer of caesium has been deposited. For barium, a monolayer is less easily defined, since the type of arrangement of the Ba atoms on the tungsten surface is not known. However, it is possible (Blewett[17]) to

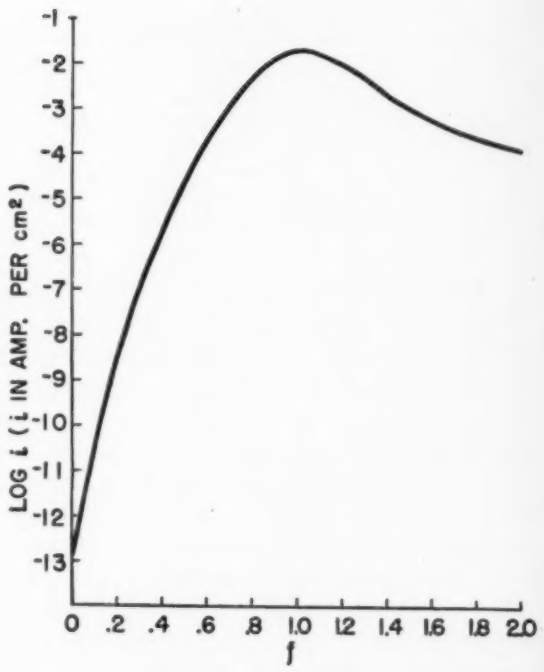

FIG. 7. Electron emission from thin films of barium on tungsten (Becker, reference 8). f is proportional to the number of barium atoms per sq. cm of tungsten surface

measure the number of Ba atoms per sq. cm of tungsten surface, which results in maximum electron emission. This number is $(5.7\pm0.5)\times10^{14}$ atoms per sq. cm of apparent tungsten surface, or $(4.1\pm0.4)\times10^{14}$ atoms per sq. cm of true tungsten surface, if we apply Taylor and Langmuir's shape factor for tungsten.

When a tungsten filament is allowed to reach equilibrium with a stream of barium vapor, the emission varies with filament temperature in the manner indicated by Fig. 8. The low temperature region of the curve corresponds to emission from a thick film of barium. As the temperature is raised, evaporation sets in, and a less and less dense layer of barium remains on the filament. The electron emission passes through a maximum and decreases to a minimum where it increases again to correspond to the emission from clean tungsten.

Ryde and Harris have determined the thermionic constants for a tungsten filament bearing the covering of barium which results in maximum emission ($f=1$). The emission is given by

$$i=1.5T^2e^{-18100/T} \text{ amp. per cm}^2.$$

They have investigated also the case of barium on oxygen on tungsten and observe a similar electron emission *vs.* f relation to the case of barium on tungsten. For the optimum electron emission in this case

$$i = 0.18T^2e^{-15600/T} \text{ amp. per cm}^2.$$

A number of further combinations of layers of oxygen and barium on tungsten have been studied by Ryde and Harris. Among other phenomena observed we note the interesting fact that a layer of oxygen on barium on tungsten appears to change, when heated, to a layer of barium on oxygen on tungsten.

An anomalous situation exists at the moment with respect to the migration of barium over tungsten surfaces. Becker[8(2)] claims that barium will migrate over a tungsten surface at observable rates in a narrow temperature range just below the point at which the barium evaporation becomes appreciable. Benjamin and Jenkins,[17] on the other hand, claim that no such migration takes place. From the published descriptions of these experiments there seems to be no way to reconcile these conflicting results.

8. *Methods for Detection of (BaSrCa)*

(a) Chemical Methods

Provided it is not necessary to distinguish between the metal and its compounds, it is a simple matter to break open the experimental tube and measure total (BaSrCa) by standard microchemical methods. As soon as air is admitted, all free metal is quickly converted to oxide, carbonate, and other compounds, so that any hope of discriminating between free metal and, say, evaporated oxide must be abandoned. Hence, if it is desired to measure only the free metal, the measurements must be made without breaking the vacuum. This can be accomplished by admission of a gas which will take part in a quantitative reaction with the metal. Reactions which suggest themselves are:

(i) $$2(\text{BaSrCa})+O_2 \rightarrow 2(\text{BaSrCa})O,$$

the consumption of oxygen being a measure of the total amount of free alkaline earth metal present.

(ii) $$(\text{BaSrCa}) + \begin{matrix} H_2O \\ 2H_2O \end{matrix} \rightarrow \begin{matrix} (\text{BaSrCa})O \\ (\text{BaSrCa})(OH)_2 \end{matrix} + H_2,$$

(iii) $$(\text{BaSrCa})+CO_2 \rightarrow (\text{BaSrCa})O+CO,$$

so that the amount of H_2 or CO set free is a measure of the free (BaSrCa).

$$3(\text{BaSrCa})+N_2 \rightarrow (\text{BaSrCa})_3N_2$$

(iv) $$(\text{BaSrCa})_3N_2+6H_2O \rightarrow 3(\text{BaSrCa})(OH)_2+2NH_3,$$

so that a determination of ammonia provides a measure of the amount present of free (BaSrCa).

All four methods, the first in particular, suffer from the fact that a certain amount of reaction with other metal (electrodes, etc.) in the tube is inevitable. In spite of this, the reaction (ii) has been used successfully by Berdennikowa[11] and by Clausing (cf. de Boer, reference 14, p. 348). Prescott and Morrison[17] claim very definite advantages for reaction (iii). Good results have been obtained from reaction (iv) by Fritz.[14] It must be emphasized, however, that extreme care is necessary both in making and interpreting measurements of this type.

(b) Direct Weighing Methods

Evaporated (BaSrCa) can be weighed directly in vacuum by mechanical methods. For instance, a tungsten or quartz spring balance can be made

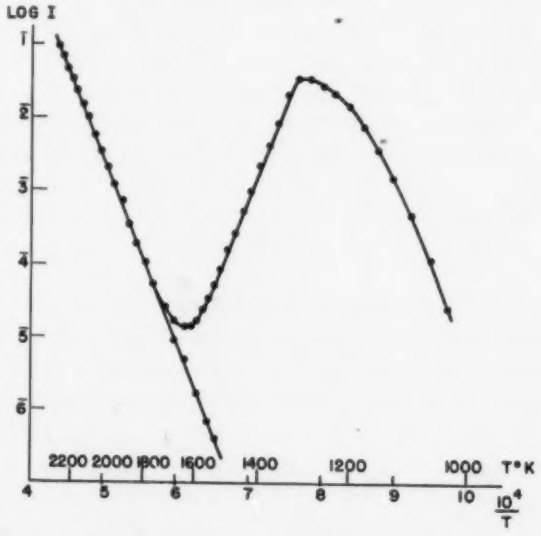

Fig. 8. Electron emission from a tungsten filament in a stream of barium vapor (Blewett, unpublished).

sufficiently sensitive. The author has described a beam balance (Blewett[18]) applicable to vacuum determinations of mass and capable of weighing 1 mg with fair accuracy. Balance methods, of course, necessitate further chemical checks to assure the operator that he has actually been weighing (BaSrCa) and not some compound or impurity.

(c) Optical Methods

Within limits it is possible to accept the opacity of a deposited layer of (BaSrCa) as a measure of the amount of the metal present. Adequate protection is necessary against the presence of gas layers on the collecting surface and against simultaneous deposition of other opaque substances. At best this method is good only with a calibration by an independent method.

(d) Electrical Methods

The most popular methods for detection of (BaSrCa) depend upon the thermionic properties of deposited films of these metals. For thick deposits, measurements of resistivity also are possible, but are complicated by the same factors which affect the optical method.

Three thermionic methods are available:

(i). *Measurement of electron emission.*—If a tungsten filament is maintained in the path of a beam of (BaSrCa), its electron emission will increase in the manner described in Section 7 above and illustrated by Becker's curve (Fig. 7). The slope of the initial region of the log emission *vs.* time curve or the time taken to reach the maximum provides an absolute measurement of the density of the vapor stream. For practical application we note the initial slope of the log i *vs.* f curve for barium on a tungsten filament at 1100°K,

$$d \log i/df = 24.5.$$

If N is the number of atoms per cm² of apparent tungsten surface, we have $N = 5.7\times10^{14}f$, so that we can deduce the rate of arrival of barium from the initial rate of increase of electron current $d \log i/dt$ from

$$\frac{dN}{dt} = 5.7\times10^{14}\frac{df}{dt} = 2.3\times10^{13}\frac{d \log i}{dt}.$$

It is generally more satisfactory to measure the time required to reach maximum electron emission, since this time is independent of the filament temperature, provided this temperature is sufficiently low (<1100°K) that reevaporation of barium is negligible.

For Sr and Ca, the number of atoms per cm² of tungsten surface corresponding to $f=1$ is not known. It is probably safe to assume that this number is of the same order of magnitude as for barium.

(ii). *Contact potential determination.*—This method is a refinement, developed by Reimann[14] and others, of method (i). The detector filament of method (i) is now maintained at room temperature. It is allowed to collect electrons from a space charge, its potential being slightly negative with respect to the emitter. Any change in work function of the detector due to deposition of (BaSrCa) will now be reflected in a change in its contact potential and hence in a voltage displacement of its volt-ampere characteristic. By this method, the work function *vs.* f relation can be traced. The work function passes through a minimum at $f=1$, corresponding to the maximum of Becker's log i *vs.* f curve. Since it avoids reevaporation and end loss uncertainties in detector temperature, this method presents decided advantages.

(iii). *Positive ion method.*—This technique is particularly applicable to Ba, although it is quite practicable for sufficiently intense sources of Sr and Ca. If a filament is maintained in a (BaSrCa) stream, its temperature being sufficiently high that no metal condenses, a certain fraction of the atoms which strike the filament will escape as positive ions. This fraction is given absolutely by the Saha-Langmuir relation:

$$\frac{n^+}{n} = \frac{\omega^+}{\omega}e^{-(I-\varphi)/kT},$$

where n^+ = number of ions evaporating per sec.
n = number of atoms arriving per sec.
ω^+ = statistical weight for $(BaSrCa)^+$
ω = statistical weight for (BaSrCa) (for (BaSrCa) $\omega^+/\omega = 2/1$)
I = ionization potential of (BaSrCa)
φ = work function of filament.

For the detector, tungsten is the most satisfactory in view of its high melting point and work

function. When the tungsten detector filament is maintained at 2500°K, the approximate fractions of alkaline earth atoms escaping as positive ions are as follows:

Ba: 10. percent
Sr: 1. percent
Ca: 0.1 percent.

This method can be checked by plotting the log of the positive ion current against $1/T$. In the range where the temperature is sufficiently high that the filament is continuously clean the plot will be a straight line whose slope corresponds to $(I-\varphi)$, as shown in Fig. 9.

Care must be taken in using this method to avoid photoelectric currents from the positive ion collector. Because of deposited layers of barium these currents may become troublesome, but they can be suppressed with a magnetic field of 100 gauss or so supplied by a Helmholtz coil.

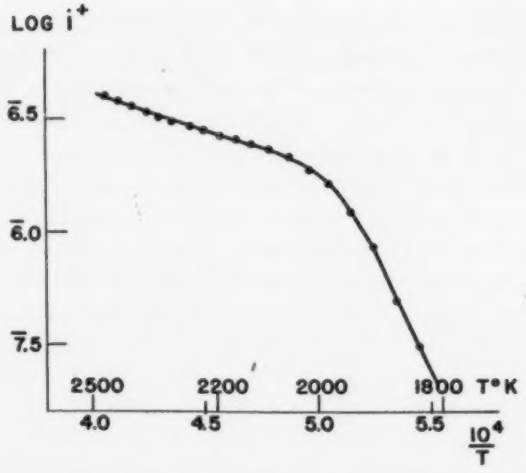

FIG. 9. Positive ion emission from a tungsten filament in a stream of barium vapor (Blewett, unpublished). Above 2000°K this curve represents ion emission from pure tungsten; below 2000°K the tungsten filament is contaminated by barium which remains on it for an appreciable time.

9. *Preparation of Oxide-Coated Cathodes*

A considerable aura of mystery and superstition surrounds the technician who prepares oxide-coated cathodes. Innumerable patents have been taken out on methods for manufacturing cathodes whose activity is high, whose life is long, and whose coating sticks tightly to the base metal.

On a few basic facts there seems to be pretty general agreement. Barium and strontium oxides are considerably better emitters than calcium oxide, and barium oxide alone is better than strontium oxide alone. A mixture of approximately 50 percent barium oxide and 50 percent strontium oxide provides a coating with satisfactory mechanical properties and appears to give a slightly more copious emission than does barium oxide alone.

The metal in most general use as a base for the coating is nickel, which is usually chosen for its convenient physical properties and relatively low cost. Many alloys have been developed for particular purposes. One alloy particularly worthy of mention is known as "Konel." Because of a small inclusion of titanium, a speedy chemical reduction of the oxide takes place, and a copious supply of the free alkaline earth metal is available for activation.

Since (BaSrCa) oxides are not stable in ordinary air, but reduce to more complex compounds such as carbonates, nitrates, hydroxides, etc., it is necessary to coat the filament with one or more of these compounds and subsequently reduce it to the oxide by heating. The compounds most generally used at present are the carbonate and the hydroxide.

Carbonate coatings are made to adhere to the base metal of the filament by the use of an organic binder. A useful binder is made up of one part of Zapon varnish to 20 parts of amyl acetate. The powdered carbonate is suspended in this binder and the filament is coated by dipping in the suspension or by spraying. If a thick coat is desired, it is preferable to apply several thin coatings and heat them between applications sufficiently to burn out the binder.

Hydroxide coatings are applied by dipping in a bath of molten hydroxide. For tungsten filaments, this method is probably the most convenient of all and results in a particularly adherent coating.

The filament may now be heated in air to a high temperature to promote reaction of the coating with the base metal. If this is done, the filament is called a "combined filament" (Becker[8(1)]). Its final appearance will be dull and grayish. If the filament is mounted without this strenuous heat treatment, the coating will remain white and the filament is described as "uncombined."

The prepared filament is now mounted in the vacuum tube in which it is to be used. The tube is evacuated and kept on the pumps while the filament is heated to a temperature of about 1400°K to reduce the coating to oxide.

Unless some powerful reducing agent has been present, the filament will still be "unactivated." By this we mean that its electron emission at the working temperature of about 1000°K is still very low (probably of the order of a few microamp.). "Activation" may be carried out in a number of ways. In some cases prolonged heating will suffice. Usually, however, a potential of several hundred volts is applied to the anode of the tube and the activation process is accelerated. When the electron emission has reached a figure of about 300 ma/cm² for a temperature of 1100°K, there will be no further increase and the filament is ready for use.

The methods just described are those in most general use. Certain other methods are worthy of note. Many attempts, some successful, have been made to use barium azide (BaN_6). This compound decomposes at about 430°K with explosive violence and liberates Ba. The barium can be converted to oxide by admitting oxygen or by depositing the barium on an oxidized surface. A mixture of 25 percent BaO and 75 percent Al_2O_3 (Ramsay and Rooksby, British Patent No. 437967) or 25 percent BaO and 75 percent BeO (Cf. Benjamin and Jenkins[17]) is stable and has a lower melting point than either component. This substance has been used in the stocking cathodes developed by Hull.[17] Barium oxalate (BaC_2O_4) possesses certain advantages, since it reduces to oxide with evolution of CO as well as CO_2. The CO acts as a reducing agent and so is conducive to freeing the system from oxygen. Patai and his school at Budapest (Patai and Tomaschek[15]) have evolved a method of deposition of alkaline earth oxide from a colloidal suspension and obtain a somewhat smoother and more closely packed coating than is achieved with the spraying or dipping methods. For their cathodes they claim more stable electron emission characteristics though at a slightly lower level of emission than is expected of the standard cathode types. Benjamin, Huck, and Jenkins[17] also have developed methods for reducing particle size in the coating.

Previous reviews of this subject (cf. Statz,[6] Simon,[7] Hodgson, Harley, and Pratt,[8] Wagner,[9] etc.) describe many other methods for preparing oxide cathodes, all leading to essentially the same final product.

For use in gas-filled tubes, a cathode of fundamentally different design has been evolved by Hull.[7, 8] The cathode takes the form of a deep cavity, often divided into several cells. A convenient form consists of an internally coated cylinder open at one end and enclosing several coated radial vanes. This assembly is heated by an axial filament. The presence of gas permits large electron currents to escape through the open end while the straight line radiation of heat can be reduced to a minimum by coaxial radiation shields. Thus very high emission efficiencies may be attained.

The recently developed "dispenser cathode" (Hull[17, 18]) is an improved variation of this technique. In this case the emitting surface consists of a set of radial vanes surrounded by a cylindrical molybdenum heat shield. This surface is initially uncoated. The heater takes the form of a "stocking" of molybdenum mesh packed with the $BaO \cdot Al_2O_3$ eutectic mentioned above. When this stocking is heated by the passage of current, barium oxide evaporates in very small quantities onto the heat shield and the radial vanes to produce a very active emitting surface. The temperatures are adjusted by suitable heat shielding so that the small losses of barium oxide from the enclosure, through the apertures in the shield, are compensated by a continuous evaporation from the stocking. These cathodes emit currents of the order of amperes per square centimeter and have such long lives that continuous operation for three years still gives no indication of exhaustion.

10. The Activation Process

Our knowledge of the activation process can be summarized as follows: *Activation of an oxide cathode takes place when (BaSrCa) is liberated from the oxide by chemical reaction, by electrolysis, by positive ion bombardment, or by a combination of these mechanisms. This free metal is distributed throughout the body of the oxide and modifies its properties in such a way as to induce a large increase in electron emission from the outer surface.*

We now consider the evidence bearing on this statement.

(a) Liberation of Alkaline Earth Metal

When sufficiently violent thermal or electrical treatment is given to an oxide cathode, a dark metallic coating appears on the inside of the vacuum tube. When air or oxygen is admitted, this coating turns white and proves on chemical analysis to have been (BaSrCa).

In the presence of a large electron current drawn from an overheated barium oxide cathode, an apple-green glow discharge appears. The spectrum of this discharge shows the characteristic lines of barium (Detels,[6] Gehrts[9]).

A tungsten filament near a heated barium oxide cathode activates in exactly the same manner as it does in a stream of free barium (Becker[8(1)]).

The presence of free (BaSrCa) in the body of the cathode can be demonstrated by the chemical methods outlined in Section 8(a) above (Berdennikowa,[11] Clausing; cf. de Boer,[14] p. 348; Fritz,[14] Prescott and Morrison[17]). It is found that in an active cathode a fraction of the order of 0.5 percent of the oxide molecules has been reduced to free (BaSrCa).

(b) Activation Due to Free Alkaline Earth Metal

If an inactive oxide coated cathode is exposed to a stream of barium vapor it will become active. Its emission in the active state will be approximately the same as if it had been activated by one of the usual methods (Becker[8(1)]).

By heating to 1600°K, at which temperature free (BaSrCa) would be evaporated, leaving only the unreduced oxides, the activity is destroyed (Koller[5]).

A cathode can be deactivated by any gas which reacts with free (BaSrCa) to restore it to (BaSrCa)O.

(c) Mechanism of Reduction of Oxide

Four choices exist for the mechanism by which the alkaline earth metal responsible for activation can be set free. The first and most obvious suggestion that thermal dissociation plays a part can be ruled out by the calculations of Villars and Dushman (Dushman[9]) and Becker.[10] These authors showed that under the most favorable assumptions the dissociation pressure of BaO at 1000°K would be less than 10^{-40} atmosphere. Even in the best attainable vacuum this amount of free barium would be converted back to BaO so speedily that its presence would never be detected. For SrO and CaO the dissociation pressures would be even lower.

Three possible mechanisms remain for liberation of (BaSrCa); namely, chemical reaction with the core metal, electrolytic reduction by the passage of the emission current, and bombardment by positive ions of the residual gas. It is probable that all three of these mechanisms play a part in the activation process.

The first mechanism can be separated from the others by observing the rate of "thermal activation" of the cathode. The cathode is heated without application of anode voltage, and the activity is measured at a low temperature by applying anode voltage for a very short time. It is hoped by this method to reduce anode voltage effects to a minimum. This type of experiment results in the conclusion that almost all oxide cathodes can be activated thermally, provided a sufficient amount of heat is applied for a sufficiently long time. Platinum core filaments seem to require particularly vigorous treatment. Experiments performed in the laboratory of the General Electric Company by Mr. G. L. Tawney indicate that cathodes with spectroscopically pure (except for a trace of Cu) platinum cores cannot be activated thermally. Nickel core cathodes activate thermally with various degrees of ease, probably depending upon the amount of chemically active impurity present in the nickel. The inclusion of chemically active components in the core metal, as Ti in Konel filaments, results in speedy thermal activation at comparatively low temperatures (Lowry,[9] Benjamin[14]).

All combinations of (BaSrCa)O and core metal will react to a certain extent in an attempt to reach the equilibrium represented by

$$(\text{BaSrCa})\text{O} + \text{Metal} \rightleftarrows \text{Metal oxide} + (\text{BaSrCa}).$$

In most cases the equilibrium vapor pressure of (BaSrCa) will be very low. If it is much lower than the vapor pressure of (BaSrCa)O, it is evident that the coating will evaporate before

thermal activation is accomplished. However, we can safely say that part, at least, of the free (BaSrCa) necessary for activation is liberated by chemical reaction with the metal of the core.

In this connection it is as well to view organic binders with some suspicion. It is generally assumed that the binder evaporates without taking part in any reactions, but it is quite possible that a small amount of carbon remains to react with the oxide and forms carbide which may easily break down to liberate the free metal. When oxide cathode tubes are broken open in a damp atmosphere, an odor of acetylene is frequently noticed—satisfactory evidence that (BaSrCa) carbide was present.

To investigate the second and third possible mechanisms (electrolysis and positive ion bombardment), we observe the phenomenon known as "voltage activation." A positive potential is applied to the anode and the rate of increase of electron emission is noted. In general it is found that the rate of activation is markedly accelerated.

When an electron current is drawn to the anode, the direction of the current through the oxide is such as to deposit (BaSrCa) at the core and liberate oxygen at the surface. It has been shown in Section 4(a) that both types of electrolysis take place. The oxygen ion current becomes very small when the filament is activated, but a fraction of the order of 10^{-5} of the current continues to be carried by barium ions. The barium will be liberated at the core and must diffuse freely through the body of the oxide, since barium evaporation continues during the life of the cathode. Probably this mechanism is of particular importance in maintaining the supply of barium and hence the activity of the cathode during the later stages of its life.

The third possible mechanism—liberation of (BaSrCa) by positive ion bombardment—is difficult to isolate or to eliminate in considerations of other mechanisms. Even at pressures of 10^{-8} mm enough positive ions may be formed to dissociate an appreciable amount of oxide, provided the dissociation process is one of high efficiency.

The experiments discussed in Section 11(f), on the effect of positive ion bombardment on the activity of cathodes, show that this treatment must play a part, if possibly a minor one, in the activation process. Certain of the curves of Berdennikowa[11] are of interest in this connection. When gas was present and a glow discharge was in evidence, the graph of quantity of barium liberated per coulomb of charge passed against time showed an unusually high initial value. As the gas was removed, the rate of evolution decreased, finally attaining a constant value corresponding with Faraday's first law. Apparently the high initial rate of evolution was connected with the positive ion bombardment. No systematic study of the effect of positive ion bombardment has yet been made. Further discussion of this mechanism can be found in the papers of Koller,[5] MacNabb,[8] and Wagner.[9]

(d) Origin of Emitted Electrons; Distribution of Free (BaSrCa)

Prior to 1931 considerable controversy took place regarding the point of origin of the thermionic emission from oxide cathodes. Certain authors, reasoning from the discovery of barium in the core of aged cathodes (Lowry[9]), or from the shapes of observed oxide conductivity curves (Reimann and Murgoci[9]), concluded that the thermionic emission of oxide cathodes originated at the surface of the core. That this was incorrect was demonstrated by the conclusive experiments of Becker and Sears.[10] These authors observed that removal by a mechanical shock of the oxide coating of an active cathode resulted in a decrease of activity by a factor greater than 1000. If the core had been the original source of the emission, the activity should have increased, or at least remained constant. Becker and Sears were able also to vary the effective size of the core without affecting the area of the oxide surface. This they accomplished by imbedding a helical ribbon "probe" in the oxide. The emission of the cathode proved to be constant whether the probe, the core, or both, were maintained at cathode potential. As mentioned in Section 10(b), the same authors demonstrated that activation of a cathode by deposition of barium on the surface shows the same characteristics as activation by the usual methods. Huxford[10] measured the surface photoelectric work function during activation of an oxide cathode and found that it was the same as the thermionic work function. These four experiments are sufficient to permit us to con-

clude that the electron emission comes from the outer surface of the cathode.

The free alkaline earth metal, on the other hand, is not localized at the oxide surface. We know (Section 10(a)) that about 0.5 percent of the oxide of an active cathode has been reduced to free metal. This quantity of metal, if concentrated on the surface, would not only produce visible changes of a sort not observed, but also it would result in the electron emission characteristic of the pure metal. Moreover, reactions of the free metal with foreign gases (cf. Section 8(a)) require periods of minutes or hours to go to completion, which would not be the case if the free metal resided on the outer surface. These facts, coupled with the parallel variations of electrical conductivity and thermionic emission, lead to the conclusion that the major part of the free metal is dispersed through the body of the oxide. Presumably it is present in atomic inclusions which assist in supplying electrons both for conduction and thermionic emission. This is essentially the mechanism described by Becker and Sears and developed theoretically in Section 4(a).

The free metal distributed through the oxide will influence the emission equation (4.2) through the factors $N_1^{\frac{1}{2}}$ and $Q/2$. The other factors, namely D and φ, depend on the nature of the oxide surface. As will be discussed in the following section, the values of these quantities suggest the presence of a potential barrier at the oxide surface. This might be due to the presence of a monatomic layer of free metal over the oxide surface. At present the experimental data are insufficient to enable us to speculate further regarding the nature of the oxide surface or its changes during activation.

11. Electrical Properties of Oxide-Coated Cathodes

(a) Emission Constants

In Section 4(a) above we obtained the relation

$$i=10^{-6}DN_1^{1/2}T^{5/4} \times e^{-(1/kT)(\varphi+Q_1/2)} \text{ amp./sq. cm,} \quad (11.1)$$

which should be obeyed by the thermionic emission of an oxide-coated cathode. It has been customary in the past to fit oxide cathode emission data to the Richardson-Dushman relation (valid for metals):

$$i=AT^2e^{-\varphi_1/kT}. \quad (11.2)$$

An equally good straight line is obtained in a semilog plot whichever relation is used, because both relations are very insensitive to the first temperature factor. Work functions φ_1 deduced from the latter relation differ by only a few hundredths of a volt from the quantity $(\varphi+Q_1/2)$. Since the spread of experimental values is much wider than this, the values for work functions quoted in the literature will be accepted as they stand.

Work functions of oxide cathodes have been measured by a variety of methods. Many thermionic determinations are available (Koller,[5] Detels,[6] Espe,[6, 8] Becker,[8(1)] Kroczek and Lübcke,[9] Reimann and his collaborators,[9, 10] Kniepkampf and Nebel,[11] Maddock,[14] Patai and his collaborators,[14, 15] and many others). Calorimetric measurements of work functions involving measurement of the cooling effect due to electron emission have been made by Davisson and Germer,[4] Michel and Spanner,[5] Rothe,[5a] and Heinze.[12] Found[13] has devised a method for measuring the zero-field electron emission from a cathode and hence he determines the true values of the thermionic constants. His method involves supplying the cathode continuously with positive ions from the plasma of a gas discharge. Heinze and Wagener[17] deduce work functions from contact potential measurements. This method is better suited to studies of variations of the work function than to determinations of its absolute value. Huxford[10] has measured the photoelectric work function of an oxide cathode.

Before 1915 the values for the work functions of (BaSrCa) oxides were quoted as between three and four electron volts. With improved vacuum technique, much lower values were observed, and the latest work function determinations lie for the most part within about 0.3 electron volt of

1.1 ev for BaO
1.4 ev for SrO
1.9 ev for CaO.

If the cathode is incompletely activated, or if some impurity is present, higher values may be observed. Found's value of 1.96 ev for BaO is

attributable to the presence of the gas necessary for the discharge employed in his method. The calorimetric measurements of work function have yielded somewhat higher values than quoted above, but thermionic measurements checked the calorimetric values, so it is probable that the cathodes were not in the same state of activation as the best cathodes studied by the thermionic method.

Since A factors in the emission equation are very sensitive to variations of work function, it is preferable to characterize an oxide cathode by its work function and its emission at an operating temperature, say 1000°K. When this is done, the agreement between the results of various experimenters is seen to be much better than a tabulation of measured A factors would suggest. The measured emission at 1000°K is usually found to lie within a factor of 10 of

10. ma per sq. cm for BaO
1. ma per sq. cm for SrO
0.1 ma per sq. cm for CaO.

A general conflict of opinion exists regarding the behavior of the emission constants during activation. Espe[8] concludes that activation is due to an increase in the A factor while the work function remains constant. Heinze and Wagener[17] claim that activation follows from a decrease in work function alone. Others (e.g., Detels,[6] Huxford[10]) show that the work function and the A factor both decrease in such a way that log A is a more or less linear function of the work function (Fig. 10).

Since we do not know the value of the transmission coefficient D of Eq. (11.1), we cannot make a direct comparison of observed A factors with the theoretical value. From the work of Berdennikowa,[11] Clausing (cf. de Boer, reference 14, p. 348), Fritz,[14] and Prescott and Morrison,[17] we know that N_1 is about 0.5 percent of N_0, the total number of molecules per cc—i.e., N_1=approximately 10^{20}. For $N_1/N_0=0.7$ percent, Prescott and Morrison's electron emission curve can be represented by

$$i=5\times10^{2}T^{5/4}e^{-16500/T}.$$

Comparing with Eq. (11.1), we find $D=5\times10^{-2}$. This value is rather low when compared with the values of D of approximately unity observed for

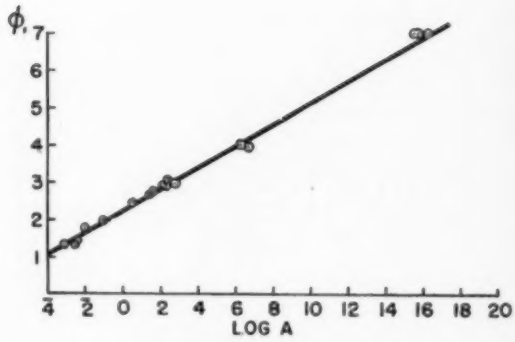

FIG. 10. Variation of log A with φ_1 (Detels, reference 6).

pure metals. It is, however, of the order of the values observed for contaminated metals (cf. Reimann, reference 13, p. 37). Even lower values than this are frequently found for D for oxide cathodes. For instance, the graph of oxide cathode emission of Fig. 1 (Dushman[9]) gives $D=4\times10^{-4}$, if we assume as before that $N_1=10^{20}$. Low transmission coefficients of this order are to be expected if the composite nature of the surface results in a surface potential barrier instead of a simple potential "step" of the sort shown in Fig. 6. This case has been dealt with theoretically by Fowler (reference 8, and Sec. 11.31 of *Statistical Mechanics*). He shows that the transmission coefficient will vary in an approximately exponential manner with the change in external work function as observed by Detels and Huxford. The slope of the log A *vs.* work function curve should have the value observed by Detels for a potential barrier a few angstroms in thickness.

The activation process may thus be broken down into two parts: first, an increase in the supply of conduction electrons as the supply of free alkaline earth metal "impurity" is increased; and, second, a decrease in external work function accompanied by the appearance of a surface potential barrier due to surface adsorption or to reorientation of the surface molecules. Depending on the initial state of the cathode and on the procedure by which the active impurities are produced, it should be possible to produce any desired type of variation of A factor or work function during activation. It is practically impossible to begin with a completely inactive cathode, since the procedures of outgassing and the mere passage of current suffice to initiate the activation process. Hence it is not surprising that

considerable disagreement is to be found in the literature on the behavior of the emission constants during activation.

(b) Anode Voltage Effect

Studies of emission constants of oxide cathodes are complicated still further because the emission current shows a marked reluctance to saturate as the anode voltage is increased (see Fig. 11). This phenomenon cannot be attributed to the presence of residual gases, because the anode current never rises above the $\frac{3}{2}$ power curve as it should if positive ions were present to neutralize part of the space charge. Probably the effect is partly attributable to heating of the oxide by the conduction current through the coating and the consequent increase in emission. A further contribution will be due to the roughness of the surface. Higher fields will penetrate hollows in the coating and draw electrons from regions protected at lower fields by space charge.

(c) Electron Temperature

The energy distribution of electrons emitted from an oxide cathode was first examined by Koller.[5] He plotted the log of the emission current for low retarding and accelerating plate voltages, against the voltage. The disturbing fact emerged that, although the line was straight, as though the electron distribution were apparently Maxwellian, the slope of the line corresponded to a temperature of 1760°K, while the cathode temperature was known to be only 1368°K. This effect was also noted by Rothe,[5a] who observed a series of electron temperatures, all about 1.6 times the known cathode temperature. An explanation has been advanced by Nottingham,[11, 15] who studied a similar effect for thoriated tungsten cathodes. Nottingham attributes the deficiency of slow electrons to an internal reflection of a type not observed for pure surfaces. He requires an internal reflection coefficient R of the form

$$R = e^{-E/C},$$

where E = electron energy and C is a constant. Evidently a reflection of this type will turn back more slow electrons than fast ones, and the temperature of the emitted electrons will apparently be decreased. Fowler's theory,[8] already discussed in Section 11(a), of reflection at a surface potential barrier leads also to a higher reflection coefficient for lower electron energies, but the variation with energy does not have precisely the form discussed by Nottingham.

(d) Shot Effect

The shot effect for oxide-coated cathodes has been studied over different frequency ranges by Johnson,[5] Kozanowski and Williams,[9] and others. Two types of abnormality appear in the results of these investigations. In the temperature limited range for frequencies below 5000 cycles the noise level is much higher than the simple theory of the shot effect would predict. This effect was studied in detail by Johnson. A theoretical discussion of the effect is given by Schottky,[5a] who agrees with Johnson in attributing it to fluctuations in the thermionic properties of the cathode surface. This interpretation inspired him to draw an analogy with fluctuating light sources and to name the abnormal behavior the "flicker effect." Schottky suggests that the fluctuations in emission correspond to appearance and disappearance of single atoms of active matter—presumably barium. From Johnson's curves he deduces that the total number of these atoms present in the surface at any time is about $\frac{1}{3}$ of all the atoms composing the surface. He estimates the average life of these adsorbed atoms to be about 0.001 second.

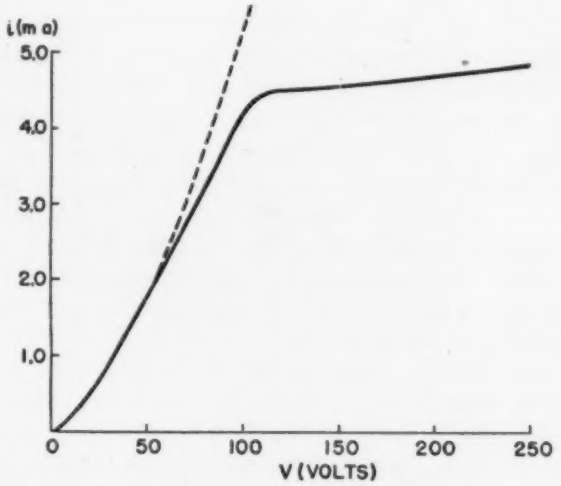

Fig. 11. Emission from an oxide cathode as a function of anode voltage (Blewett, reference 18).

The second type of abnormal shot effect is found when the current is space-charge limited. As the anode potential is increased through the space charge region, the noise level rises to a value considerably higher than the theoretical value, passes through a maximum and decays as the current becomes emission-limited, provided the frequency is high enough, to the theoretical value. Kozanowski and Williams attribute this effect to emission by the cathode of positive ions which are trapped in the minimum of potential due to the space charge. By virtue of its large mass and consequent low mobility, a single positive ion can release as many as several hundred electrons from space charge and so produce a comparatively large fluctuation in the anode current. This hypothesis is amply supported by the further experiments of Kozanowski and Williams in which they supplied positive ions from an external source to the space charge around a pure tungsten filament. The shot effect observed in this case behaved in much the same manner as did that of the oxide cathode.

The noise level due to shot effect in a commercial triode employing an oxide-coated cathode has been studied as a function of temperature by Szepesi.[18] He points out that a variety of effects contribute to make the shot noise increase rapidly if the cathode is operated above or below the temperature range 875–1050°K.

(e) Photoelectric Effect and Secondary Emission

At low temperatures the only sources of electrons for the photoelectric effect will be the filled band and the unexcited impurity energy levels (see Fig. 6, Part I). The photoelectric work function deduced from the long wave limit of the photoeffect should thus give the same value as the thermionic work function, namely $(\varphi+Q_1/2)$. This appears to be the case. Huxford[10] has measured the photoelectric and thermionic work functions of the same cathode and obtained the same value of about 1.3 ev.

At higher temperatures a new source of photoelectrons appears, since electrons are now excited in appreciable numbers to the conduction band. These electrons require only the energy φ to remove them from the oxide. As the temperature is raised, more electrons will be available in the conduction band, and the photoelectric current may be expected to increase. This explanation is advanced by Morgulis and Nagorsky[17] to account for the anomalous increase in photocurrent observed by Bodemann,[8] Newbury,[8] Newbury and Lemery,[11] and others.

The same increase with temperature has been observed by Morgulis and Nagorsky[17] for the secondary electron emission from oxide cathodes. These authors were successful in measuring the temperature dependence of the "anomalous" part of the secondary emission. A semilog plot of anomalous secondary emission against $1/T$ gave a good straight line whose slope corresponded to an energy of about 0.7 ev. If this emission is attributable to the increased number of electrons in the conduction band, we may conclude that $Q_1/2=0.7$ ev and $Q_1=1.4$ ev, in good agreement with the value of 1.6 ev deduced in Section 4(a) from the electrical conductivity.

(f) Time Effects

When emission-limited current is drawn from an active oxide-coated cathode, the emission decays rapidly at first, then slowly approaches a steady final value which may be less by a factor of ten or more than the initial current. At operating temperatures of commercial cathodes this decay takes place so rapidly as to be unobservable without special technique. For lower temperatures, however, the decay is slower, so that around 600°K it may require several hours to approach within 10 percent of its steady final value. This effect has been studied by Becker,[8(1)] Becker and Sears,[10] Kniepkamp and Nebel,[11] and Blewett.[18] Fig. 12 shows the emission from an oxide cathode at 880°K as a function of time after application of anode voltage. The right-hand part of the curve demonstrates the recovery of the emission when the cathode is glowed without drawing current.

It has been shown (Blewett[18]) that the effect depends on the emission current and not on the anode potential, indicating that it is a volume effect rather than a surface effect. Probably the decay is due either to electrolytic removal of barium from the surface or to electrolytic deposition of oxygen at the surface with consequent neutralization of the active surface layer of free barium. Becker, and Kniepkamp and Nebel

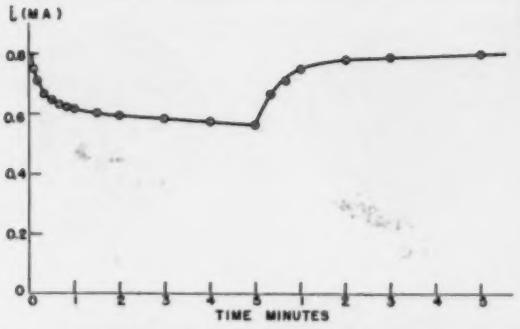

FIG. 12. Decay and recovery of emission from an oxide cathode (Blewett, reference 18). The first half of the curve shows the decay of emission when current is drawn; the second half, the recovery of the activity when the cathode is merely glowed without drawing current.

favor the latter viewpoint, since it is known that oxygen is evolved during this decay process. Becker has noted, however, that the evolution of oxygen is a surface phenomenon, depending on the anode potential. In the absence of further evidence it seems impossible to discriminate between the two alternatives. In either case the electrolytic current will set up a concentration gradient through the oxide. A back diffusion of atoms or ions will result, and the decay process will finally be complete when the two rates of transport become equal. The temperature dependence of the recovery process indicates that the heat of diffusion is about 17 kcal. (Blewett[18]).

The equilibrium between electrolysis and diffusion will be disturbed if the cathode temperature is varied, and the electron emission will drift gradually to a value corresponding to the new equilibrium state. An effect of this type has been observed by Davisson and Germer.[4]

It is evident that, in a tube employing an emission-limited oxide cathode, changes in electrode potentials or cathode temperature will result, in general, in more gradual changes in electron current. Since most commercial oxide cathodes are run space-charge limited, however, these effects are not often troublesome.

(g) Influence of Gases on Electron Emission

In the presence of active gases the emission from an oxide cathode may be found to undergo very radical changes. Of all ordinary gases yet tested, oxygen seems to be the most detrimental. At pressures as low as 10^{-4} mm, oxygen may decrease the emission of an oxide cathode by several powers of ten; a pressure of 10^{-3} is sufficient to poison it completely (Koller,[5] Reimann and Murgoci[9]). If the oxygen is removed, it may be possible to recover the emission by vigorous heating or by positive ion bombardment in an inert gas. Benjamin and Rooksby[12] note the fact that a BaO cathode poisoned by oxygen can always be reactivated, but a BaO+SrO cathode may be so affected by oxygen poisoning that reactivation is impossible.

Water vapor also is an effective poison for an oxide cathode (Koller[5]). Its behavior is qualitatively similar to that of oxygen.

According to Koller,[5] reducing gases such as CO and H_2 are beneficial. Arnold[3] claims that hydrogen is very beneficial and may restore a deactivated cathode. On the other hand, Reimann and Murgoci[9] assert that hydrogen is slightly detrimental to a fully activated cathode.

Neutral gases like CO_2 and N_2 effect small changes in emission. CO_2 is claimed by Arnold[3] to have a slight poisoning effect; by Koller[5] it is considered to be slightly beneficial; Prescott and Morrison[17] have shown that long exposure to CO_2 will completely deactivate a cathode; Reimann (reference 13, p. 203) states that nitrogen may be effective in restoring a deactivated cathode.

Argon was studied by Koller[5] and gave a slight improvement in emission.

Glowing in methane (Prescott and Morrison[17]) or in certain other organic vapors is so conducive to activation that sometimes no other activating procedure is necessary.

It seems probable, however, that no gas is capable of changing a cathode to a more active state than could be achieved by the best activation technique in high vacuum.

(h) Influence of Positive Ion Bombardment on Electron Emission

According to Koller,[5] bombardment by positive ions of CO_2 and other gases improves the emission from an oxide cathode. Reimann (reference 13, p. 203) has also observed this effect, but he asserts that continued bombardment by positive ions results eventually in deactivation. Hull[8] remarks on the detrimental effects of bombard-

ment by ions of mercury and the rare gases if the ion energy is greater than 20–25 volts.

The detrimental effects of continued or violent ion bombardment in rare gases may be attributed to sputtering away of an active surface layer of the cathode.

(i) Surface Distribution of Emission

Microscopic investigation of oxide cathodes shows that preparation by the usual procedures results in a rough and irregular surface. This causes thermal variations as well as local concentrations of electric field at the tops of the small peaks and ridges. If the coating is particularly rough, local heating may take place at points where high current is drawn, with consequent further increase in emission current. Probably this accounts for the bright spots which are often observed on the surface of a cathode delivering a heavy current (cf. Espe[6]).

When a comparatively smooth surface is achieved, however, a very spotty emission pattern can still be observed with the aid of the electron microscope. Fig. 13 (a and b), taken from the paper of Heinze and Wagener,[18] shows an optical microphotograph and an electron microphotograph of the same cathode, from which it is evident that there is no correlation between the surface irregularities and the regions of high emission. An exhaustive study of this phenomenon has recently been completed by Heinze and Wagener,[18] who demonstrate that the irregularities in surface distribution of emission are due mainly to the differences in work function between the individual crystal faces which happen to be exposed. They show that the faces of a barium oxide crystal may vary in work function by as much as 0.4 volt, so that the emission is due almost wholly to those crystallites which happen to be so oriented that surfaces of low work function are exposed.

A number of excellent electron microphotographs of oxide cathodes are to be found in the papers of Brüche and Johannson,[11] Richter,[12] Knecht,[13] Brüche,[14] Heinze and Wagener,[15, 18] Benjamin, Huck, and Jenkins,[17] and many others.

As can be seen from Fig. 13, it is possible to decrease the local variations in emission to the point of invisibility by special techniques of preparation. Fig. 13 (c and d) (Heinze and Wagener[18]) shows an optical microphotograph and an electron microphotograph of a cathode prepared by the colloidal deposition method of Patai and Tomaschek.[16]

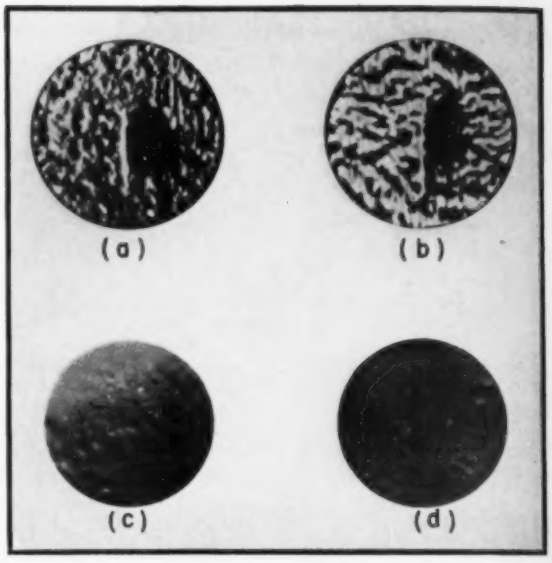

Fig. 13. Optical and electron microphotographs of oxide cathodes (Heinze and Wagener, references 15 and 18). (a) Optical microphotograph of ordinary oxide cathode. (b) Electron microphotograph of the cathode shown in (a). (c) Optical microphotograph of cathode prepared by the method of Patai and Tomaschek. (d) Electron microphotograph of the cathode shown in (c).

(j) Effect of Particle Size on Emission

The work of Benjamin, Huck, and Jenkins[17] indicates that the emission per watt input from BaSr oxide cathodes is increased as the particle size of the oxide is decreased. Although no continuous trend is evident from their results, it would appear that the emission is increased by a factor of about two as the particle size is decreased from 100μ to 3–7μ. Von Buzágh[15] has studied the emission from cathodes composed of colloidal particles and shows that the emission efficiency decreases as the particle size is decreased through the range of colloidal dimensions. There seems to be a value of particle size just below the upper limit of colloid size for which the efficiency is a maximum. In these experiments emission is measured for a fixed power input to the filament, so temperature variations may exist due to changes in surface emissivity. It is hence quite possible that there is no real variation either in

work function or A factor of the variously prepared cathodes.

(k) Decay of Emission

Any completely satisfactory theory of the activation process must be able to explain the fact that the emission from an oxide-coated cathode may decay to so low a value as to render the cathode useless long before the supply of oxide is exhausted. As far as visual observation can detect, the "dead" cathode may present the same appearance as it did while still active. In this state it is frequently impossible to restore the activity by any of the usual methods.

According to Clausing (de Boer, reference 14, p. 358), this decay is attributable to a decrease in the A factor of the emission equation. The work function seems to remain more or less constant. Apparently the supply of free (BaSrCa) is no longer available, so that $N_1^{\frac{1}{3}}$ of Eq. (4.2) has dropped to very low values.

This phenomenon is quite comprehensible for mixed oxide cathodes. For instance, in a BaO-SrO cathode, the BaO will evaporate preferentially out of the surface layers, leaving only the less active SrO (cf. Benjamin and Rooksby[12]). Many other explanations have been advanced to cover the decay phenomenon for other forms of oxide cathodes. Reimann and Murgoci[9] suggest that free oxygen and (BaSrCa) recombine throughout the coating and eventually fill the vacant pores. The coating eventually becomes so dense that free diffusion is impossible. If a chemical reaction with the core has been important in maintaining the supply of free (BaSrCa), it is possible that the supply of active impurities may become exhausted, or that a layer of oxide of the core metal is built up and separates the reacting components.

12. Conclusion

A large number of compounds have been tested as thermionic emitters (cf. Dushman[9]), but none have been found which are nearly as efficient as the oxides of the alkaline earths. It is probable that the emission from these substances cannot be increased by more than a factor of ten over what has been achieved already; nevertheless a great number of troublesome problems remain to be solved before oxide cathodes can be considered completely satisfactory and reproducible.

A major drawback in the experimental work in the past has been the lack of definition of the mechanical state of the oxide. Frequently measurements of volume properties must have been obscured by surface effects to a degree depending on the size of the individual single crystals. It is obvious that further progress must involve investigations of the properties of single crystals of the alkaline earth oxides. This mode of attack has been initiated by Heinze and Wagener[18] in their study of thermionic emission from the various crystal faces of small single crystals of barium oxide. There is little doubt that a complete study of the properties of single crystals of the alkaline earth oxides and an extension to coatings of known particle size and porosity will clear away most of the anomalies and contradictions which now obscure our understanding of oxide-coated cathodes.

13. Bibliography and Acknowledgments

A list is appended of about a hundred and twenty references. We believe this list to be fairly complete for the period since 1925. Earlier references can be traced through the review articles mentioned below. The parentheses after each paper are supposed to suggest the feature of the paper of particular interest in connection with oxide cathodes.

The writer wishes to acknowledge his indebtedness to Dr. A. W. Hull, Dr. S. Dushman, and his other colleagues in the laboratory for their helpful criticism and advice during the preparation of this paper.

Bibliography

1. *1904*

A. Wehnelt, Ann. d. Physik **14**, 425 (1904).

2. *1906*

F. Horton, Phil. Mag. **11**, 505 (1906). (Conductivity of CaO and BaO.)

3. *1920*

H. D. Arnold, Phys. Rev. **16**, 70 (1920). (Oxide cathode phenomena.)

C. Davisson and H. A. Pidgeon, Phys. Rev. **15**, 553 (1920). (Activation of tungsten filament in BaO vapor.)

3a. *1923*

J. W. Mellor, *Treatise on Inorganic Chemistry*, Vol. 3. p. 660.

4. *1924*

C. Davisson and L. H. Germer, Phys. Rev. **24**, 666 (1924). (Calorimetric determination of work function of oxide coated platinum.)

H. J. Spanner, Ann. d. Physik **75**, 609 (1924). (Conductivity and thermionic emission of BaO, SrO and CaO.)

5. *1925*

H. A. Barton, Phys. Rev. **26**, 360 (1925). (Negative oxygen ions from oxide cathodes.)

J. B. Johnson, Phys. Rev. **26**, 71 (1925). ("Flicker" effect for oxide cathodes, cf. W. Schottky, 1926.)

L. R. Koller, Phys. Rev. **25**, 671 (1925). (Electron emission from oxide cathodes.)

G. Michel and H. J. Spanner, Zeits. f. Physik **35**, 395 (1925). (Calometric determination of work function of BaO, SrO and CaO.)

5a. *1926*

M. S. Glass, Phys. Rev. **28**, 521 (1926). (Variation with temperature of the work function of oxide coated platinum.)

H. Rothe, Zeits. f. Physik **36**, 737 (1926). (Work function of oxide cathodes.) Zeits. f. Physik **37**, 414 (1926). (Electron temperatures for oxide cathodes.)

W. Schottky, Phys. Rev. **28**, 74 (1926). (Explanation of results of J. B. Johnson, 1925.)

E. E. Schumacher, J. Am. Chem. Soc. **48**, 396 (1926). (Melting points of CaO, SrO and BaO.)

6. *1927*

F. Detels, Zeits. f. Hochfrequenz. **30**, 10 and 52 (1927). (Formation processes in oxide cathodes.)

W. Espe, Wiss. Veröff. aus der. Siemens-Konzern **5** (III), 29 and 46 (1927). (Emission processes and thermionic constants of oxide cathodes.)

W. Statz, Zeits. f. tech. Physik **8**, 451 (1927). (Methods for preparing oxide cathodes.)

7. *1928*

J. M. Eglin, Phys. Rev. **31**, 1127 (1928) (Abstract). (Emission constants of oxide cathodes.)

A. W. Hull, Trans. A. I. E. E. **47**, 753 (1928). (Cavity type of cathode.)

W. Schottky and H. Rothe, *Handbuch der Experimental Physik* (1928), Vol. **13**, Pt. 2, pp. 215–232.

H. Simon, *Handbuch der Experimental Physik* (1928), Vol. **13**, Pt. 2, 305–314. (Review articles.)

M. de K. Thompson and W. G. Armstrong, Trans. Am. El. Chem. Soc. **54**, 85 (1928). (Vapor pressure of BaO.)

C. Zwikker, Physica **8**, 241 (1928) (in Flemish). (Vapor Pressure of BaO.)

8. *1929*

J. A. Becker (1) Phys. Rev. **34**, 1323 (1929). (Activation and emission of oxide cathodes.) (2) Trans. Am. El. Chem. Soc. **55**, 153 (1929). ("Life history of adsorbed atoms and ions.")

A. Bodemann, Ann. d. Physik **3**, 614 (1929). (Photoelectric effect for oxide cathodes.)

W. Espe, Zeits. f. tech. Physik **10**, 489 (1929). (Thermionic constants of oxide cathodes.)

R. H. Fowler, Proc. Roy. Soc. **122**, 36 (1929). (The thermionic constant A.)

B. Hodgson, L. S. Harley and O. S. Pratt, J. I. E. E. **67**, 762 (1929). (Preparation of oxide cathodes.)

A. W. Hull, Gen. Elec. Rev. **32**, 213 and 390 (1929). (Effect of positive ion bombardment of oxide cathodes.)

V. C. MacNabb, J. Opt. Soc. Am. and Rev. Sci. Inst. **19**, 33 (1929). (Activation of oxide cathodes.)

K. Newbury, Phys. Rev. **34**, 1418 (1929). (Photoelectric effect for oxide cathodes.)

9. *1930*

N. C. Beese, Phys. Rev. **36**, 1309 (1930). (Ba-Ni alloy core for oxide cathodes.)

S. Dushman, Rev. Mod. Phys. **2**, 381 (1930). (Review article; pp. 418–444 are on oxide cathodes.)

A. Gehrts, Zeits. f. tech. Physik **11**, 246 (1930). (Review article.)

H. N. Kozanowski and N. H. Williams, Phys. Rev. **36**, 1314 (1930). (Shot effect for oxide cathodes.)

J. Kroczek and E. Lübcke, Wiss. Veröff. aus der Siemens-Konz. **9** (II), 252 (1930). (Conductivity and emission of oxide cathodes.)

E. F. Lowry, Phys. Rev. **35**, 1367 (1930). (Role of core metal in oxide cathodes.)

A. L. Reimann and R. Murgoci, Phil. Mag. **9**, 440 (1930). (Emission and conductivity of oxide cathodes.)

E. R. Wagner, Electronics **1**, 178 (1930). (Preparation and activation of oxide cathodes.)

10. *1931*

W. Albricht, Physica **11**, 146 (1931) (in Flemish). (Relation between electron emission and conductivity of oxide during activation.)

J. A. Becker, Trans. Am. El. Chem. Soc. **59**, 207 (1931). (Conductivity of BaO+SrO.)

J. A. Becker and R. W. Sears, Phys. Rev. **38**, 2193 (1931). (The activation process in oxide cathodes.)

W. S. Huxford, Phys. Rev. **38**, 379 (1931). (Photoelectric emission from oxide cathodes.)

H. Nelson, Physics **1**, 84 (1931). (Properties of barium films on tungsten.)

K. Newbury and F. Lemery, J. Opt. Soc. Am. **21**, 276 (1931). (Photoelectric effect for oxide cathodes.)

A. L. Reimann and L. R. G. Treloar, Phil. Mag. **12**, 1073 (1931). (Emission and conductivity of oxide cathodes.)

N. H. Williams and W. S. Huxford, Phys. Rev. **37**, 463 (1931) (Abstract). (Conductivity of oxide coatings.)

11. *1932*

T. P. Berdennikowa, Physik. Zeits. der Sowjetunion **2**, 77 (1932). (Chemical determination of free barium in oxide cathodes.)

E. Brüche and H. Johannson, Naturwiss. **20**, 353 (1932); Ann. d. Physik **15**, 145 (1932). (Electron microscope study of oxide cathodes.)

A. Gehrts, Naturwiss **20**, 732 (1932). (Review article.)
H. Kniepkampf and C. Nebel, Wiss. Veröff aus der Siemens-Konzern **11** (II), 75 (1932). (Emission mechanism of oxide cathodes.)
W. Meyer and A. Schmidt, Zeits. f. tech. Physik **13**, 137 (1932). (Conductivity of BaO.)
W. B. Nottingham, Phys. Rev. **41**, 793 (1932). (Emission from composite surfaces.)

12. *1933*

M. Benjamin and H. P. Rooksby, Phil. Mag. **15**, 810 (1933); **16**, 519 (1933). (Emission and structure of oxide cathodes.)
W. G. Burgers, Zeits. f. Physik **80**, 352 (1933). (X-ray analyses of BaO+SrO cathodes.)
A. Claassen and C. F. Veenemans, Zeits. f. Physik **80**, 342 (1933). (Vapor pressures of BaO, SrO and CaO.)
P. Clausing and J. B. Ludwig, Physica **13**, 193 (1933). (Emissivity of oxide coatings.)
W. Heinze, Ann. d. Physik **16**, 41 (1933). (Calorimetric determination of work function for oxide cathodes.)
E. F. Richter, Zeits. f. Physik **86**, 697 (1933). (Electron microscope study of oxide cathodes.)
J. B. Taylor and I. Langmuir, Phys. Rev. **44**, 423 (1933). (Properties of cesium films on tungsten.)

13. *1934*

C. G. Found, Phys. Rev. **45**, 519 (1934). (Gas discharge methods for measuring work functions.)
W. Knecht, Ann. d. Physik **20**, 161 (1934). (Electron microscope pictures of oxide cathodes.)
L. Piatti, N. Cim. **11**, 77 (1934). (Review article.)
A. L. Reimann, *Thermionic Emission* (Wiley, 1934). (Chap. VI deals with oxide cathodes.)

14. *1935*

P. A. Anderson, Phys. Rev. **47**, 958 (1935). (Work function of barium, see Anderson, 1938.)
J. A. Becker, Rev. Mod. Phys. **7**, 95 (1935). (General review of thermionic emission.)
M. Benjamin, Phil. Mag. **20**, 1 (1935). (Influence of metallic impurities in the core of oxide cathodes.)
J. H. de Boer, *Electron Emission and Adsorption Phenomena* (Cambridge University Press, 1935). (Chapter XIV deals with oxide cathodes.)
E. Brüche, Zeits. f. Physik **98**, 77 (1935). (Electron microscope study of oxide cathodes.)
H. Fritz, Mikrochemie **17**, 191 (1935). (Microchemical determination of free barium in oxide cathodes.)
H. Gaertner, Phil. Mag. **19**, 82 (1935). (Electron diffraction in oxide cathodes.)
K. K. Kelley, Bulletins of the U. S. Dept. of the Interior, Bureau of Mines: Bulletin 383—*Vapor Pressures of Inorganic Substances;* Bulletin 394—*A Revision of the Entropies of Inorganic Substances.*
A. J. Maddock, Phil. Mag. **19**, 422 (1935). (Activation of oxide cathodes.)
E. Patai and G. Frank, Zeits. f. tech. Physik **16**, 254 (1935). (Emission constants of oxide cathodes.)
A. L. Reimann, Phil. Mag. **20**, 594 (1935). (Contact potential method for measuring work functions.)
E. Rudberg and J. Lempert, J. Chem. Phys. **3**, 627 (1935). (Vapor pressure of barium, cf. Van Liempt, 1936.)
W. Schottky, Naturwiss. **23**, 116 (1935). (Theory of semiconductors.)

15. *1936*

J. P. Blewett and E. J. Jones, Phys. Rev. **50**, 464 (1936). (Ion emission from heated salts.)
J. H. de Boer and E. J. W. Verwey, Rec. Trav. Chim. d. Pays-Bas **55**, 443 (1936). (Energy and structure of molecules of alkaline earth oxides.)
A. von Buzágh, Kolloid Zeits. **77**, 172 (1936). (Effect of particle size on emission from oxide cathodes.)
A. N. Guthrie, Phys. Rev. **49**, 868 (1936) (Abstract). (Surface ionization of barium on tungsten.)
W. Heinze and S. Wagener, Zeits. f. tech. Physik **17**, 645 (1936). (Surface distribution of emission from oxide cathodes.)
J. A. M. van Liempt, Rec. Trav. Chim. d. Pays-Bas **55**, 468 (1936). (Vapor pressure of barium).
G. Mönch, Ann. d. Physik **26**, 481 (1936). (Thermoelectric effect for Cu_2O, includes references to earlier work.)
W. B. Nottingham, Phys. Rev. **49**, 78 (1936). (Emission from composite surfaces.)
E. Patai and Z. Tomaschek, Kolloid Zeits. **74**, 253 (1936); **75**, 80 (1936). (Preparation of oxide coatings in colloidal form.)

16. *1937*

G. Herrmann, Zeits. f. physik. Chemie **35B**, 298 (1937). (Vapor pressure of BaO.)
H. Isensee, Zeits. f. physik. Chemie **35B**, 309 (1937). (Evolution of oxygen during activation of an oxide cathode.)
E. A. Lederer and D. H. Walmsley, RCA Review **2**, 117 (1937. (Reduction of BaO by Ta.)
M. Schriel, Zeits. f. Anorg. Allgem. Chemie **231**, 313 (1937). (Search for suboxide of barium.)

17. *1938*

P. A. Anderson, Phys. Rev. **54**, 753 (1938). (Contact potential difference between Ba and Mg.)
C. H. Bachman and C. W. Carnahan, Proc. I. R. E. **26**, 529 (1938). (Negative ion emission from oxide cathodes.)
M. Benjamin and R. O. Jenkins, Phil. Mag. **26**, 1049 (1938). (Migration of barium on tungsten and nickel.)
M. Benjamin, R. J. Huck and R. O. Jenkins, Proc. Phys. Soc. **50**, 345 (1938). (Influence of particle size on emission of oxide cathodes.)
J. P. Blewett, Phys. Rev. **53**, 935 (1938) (Abstract). (Chemical reactions of BaO.)
E. U. Condon, Phys. Rev. **54**, 1089 (1938). (External photoelectric effect for semi-conductors.)
J. A. Darbyshire, Proc. Phys. Soc. **50**, 635 (1938). (Electron diffraction in oxide cathodes.)
B. Gsaye and S. Wagener, Zeits. f. Physik **110**, 145 (1938). (Contact potentials between metals and dielectrics.)
W. Heinze and S. Wagener, Zeits. f. Physik **110**, 164 (1938). (Variation of emission constants of oxide cathodes during activation.)

W. Heinze and W. Hass, Zeits. f. tech. Physik **19**, 166 (1938). (Contact potential method for temperature measurement.)
A. W. Hull, Phys. Rev. **53**, 936 (1938) (Abstract). (A new type of oxide cathode; the "migration" cathode.)
J. E. Mayer and I. H. Wintner, J. Chem. Phys. **6**, 301 (1938). (Vapor pressures of alkali halides.)
N. Morgulis and A. Nagorsky, Tech. Phys. U. S. S. R. **5**, 848 (1938). (Secondary emission from oxide cathodes.)
C. H. Prescott and J. Morrison, J. Am. Chem. Soc. **60**, 3047 (1938). (Chemical measurement of free Ba in active cathodes.)
R. Suhrmann and C. Frühling, Naturwiss. **26**, 108 (1938) (Letter). (Emission from oxide cathodes.)

18. *1939*

J. P. Blewett, Phys. Rev. **55**, 713 (1939). (Decay of emission from oxide cathodes.)
J. P. Blewett, Rev. Sci. Inst. **10**, 231, (1939). (Vacuum balance.)
J. P. Blewett, H. A. Liebhafsky and E. F. Hennelly, J. Chem. Phys. **7**, 478 (1939). (Rate of evaporation of BaO.)
L. F. Broadway and A. F. Pearce, Proc. Phys. Soc. **51**, 335 (1939). (Negative ion emission from oxide cathodes.)
R. J. Cashman and E. Bassoe, Phys. Rev. **55**, 63 (1939). (Photoelectric properties of Ba.)
W. Heinze and S. Wagener, Zeits. f. tech. Physik **20**, 16 (1939). (Electron microscope study of oxide cathode emission.)
A. W. Hull, Phys. Rev. **55**, 1145 (1939) (Abstract); **56**, 86 (1939). (The "dispenser" cathode.)
C. H. Prescott and J. Morrison, Rev. Sci. Inst. **10**, 36 (1939). (Temperature scale for oxide cathodes.)
Z. Szepesi, Wireless Eng. **16**, 67 (1939). (Temperature variations in shot effect for oxide cathodes.)

Contributed Original Research

Matrix Theory of Oscillatory Networks

LOUIS A. PIPES
Graduate School of Engineering, Harvard University, Cambridge, Massachusetts
(Received April 26, 1939)

Starting with the energy functions of a general, linear, bilateral, resistanceless, lumped network the canonical equations of the circuit are obtained. These equations are solved in a general form taking into account applied electromotive forces and initial charges and currents by a matrix multiplication process. It is shown how the matrix multiplication process replaces the usual "frequency equation" which determines the normal modes of the system. Initial charges and currents in the various component parts of the network are considered for generality. The method given appears to have some computational advantages in certain classes of problems over the method of the "Heaviside calculus." The discussion is concluded with a discussion of normal coordinates and an illustrative numerical example is given. Since oscillatory networks are used extensively in communication engineering it is hoped that the present discussion will be of value. Since, if the circuit has a small amount of resistance present it may be shown that periods of oscillation are affected only by the squares of small quantities, it is seen that the method given is applicable to many technical problems. A method is given by which the attenuation due to the presence of small resistances in the system may be readily calculated.

INTRODUCTION

A GREAT deal has been written concerning the methods of solution of linear dynamical systems. As early as 1788 in the "Mecanique Analytique" of Lagrange[1] a method for the solution of the resulting systems of equations had been presented. The English physicists, Routh and Rayleigh further developed the subject and introduced methods of great power. The problem attracted the attention of Oliver Heaviside (1850–1925) and he further developed the subject by the development and application of his "Heaviside calculus" to the problem. Subsequent workers in the field such as Bromwich, Jeffreys, Carson, Van der Pol, and many others greatly extended the theory. In 1934 two English investigators, W. J. Duncan and A. R. Collar published a paper[2] that attacked the problem from an entirely different point of view. By the introduction of matrix algebra, a mathematical tool which plays such a prominent role in the new quantum mechanics, they were able to make a notable advance in the development of the subject. It is the purpose of this discussion to apply the methods of Duncan and Collar to the general problem of dissipationless electrical circuits and to make certain extensions and simplifications. By the application of this method problems of many degrees of freedom which present formidable computational difficulties when considered by conventional methods may be solved. A method which gives the solution of systems when there is a small amount of resistance present is presented. A knowledge of the fundamentals of matrix algebra such as that given in Section II of reference 3 will be assumed.

I. THE ENERGY FUNCTION

Consider a general, linear, lumped, dissipationless network consisting of n independent meshes or circuits. Let these meshes be numbered from 1 to n and let the corresponding mesh charges be the elements of the columnar matrix $\{q\}$ defined by:

$$\{q\} = \begin{Bmatrix} q_1 \\ q_2 \\ \cdot \\ q_n \end{Bmatrix}. \qquad (1)$$

[1] Lagrange, *Mecanique Analytique* (1788), Vol. 7, p. 390.
[2] W. J. Duncan, and A. R. Collar, "Matrices Applied to the Motions of Damped Systems," Phil. Mag. [7] **19**, 197 (1935).
[3] L. A. Pipes, "Matrices in Engineering," Elec. Eng. **56**, 1177–1190 (1937).

Let the elements of the square matrix $[L]$ defined by:

$$[L]=\begin{bmatrix} L_{11} & L_{12} & \cdots & L_{1n} \\ \cdot & \cdot & \cdot & \cdot \\ L_{n1} & L_{n2} & \cdots & L_{nn} \end{bmatrix} \tag{2}$$

be the total and mutual inductance coefficients of the meshes of the network. Since $L_{mn}=L_{nm}$ the matrix $[L]$ is symmetric.

Let the elements of the matrix $[S]$ defined by

$$[S]=\begin{bmatrix} S_{11} & \cdots & S_{1n} \\ \cdot & \cdot & \cdot \\ S_{n1} & \cdots & S_{nn} \end{bmatrix} \tag{3}$$

be the total and mutual elastance coefficients of the meshes of the network. Since $S_{mn}=S_{nm}$ the matrix $[S]$ is symmetric.

Let the elements of the matrix i defined by

$$\{i\}=\{\dot{q}\} \tag{4}$$

be the mesh currents of the network. We then have:

$$T=\frac{\{i\}'[L]\{i\}}{2}, \tag{5}$$

where T is a scalar quantity that represents the total instantaneous magnetic energy of the system and $\{i\}'$ is the transposed matrix of $\{i\}$.

If we let the scalar V represent the total instantaneous electric energy of the system we have:

$$V=\frac{\{q\}'[S]\{q\}}{2}, \tag{6}$$

where $\{q\}'$ is the transposed matrix of $\{q\}$. Since the quantities T and V represent the magnetic and electric energies of the system it is obvious from physical considerations that they are positive for all values of the elements of the matrices $\{q\}$ and $\{i\}$.

II. The Canonical Equations

If we let the elements of the columnar matrix e defined by:

$$\{e\}=\begin{Bmatrix} e_1 \\ \cdot \\ e_n \end{Bmatrix} \tag{7}$$

be the electromotive forces applied to the n meshes we may write the Lagrangian equations expressing the dynamic equilibrium of the system in the form:

$$(d/dt)(\partial T/\partial i_k)+\partial V/\partial q_k=e_k\ (k=1, 2, \cdots n). \tag{8}$$

Performing the indicated operations, we may write the system of Eqs. (8) in the form:

$$[L](\ddot{q})+[S](q)=\{(e)\}. \tag{8a}$$

These are the canonical equations of the general electric network devoid of resistance. Such a network is called an oscillatory network. The circuit containing resistance will be discussed in a later section.

Our general problem is to obtain the solution of the canonical Eqs. (8a) when we know the arbitrary electromotive forces impressed on the network and the initial charges and currents of the system at time $t=0$.

As a step toward the solution, let us assume that the charge matrix is the sum of two matrices given by:

$$(q)=(q)_t+(q)_s, \tag{9}$$

where we specify that the matrices $(q)_t$ and $(q)_s$ satisfy the following equations:

$$[L](\ddot{q})_t+[S](q)_t=(0), \tag{10}$$

$$[L](\ddot{q})_s+[S](q)_s=(e). \tag{11}$$

That is, the elements of $(q)_t$ are the various transient oscillations and $(q)_s$ has elements that represent the various forced or steady-state terms.

III. The Steady-State Solution

Let us assume that the various electromotive forces impressed on the meshes of the system are periodic. If the impressed electromotive forces are periodic functions of fundamental period T, they may be represented within certain restrictions on continuity in the complex Fourier series form

$$e_k(t)=\sum_{n=-\infty}^{n=+\infty} a_{kn}e^{jnwt}, \tag{12}$$

where

$$w=2\pi/T \tag{13}$$

and the coefficients a_{kn} are given by:

$$a_{kn}=\frac{w}{2\pi}\int_0^{2\pi/\omega} e_k(t)e^{-jnwt}dt. \tag{14}$$

If we introduce a column matrix $(a)_r$ defined by the equation:

$$(a)_r=\begin{Bmatrix} a_{1r} \\ \cdot \\ a_{nr} \end{Bmatrix}, \tag{15}$$

we may write the electromotive force matrix in the form:

$$(e)=\sum_{r=-\infty}^{r=+\infty}(a)_r e^{jrwt}. \tag{16}$$

We must now solve the Eq. (11) for the various steady-state mesh charges produced by the impression of the general electromotive force matrix (16). To obtain this solution let D represent the operator d/dt, we may then write (11) in the form:

$$([L]D^2+[S])(q)_s=(e). \tag{17}$$

Let us assume a solution of the form:

$$(q)_s=\sum_{r=-\infty}^{r=+\infty}(Q)_r e^{jrwt}, \tag{18}$$

where $(Q)_r$ is a matrix whose elements are amplitudes to be determined of the form:

$$(Q)_r=\begin{Bmatrix} Q_{1r} \\ Q_{2r} \\ \cdot \\ Q_{nr} \end{Bmatrix}. \tag{19}$$

Substituting (18) and (16) into (17) and performing the indicated differentiation, we obtain

$$\sum_{r=-\infty}^{r=+\infty}([L](-r^2w^2)+[S])(Q)_r e^{jrwt}=\sum_{r=-\infty}^{r=+\infty}(a)_r e^{jrwt}. \tag{20}$$

Equating coefficients of like harmonic terms, we have:

$$([L](-r^2w^2)+[S])(Q)_r=(a)_r. \tag{21}$$

Letting

$$[f(jwr)]=[S]-r^2w^2[L], \tag{22}$$

$$|\Delta(jwr)|=|f(jwr)| \tag{23}$$

and $[F(jwr)]$ be the adjoint matrix of the matrix $[f(jwr)]$ defined by the relation

$$[f(jwr)][F(jwr)]=\Delta(jwr)I, \tag{24}$$

where I is the unit matrix of the nth order, we have:

$$(Q)_r=[F(jwr)](a)_r/\Delta(jwr) \tag{25}$$

for the amplitude matrix of the rth harmonic. Substituting this into (18) we have the steady-state solution for the general periodic electromotive forces (16)

$$(q)_s=\sum_{r=-\infty}^{+\infty}\frac{[F(jwr)](a)_r e^{jwrt}}{\Delta(jwr)}. \tag{26}$$

This solution fails for the exceptional case $\Delta(jwr)=0$. This occurs when one of the impressed electromotive forces has a component frequency that is a resonant frequency of the system. By a limiting process, the steady state for a component voltage for which $\Delta(jws)=0$ is found to be:

$$\frac{e^{jwst}}{\Delta'(jws)}([F(jws)]'+t[F(jws)])(a)_s, \tag{27}$$

where

$$\Delta'(jws)=\frac{d}{d(jws)}(jws), \tag{28}$$

$$[F(jws)]'=\frac{d}{d(jws)}[F(jws)]. \tag{29}$$

IV. Transient Solution

Having obtained the steady-state solution for a general class of electromotive forces, we turn now to a discussion of the free or transient oscillations of the network. These oscillations are governed by the equation:

$$[L](\ddot{q})_t+[S](q)_t=(0). \tag{30}$$

To solve this equation let us assume the solution:

$$(q)_t=e^{jwt}(k), \tag{31}$$

where e^{jwt} is a scalar multiplier and (k) is a columnar matrix of n constants to be determined. Substituting (31) into (30) we obtain on dividing out the scalar e^{jwt} factor, the following equation:

$$(-w^2[L]+[S])(k)=(0). \tag{32}$$

If we premultiply both sides of (32) by $[S]^{-1}$ the inverse of the elastance matrix, we obtain

$$(-w^2[S]^{-1}[L]+I)(k)=(0), \tag{33}$$

where I is the unit matrix of the nth order. If we let

$$w^2=1/m \quad \text{and} \tag{34}$$

$$[u]=[S]^{-1}[L], \tag{35}$$

then (33) becomes:

$$(mI-[u])(k)=(0). \tag{36}$$

The square matrix of the nth order $[u]$ will be called the "dynamical matrix." Eq. (36) may be written in the following form:

$$[u](k)=m(k). \tag{37}$$

Premultiplying the equation by $[u]$ we obtain:

$$[u]^2(k)=m[u](k)=m^2(k). \tag{38}$$

By repeating this procedure, it may be shown that

$$[u]^s(k)=m^s(k) \tag{39}$$

for s a positive or negative integer.

Now in order for the linear Eqs. (36) to be consistent, we must have:

$$|mI-[u]|=0. \tag{40}$$

This determinantal equation will, in general, have n distinct real roots m_j. These are the latent roots of the dynamical matrix $[u]$. Every latent root m_j has associated with it a columnar matrix (k_j). These columnar matrices satisfy n equations of the form:

$$[u]^s(k_j)=m_j{}^s(k_j) \qquad (j=1, 2, \cdots n), \tag{41}$$

where s is a positive or negative integer. This set of matrix equations may be written in the form:

$$[u]^s[(k_1)(k_2)\cdots(k_n)] = [m_1{}^s(k_1)m_2{}^s(k_2)\cdots m_n{}^s(k_n)], \tag{42}$$

where the square matrices of both members of (42) are partitioned matrices formed from the (k_j) columns as indicated. If we introduce the square matrix $[k]$ defined by the equation

$$[k]=[(k_1)(k_2)\cdots(k_n)], \tag{43}$$

we may write (42) in the form

$$[u]^s[k]=[k]\begin{bmatrix} m_1{}^s & 0 & \cdots & 0 \\ 0 & m_2{}^s & \cdots & 0 \\ \cdot & \cdot & \cdot & \cdot \\ 0 & \cdot & \cdot & m_n{}^s \end{bmatrix}. \tag{44}$$

The matrix $[k]$ will be called the modal matrix; if the latent roots m_j are distinct, the modal matrix has an inverse and by post multiplying (44) by $[k]^{-1}$ we obtain:

$$[u]^s=[k]\begin{bmatrix} m_1{}^s & 0 & 0 & 0 & \cdots & 0 \\ 0 & m_2{}^s & 0 & 0 & \cdots & 0 \\ \cdot & \cdot & \cdot & \cdot & \cdot & \cdot \\ 0 & 0 & 0 & 0 & \cdots & m_n{}^s \end{bmatrix}[k]^{-1}. \tag{45}$$

Let us place

$$[A]=[k]^{-1}. \tag{46}$$

Then, by direct multiplication, we obtain:

$$[u]^s=\sum_{r=1}^{n} m_r{}^s[u_r], \tag{47}$$

where

$$[u]_r=\begin{bmatrix} k_{1r}A_{r1} & k_{1r}A_{r2} & \cdots & k_{1r}A_{rn} \\ k_{2r}A_{r1} & k_{2r}A_{r2} & \cdots & k_{2r}A_{rn} \\ \cdot & \cdot & \cdot & \cdot \\ k_{nr}A_{r1} & k_{nr}A_{r2} & \cdots & k_{nr}A_{rn} \end{bmatrix}. \tag{48}$$

For convenience, let the latent roots be arranged in order of decreasing magnitude. We then have

$$|m_1|>|m_2|\cdots>|m_n|. \tag{49}$$

Then when s is a large positive integer, only the terms corresponding to the dominant root need be retained in (47). We have, therefore, for s sufficiently large:

$$\lim_{s\to\infty}[u]^s=m_1{}^s\begin{bmatrix} k_{11}A_{11} & k_{11}A_{12} & \cdots & k_{11}A_{1n} \\ k_{21}A_{11} & k_{21}A_{12} & \cdots & k_{21}A_{1n} \\ \cdot & \cdot & \cdot & \cdot \\ k_{n1}A_{11} & k_{n1}A_{12} & \cdots & k_{n1}A_{1n} \end{bmatrix}. \tag{50}$$

If we premultiply Eq. (45) by $[k]^{-1}$ we obtain:

$$[k]^{-1}[u]^s=\begin{bmatrix} m_1{}^s & 0 & \cdots & 0 \\ 0 & m_2{}^s & \cdots & 0 \\ \cdot & \cdot & \cdot & \cdot \\ 0 & & & m_n{}^s \end{bmatrix}[k]^{-1}. \tag{51}$$

Placing $s=1$ and $[k]^{-1}=[A]$ we have:

$$[A][u]=\begin{bmatrix} m_1 & 0 & \cdots & 0 \\ 0 & m_2 & \cdots & 0 \\ \cdot & \cdot & \cdot & \cdot \\ 0 & \cdots & \cdots & m_n \end{bmatrix}[A]. \quad (52)$$

If we now consider the matrix $[A]$ to be partitioned into n rows as shown

$$[A]=\begin{bmatrix} A_{11} & A_{12} & \cdots & A_{1n} \\ A_{21} & A_{22} & \cdots & A_{2n} \\ \cdot & \cdot & \cdot & \cdot \\ A_{n1} & A_{n2} & \cdots & A_{nn} \end{bmatrix} \quad (53)$$

and let

$$[A_r]=[A_{r1}A_{r2}\cdots A_{rn}], \quad (54)$$

then, by virtue of (52) we have the relation:

$$[A_r][u]=m_r[A_r] \quad (r=1, 2, \cdots n). \quad (55)$$

It will now be shown how it is possible to obtain a row proportional to $[A_r]$ from the column (k_r) in a simple manner.

If we substitute $[u]=[S]^{-1}[L]$ in the set of Eqs. (41) we obtain

$$m_r(k_r)=[S]^{-1}[L](k_r) \quad (r=1, 2, \cdots n). \quad (56)$$

Now if we remultiply (56) by $[L]$, we obtain:

$$m_r[L](k_r)=[L][S]^{-1}[L](k_r). \quad (57)$$

If we take the transpose of both sides of this Eq. (57) and make use of the reversal law for transposed products, we obtain:

$$m_r(k_r)'[L]'=(k_r)'[L]'[S]^{-1'}[L]'. \quad (58)$$

Since the square matrices $[L]$ and $[S]$ are symmetric, we obtain:

$$m_r(k_r)'[L]=(k_r)'[L][u]. \quad (59)$$

Considering Eqs. (55) and (59) it is seen that we must have

$$[A_r]=a_r(k_r)'[L], \quad (60)$$

where a_r is a constant. The relation (60) is most useful in obtaining the transient solution, as will be shown. Since $[A]=[k]^{-1}$, we have:

$$[A_r](k_s)=\begin{cases} 0 & \text{if} \quad r\neq s \\ 1 & \text{if} \quad r=s. \end{cases} \quad (61)$$

Hence:

$$(k_r)'[L](k_s)=0 \quad r\neq s. \quad (62)$$

This expresses the orthogonal properties of the modal columns.

After the above digression into the theory of modal columns, let us continue our solution of the Eq. (30). The problem has resolved itself into finding the latent roots of the dynamical matrix. These are related to the natural frequencies of the system by the Eq. (34). We must also determine the various modal columns (k_r), associated with the various natural frequencies. It is in the numerical simplicity of these operations that the matrix method has distinct advantages.

V. Determination of the Fundamental Frequency

We shall now consider a procedure which will yield the fundamental natural frequency of the system. Let us select an *arbitrary* columnar matrix $(x)_0$ and form the following sequence.

$$\begin{aligned} [u](x)_0&=(x)_1 \\ [u](x)_1&=[u]^2(x)_0=(x)_2 \\ &\cdot \quad \cdot \quad \cdot \quad \cdot \quad \cdot \quad \cdot \quad \cdot \quad \cdot \\ [u](x)_{s-1}&=[u]^s(x)_0=(x)_s. \end{aligned} \quad (63)$$

Then, in view of Eq. (50), we have, for a sufficiently large s,

$$[u]^s(x)_0=[u]^s\begin{Bmatrix} x_{10} \\ \cdot \\ x_{n0} \end{Bmatrix}=m_1{}^s\begin{Bmatrix} k_{11}R_1 \\ \cdot \quad \cdot \\ k_{n1}R_1 \end{Bmatrix}, \quad (64)$$

where $R_1=A_{11}x_{10}+A_{12}x_{20}+--+A_{1n}x_{n0}$ and we see that for a sufficiently large s in the sequence (63), we have the relations

$$x_{js}/x_{rs}=k_{j1}/k_{r1}, \quad (65)$$

$$m_1=x_{j,\,s+1}/x_{j,\,s}. \quad (66)$$

From the relations (65) and (66) we determine the slowest natural frequency given by

$$w_1=1/(m_1)^{\frac{1}{2}} \quad (67)$$

and the modal column (k_1). The row matrix $[A_1]$ is given by

$$[A_1]=a_1(k_1)'[L], \quad (68)$$

where a_1 is an arbitrary constant.

VI. Completion of the Solution

Having determined the fundamental frequency w_1 and the modal column (k_1) we must now proceed to a determination of the overtones

and the modal columns associated with the overtones. In terms of the modal columns (k_1) the solution of the Eq. (30) may be written in the following form:

$$(q)_t=\sum_{r=1}^{n}(k_r)(B_r\sin(w_rt)/w_r+D_r\cos(w_rt)), \quad (69)$$

where (k_r) is the modal column of the rth mode and B_r and D_r are arbitrary constants associated with the rth mode and to be determined from the initial boundary conditions. Let us premultiply (69) by the line matrix $[A_s]$; then in view of the relation (61) we obtain:

$$[A_s](q)_t=B_s\sin(w_st)/w_s+D_s\cos(w_st). \quad (70)$$

Then if the mode corresponding to w_s is absent,

$$[A_s](q)_t=0. \quad (71)$$

In particular, if the dominant mode w_1 is absent, the coordinates must satisfy the homogeneous linear scalar equation:

$$[A_1](q)_t=0. \quad (72)$$

Now, after the sequence (63) has been formed, (k_1) is determined and $[A_1]$ is given by (68).

Expanding Eq. (71) we obtain:

$$A_{11}q_{1t}+A_{12}q_{2t}+\cdots+A_{1n}q_{nt}=0. \quad (73)$$

If we solve for q_{1T} in (73) we have:

$$q_{1t}=-A_{12}q_{2t}/A_{11} -A_{13}q_3t/A_{11}\cdots-A_{1n}q_{nt}/A_{11}. \quad (74)$$

Accordingly, when the fundamental mode is absent, we have

$$\begin{Bmatrix}q_{1t}\\q_{2t}\\\cdot\\q_{nt}\end{Bmatrix} =\begin{bmatrix}0&-A_{12}/A_{11}&-A_{13}/A_{11}&\cdots&A_{1n}/A_{11}\\0&1&0&\cdots&0\\\cdot&\cdot&\cdot&\cdot&\cdot\\0&0&0&\cdots&1\end{bmatrix} \times\begin{Bmatrix}q_{1t}\\q_{2t}\\\cdot\\q_{nt}\end{Bmatrix}. \quad (75)$$

Now, if we substitute (75) for the right member of Eq. (37), we obtain:

$$m(q)_T=[u]_1(q)_T, \quad (76)$$

where

$$[u]_1=[u]\begin{bmatrix}0&-A_{12}/A_{11}&\cdots&-A_{1n}/A_{11}\\0&1&\cdots&0\\\cdot&\cdot&\cdot&\cdot\\0&0&\cdots&1\end{bmatrix}. \quad (77)$$

Now $[u]_1$ is the dynamical matrix for a system whose fundamental mode is m_2. A sequence similar to that of (63) is now set up. This new sequence gives us the first overtone w_2 and the second modal column (k_2). From the second modal column we obtain

$$[A_2]=(k_2)'[L]. \quad (78)$$

A condition that insures that the overtone w_2 is absent is

$$[A_2](q)_t=0. \quad (79)$$

This equation combined with Eq. (72) enables us to obtain a matrix $[u]_2$ which is the dynamical matrix of a system having both lowest frequencies w_1 and w_2 absent. Continuing this process, we obtain the n angular frequencies w_j and the n modal columns (k_r). The Eq. (60) enables us to find the n modal rows $[A_r]$. From the modal columns and rows, we may construct the matrices $[k]$ and $[A]$ which, as we shall see, enable us to evaluate the arbitrary constants.

VII. Evaluation of the Arbitrary Constants

From Eq. (9) we have:

$$(q)=(q)_t+(q)_s. \quad (9)$$

Suppose the system has the n initial mesh charges at $t=0$ denoted by the matrix,

$$(q^0)=\begin{Bmatrix}q_1{}^0\\q_2{}^0\\\cdot\\q_n{}^0\end{Bmatrix} \quad (80)$$

and the n initial mesh currents at $t=0$ denoted by the matrix

$$(i^0)=\begin{Bmatrix}i_1{}^0\\i_2{}^0\\\cdot\\i_n{}^0\end{Bmatrix}. \quad (81)$$

Then we have from (9)

$$(q^0)_t=(q^0)-(q^0)_s, \tag{82}$$

$$(i^0)_t=(i^0)-(i^0)_s, \tag{83}$$

where $(q^0)_t$ and $(i^0)_t$ are the transient charges and currents at $t=0$. Placing $t=0$ in Eq. (69), we obtain:

$$(q^0)_t=\sum_{r=1}^{n}(k_r)D_r. \tag{84}$$

This may be written in the matrix form:

$$(q^0)_t=\begin{bmatrix} k_{11} & k_{12} & \cdots & k_{1n} \\ k_{21} & k_{22} & \cdots & k_{2n} \\ \cdot & \cdot & \cdots & \cdot \\ k_{n1} & k_{n2} & \cdots & k_{nn} \end{bmatrix}\begin{Bmatrix} D_1 \\ D_2 \\ \cdot \\ D_n \end{Bmatrix}. \tag{85}$$

If we introduce the columnar matrix of arbitrary constants defined by

$$(D)=\begin{Bmatrix} D_1 \\ D_2 \\ \cdot \\ D_n \end{Bmatrix}, \tag{86}$$

then in view of (43), we may write Eq. (85) in the form

$$(q^0)_t=[k](D), \tag{87}$$

$$(D)=[k]^{-1}(q^0)_t=[A](q^0)_t. \tag{88}$$

Similarly, from (69), we obtain

$$(i^0)_t=(q^0)_t=\sum_{r=1}^{n}(k_r)B_r \tag{89}$$

and if we introduce a columnar matrix of arbitrary constants (B) defined by

$$(B)=\begin{Bmatrix} B_1 \\ B_2 \\ \cdot \\ B_n \end{Bmatrix}, \tag{90}$$

we have

$$(B)=[A](i^0)_t. \tag{91}$$

From this it is seen that we have the $2n$ arbitrary constants $(D_1\cdots D_n)$, $(B_1\cdots B_n)$ determined by the Eqs. (88) and (91).

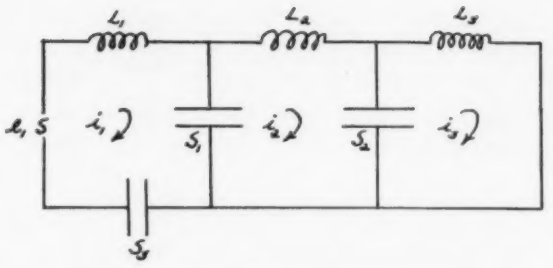

FIG. 1.

VIII. NORMAL COORDINATES

Equation (69) may be written in the matrix form

$$\begin{aligned}(q)_t=&[k]\\ &\times\begin{bmatrix} \sin(w_1t)/w_1 & 0 & \cdots & 0 \\ 0 & \sin(w_2t)/w_2 & \cdots & 0 \\ \cdot & \cdot & \cdots & \cdot \\ 0 & 0 & \cdots & \sin(w_nt)/w_n \end{bmatrix}\\ &\times\begin{Bmatrix} B_1 \\ B_2 \\ \cdot \\ B_n \end{Bmatrix}+[k]\\ &\times\begin{bmatrix} \cos(w_1t) & 0 & \cdots & 0 \\ 0 & \cos(w_2t) & \cdots & 0 \\ \cdot & \cdot & \cdots & \cdot \\ 0 & 0 & \cdots & \cos(w_nt) \end{bmatrix}\begin{Bmatrix} D_1 \\ D_2 \\ \cdot \\ D_n \end{Bmatrix}. \end{aligned} \tag{92}$$

If we introduce the coordinates Q defined by:

$$(Q)=[k]^{-1}(q)_t=[A](q)_t, \tag{93}$$

then, the Eq. (92) on premultiplication by $[k]^{-1}$ reduces to:

$$\begin{aligned}(Q)=&\begin{bmatrix} \sin(w_1t)/w_1 & 0 & \cdots & 0 \\ 0 & \sin(w_2t)/w_2 & \cdots & 0 \\ \cdot & \cdot & \cdots & \cdot \\ 0 & \cdots & \cdots & \sin(w_nt)/w_n \end{bmatrix}(B)\\ &+\begin{bmatrix} \cos(w_1t) & 0 & \cdots & 0 \\ 0 & \cos(w_2t) & \cdots & 0 \\ \cdot & \cdot & \cdots & \cdot \\ 0 & 0 & \cdots & \cos(w_nt) \end{bmatrix}(D). \end{aligned} \tag{94}$$

By multiplication, we have the general relations:

$$(Q_r)=\sin(w_rt)B_r/w_r+\cos(w_rt)D_r \qquad (r=1, 2, \cdots n), \tag{95}$$

that is, the motion of any normal coordinate such as Q_s is independent of the motion of any of the other normal coordinates Q_r. The motions of the several normal coordinates Q_r is thus seen to be uncoupled.

IX. Illustrative Example

To illustrate the above general theory, let us consider the circuit of Fig. 1. Let

$$L_1=L_2=L_3=1 \text{ henry.}$$
$$S_1=\tfrac{1}{3}\times 10^6 \text{ darafs.}$$
$$S_2=\tfrac{1}{6}\times 10^6 \text{ darafs.}$$
$$S_3=\tfrac{1}{2}\times 10^6 \text{ darafs.}$$

The inductance and elastance matrices are therefore given by the equations

$$[L]=\begin{bmatrix}1&0&0\\0&1&0\\0&0&1\end{bmatrix} \quad [S]=\begin{bmatrix}\frac{5}{6}&-\frac{1}{3}&0\\-\frac{1}{3}&\frac{1}{2}&-\frac{1}{6}\\0&-\frac{1}{6}&\frac{1}{6}\end{bmatrix}10^{-6}. \tag{96}$$

The dynamical matrix is, therefore,

$$[u]=[S]^{-1}[L]=10^{-6}\begin{bmatrix}2&2&2\\2&5&5\\2&5&11\end{bmatrix}\begin{bmatrix}1&0&0\\0&1&0\\0&0&1\end{bmatrix}, \tag{97}$$

$$[u]=10^{-6}\begin{bmatrix}2&2&2\\2&5&5\\2&5&11\end{bmatrix}.$$

Determination of natural frequencies

Substituting the above value of $[u]$ into (37) gives

$$10^{-6}\begin{bmatrix}2&2&2\\2&5&5\\2&5&11\end{bmatrix}(k)=m(k). \tag{98}$$

If we let

$$\bar{m}=10^6 m, \tag{99}$$

the numerical factor 10^{-6} is absorbed and we have:

$$\begin{bmatrix}2&2&2\\2&5&5\\2&5&11\end{bmatrix}(k)=\bar{m}(k). \tag{100}$$

The natural frequencies are given by the equation

$$w_r=10^3/\sqrt{\bar{m}_r}. \tag{101}$$

To determine the fundamental frequency, let us form the sequence (63). As our arbitrary vector (x_0) let us choose:

$$(x)_0=\begin{Bmatrix}1\\1\\1\end{Bmatrix}. \tag{102}$$

We then begin the sequence:

$$[u](x)_0=\begin{bmatrix}2&2&2\\2&5&5\\2&5&11\end{bmatrix}\begin{Bmatrix}1\\1\\1\end{Bmatrix}=\begin{Bmatrix}6\\12\\18\end{Bmatrix}=18\begin{Bmatrix}.3\\.6\\1\end{Bmatrix}. \tag{103}$$

Now, it is unnecessary to carry the common factor 18 in the further operations since it is the *ratios* of successive elements in the multiplications that are important.

Dropping the factor 18 and continuing, we have:

$$\begin{bmatrix}2&2&2\\2&5&5\\2&5&11\end{bmatrix}\begin{Bmatrix}.3\\.6\\1\end{Bmatrix}=\begin{Bmatrix}4\\9\\15\end{Bmatrix}=15\begin{Bmatrix}.26\\.6\\1\end{Bmatrix} \tag{104}$$

and, after repeating the multiplication 9 times, we obtain

$$\begin{bmatrix}2&2&2\\2&5&5\\2&5&11\end{bmatrix}\begin{Bmatrix}0.254885\\0.584225\\1\end{Bmatrix}=14.43\begin{Bmatrix}0.254885\\0.584225\\1\end{Bmatrix}. \tag{105}$$

Repeating the process farther only multiplies the columnar matrix by the same factor 14.43. Accordingly, we need not go any farther in the sequence. We then have:

$$\bar{m}_1=14.43 \tag{106}$$

and the fundamental angular frequency is

$$w_1=10^3/(14.43)^{\frac{1}{2}}=263. \tag{107}$$

The fundamental frequency is:

$$f_1=w_1/2=41.9 \text{ cycles/sec.} \tag{108}$$

The fundamental modal column may be taken to be:

$$(k_1)=\begin{Bmatrix}0.254885\\0.584225\\1\end{Bmatrix}. \tag{109}$$

The row $[A_1]$ to an arbitrary constant, is given by Eq. (68). If we let the arbitrary constant $a_1=1$. We do not lose the orthogonal properties (61) so that we may take

$$\begin{aligned}[A_1]&=[(0.254885)(0.584225)1][L]\\&=[(0.254885)(0.584225)1].\end{aligned} \tag{110}$$

Now by (72) in any oscillation from which the fundamental mode is absent, we must have:

$$[A_1](q)_t = 0.254885q_{1t} + 0.584225q_{2t} + q_{3t} = 0 \quad (111)$$

or

$$q_{1t} = -2.29211q_{2t} - 3.92334q_{3t}.$$

In this case, Eq. (75) becomes:

$$\begin{Bmatrix} q_{1t} \\ q_{2t} \\ q_{3t} \end{Bmatrix} = \begin{bmatrix} 0 & -2.29211 & -3.92334 \\ 0 & 1 & 0 \\ 0 & 0 & 1 \end{bmatrix} \begin{Bmatrix} q_{1t} \\ q_{2t} \\ q_{3t} \end{Bmatrix}. \quad (112)$$

The matrix (77) is now given by

$$[u]_1 = \begin{bmatrix} 2 & 2 & 2 \\ 2 & 5 & 5 \\ 2 & 5 & 11 \end{bmatrix} \begin{bmatrix} 0 & -2.29211 & -3.92334 \\ 0 & 1 & 0 \\ 0 & 0 & 1 \end{bmatrix} = \begin{bmatrix} 0 & -2.58422 & -5.84668 \\ 0 & .41578 & -2.84668 \\ 0 & .41578 & 3.15332 \end{bmatrix}. \quad (113)$$

This is the dynamical matrix for a system whose fundamental mode is $\bar{m}_2$

We again set up a sequence similar to that of (63). We again choose the arbitrary vector (102). It is unnecessary to compute the leading element of any column since this is always multiplied by 0 in the succeeding step. We thus find

$$[u]_1 \begin{Bmatrix} 1 \\ 1 \\ 1 \end{Bmatrix} = \begin{Bmatrix} \cdot & \cdot & \cdot \\ -2.4309 \\ 3.5691 \end{Bmatrix} = 3.5691 \begin{Bmatrix} \cdot & \cdot & \cdot \\ -0.68110 \\ 1 \end{Bmatrix}, \quad (114)$$

$$[u]_1 \begin{Bmatrix} \cdot & \cdot & \cdot \\ -0.68110 \\ 1 \end{Bmatrix} = \begin{Bmatrix} \cdot & \cdot & \cdot \\ -3.1299 \\ 2.8701 \end{Bmatrix} = 2.8701 \begin{Bmatrix} \cdot & \cdot & \cdot & \cdot \\ -1.09049 \\ 1 \end{Bmatrix}. \quad (115)$$

After fifteen approximations, the column repeats itself, the scalar multiple is

$$\bar{m}_2 = 2.6152. \quad (116)$$

The modal column (k_2) is then given by:

$$(k_2) = \begin{Bmatrix} -0.95670 \\ -1.29429 \\ 1 \end{Bmatrix}. \quad (117)$$

The angular frequency of the first overtone is given by:

$$w_2 = 10^3/(2.6152)^{\frac{1}{2}} = 618. \quad (118)$$

The natural frequency of the first overtone is:

$$f_2 = w_2/2\pi = 98.4 \text{ cycles/sec.} \quad (119)$$

The row $[A_2]$ is now given by (60) to an arbitrary constant placing this constant equal to 1, we may take

$$[A_2] = (k_2)'[L] = [(-0.95670)(-1.29429)1]. \quad (120)$$

The necessary condition that the first overtone be absent from the motion is

$$[A_2](q)_t = -0.95670q_{1t} - 1.29429q_{2t} + q_{3t} = 0 \quad (121)$$

or

$$q_{1t} = -1.35287q_{2t} + 1.04526q_{3t}. \quad (122)$$

Equation (111) gives the necessary condition: that the fundamental mode be absent from the motion. Hence eliminating q_{1T} between equations (111) and (122) gives

$$0 = 0.93924q_{2t} + 4.96860q_{3t} \quad (123)$$

or

$$q_{2t} = -5.2900q_{3t}. \quad (124)$$

Hence for a motion that has the fundamental and first overtone absent, we have:

$$\begin{Bmatrix} q_{1t} \\ q_{2t} \\ q_{3t} \end{Bmatrix} = \begin{bmatrix} 1 & 0 & 0 \\ 0 & 0 & -5.290 \\ 0 & 0 & 1 \end{bmatrix} \cdot \begin{Bmatrix} q_{1t} \\ q_{2t} \\ q_{3t} \end{Bmatrix}. \quad (125)$$

Now, in terms of the matrix $[u]_1$ as given by (113), we have Eq. (76) in the form:

$$\bar{m}(q)_t = [u]_1(q)_t. \quad (76)$$

Substituting the relation $(q)_T$ as given by (125) into the right side of (76) gives

$$\bar{m} \begin{Bmatrix} q_{1t} \\ q_{2t} \\ q_{3t} \end{Bmatrix} = [u]_1 \begin{bmatrix} 1 & 0 & 0 \\ 0 & 0 & -5.290 \\ 0 & 0 & 1 \end{bmatrix} \begin{Bmatrix} q_{1t} \\ q_{2t} \\ q_{3t} \end{Bmatrix}. \quad (126)$$

Let us define $[u]_2$ by the following equation:

$$[u]_2 = [u]_1 \begin{bmatrix} 1 & 0 & 0 \\ 0 & 0 & -5.2900 \\ 0 & 0 & 1 \end{bmatrix} \quad (127)$$

or

$$[u]_2 = \begin{bmatrix} 0 & 0 & 7.8238 \\ 0 & 0 & -5.0461 \\ 0 & 0 & 0.9539 \end{bmatrix}.$$

The matrix $[u]_2$ is the dynamical matrix of a system having the fundamental w_1 and the first

overtone w_2 absent. Setting up the sequence (63) as before, we have

$$[u]_2\,(x)_0=\begin{bmatrix}0&0&7.8238\\0&0&-5.0461\\0&0&0.9539\end{bmatrix}\begin{Bmatrix}1\\1\\1\end{Bmatrix}$$

$$=\begin{Bmatrix}7.8238\\-5.0461\\0.9539\end{Bmatrix}=.9539\begin{Bmatrix}8.2019\\-5.2900\\1\end{Bmatrix}. \quad (128)$$

Discarding the factor 0.9539 and repeating the process, we have:

$$[u]_2^2(x)_0=.9539\begin{Bmatrix}8.2019\\-5.290\\1\end{Bmatrix}. \quad (129)$$

Since the vector repeats itself it is not necessary to go further, and we have directly

$$\bar{m}_3=0.9539. \quad (130)$$

The angular frequency of the first overtone w_3 is given by:

$$w_3=10^3/(\bar{m}_3)^{\frac{1}{2}}=1025. \quad (131)$$

The highest natural frequency of the system, is, therefore:

$$f_3=w_3/2\pi=163 \text{ cycles/second}. \quad (132)$$

The third modal column may be taken to be

$$(k_3)=\begin{Bmatrix}8.2019\\-5.2900\\1\end{Bmatrix}. \quad (133)$$

The row $[A_3]$ may be taken to be:

$$[A_3]=[(8.2019)(-5.2900)1]. \quad (134)$$

From (109), (117) and (133) we may construct the modal matrix

$$[k]=\begin{bmatrix}(0.254885)&(-0.95670)&(8.2019)\\(.584225)&(-1.29429)&(-.52900)\\1&1&1\end{bmatrix}. \quad (135)$$

And from (110), (120) and (134) we may form the matrix $[A]$ given by:

$$[A]=\begin{bmatrix}(0.254885)&(0.584225)&1\\(-.95670&(-1.29429)&1\\(8.2019)&(-5.2900)&1\end{bmatrix}. \quad (136)$$

In this particular example since $[L]=[I]$ the unit matrix of the third order, the matrix $[A]$ may be taken to be $[k]'$.

Completion of the solution

The steady-state solution for arbitrary periodic electromotive forces is given by the methods of Section III. Let the steady-state solution be $(q)_s$, then, we have the solution:

$$(q)_t=\sum_{r=1}^{3}(k_r)(B_r\sin(w_rt)/w_r+D_r\cos(w_rt)), \quad (69)$$

where if (q^0) and (i^0) are columnar matrices whose elements are the initial charges and currents, we have:

$$\begin{Bmatrix}D_1\\D_2\\D_3\end{Bmatrix}=[A]((q^0)-(q^0)_s), \quad (137)$$

$$\begin{Bmatrix}B_1\\B_2\\B_3\end{Bmatrix}=[A]((i^0)-(i^0)_s) \quad (138)$$

from (88) and (91).

Since we know $[A]$, $[k]_r$ and the various angular frequencies, the arbitrary constants are easily evaluated by (137) and (138) and the solution is complete. The solution is then given by (9). The ease by which the natural frequencies and modal columns are obtained is apparent from this example.

X. Effect of Small Resistance Terms

Thus far in our discussion, we have neglected the effect of resistances that may be present in the general network. As soon as resistance enters into the problem, and in actual cases it always does, the work necessary to obtain the solution increases considerably. In practice, however, it happens quite frequently that although resistances are present, they are very small and cause only a relatively slow attenuation. Practically every network used in communication theory comes under this category.

It appears logical, therefore, to extend the theory to the slightly damped case. The method here presented will illustrate how the effect of a small amount of dissipation may be taken into account.

XI. The Potential Function

In order to obtain the transient solution of the slightly damped case, let us introduce the following functions.

$$A=(q)_t'[L](q)_t/2, \tag{139}$$

$$B=(q)_t'[R](q)_t/2, \tag{140}$$

$$C=(q)_t'[S](q)_t/2, \tag{141}$$

where $[R]$ is a square matrix whose elements are the self and mutual mesh resistances of the circuit. The scalar functions A, B, and C may be called the potentials of the magnetic forces, the resistance forces, and the electric forces.

In terms of these potential functions, the canonical equations of the free or transient oscillations are:

$$\frac{d^2}{dt^2}(\partial A/\partial q_{kt})+\frac{d}{dt}(\partial B/\partial q_{kt})+\partial C/\partial q_{kt}=0 \qquad (k=1, 2, \cdots -n) \tag{142}$$

or
$$[L](\ddot{q})_t+[R](\dot{q})_t+[S](q)_t=(0). \tag{143}$$

Let us assume the solution:

$$(q)_t=\sum_{r=1}^{2n}(x_r)e^{m_r t} \tag{144}$$

for the set (143), where (x_r) are the various modal columns and m_r the several modes.

Substituting (144) into (143), we obtain:

$$m_r^2[L](x_r)+m_r[R](x_r)+[S](x_r)=(0) \qquad (r=1, 2, \cdots 2n) \tag{145}$$

for the various amplitudes (x_r) of the several modes m_r.

If we premultiply (145) by $(x_r)'$ the transposed matrix of (x_r) we obtain the following scalar equations:

$$m_r^2(x_r)'[L](x_r)+m_r(x_r)'[R](x_r)+(x_r)'[S](x_r)=0 \quad (r=1, 2, \cdots 2n). \tag{146}$$

Comparing the three members of the equation with the potential function (131), (140), and (141), let us introduce the following potential functions for the several modes x_r:

$$A_r=(x_r)'[L](x_r)/2, \tag{147}$$

$$B_r=(x_r)'[R](x_r)/2, \tag{148}$$

$$C_r=(x_r)'[S](x_r)/2. \tag{149}$$

In terms of these potentials, the scalar Eqs. (146) become

$$m_r^2A_r+m_rB_r+C_r=0 \quad (r=1, 2, \cdots 2n). \tag{150}$$

Solving for the modes m_r, we have:

$$m_r=-B_r/2A_r\pm(B_r^2/4A_r^2-C_r/A_r)^{\frac{1}{2}}. \tag{151}$$

Now if the network has no resistance, we have:

$$B_r=0, \tag{152}$$

$$m_r=\pm jC_r/A_r \tag{153}$$

and we have a solution of the type (69) where

$$w_r=(C_r/A_r)^{\frac{1}{2}}. \tag{154}$$

Now, in the case of small damping we have

$$C_r/A_r\gg(B_r/2A_r)^2 \quad (r=1, 2, \cdots 2n), \tag{155}$$

so that
$$m_r=-B_r/2A_r\pm j(C_r/A_r)^{\frac{1}{2}}. \tag{156}$$

In this case, the motion is only slightly perturbed from the undamped case and the solution (69) must be modified to

$$(q)_t=\sum_{r=1}^{n}(k_r)e^{-\alpha_r t}\{B\sin(w_r t)/w_r+D\cos(w_r t),\} \tag{157}$$

where
$$\alpha_r=-B_r/2A_r \tag{158}$$

is the attenuation constant and the natural frequencies w_r and amplitudes may be calculated as before, since if the relation (155) is satisfied the frequencies and amplitudes of the undamped system differ from those of the damped system by quantities of higher order.

XII. Computation of the Attenuation Constants

We have seen that if the relation (155) is satisfied so that the frequencies of the system may be computed by neglecting the resistance terms, then the solution for the damped case given by (157) differs from that of the undamped case (69) by the presence of the attenuation constants (157). These are given by (158). The modal columns (x_r) may be taken proportional to the modal column (k_r). Substituting these into (158) we have:

$$\alpha_r=-(k_r)'[R](k_r)/2(k_r)'[L](k_r). \tag{159}$$

The procedure to be followed in the transient solution of the oscillatory network is first to neglect the resistance matrix $[R]$ and to obtain the natural frequencies w_r and the modal matrices (k_r) by the methods of the first part of this paper.

Then if the relation (155) which may be written in the form

$$(k_r)'[S](k_r)/(k_r)'[L](k_r) \gg ((k_r)'[R](k_r)/2(k_r)'[L](k_r))^2 \quad (160)$$

is satisfied the solution is given by (157) and the various attenuation constants are obtained from (159) by direct matrix multiplication. The rest of the solution proceeds as before.

XIII. Conclusion

The simplicity and power of the iterative matrix method of solution for the transient and steady-state behavior of oscillatory circuits is evident from the above discussion. If the amount of resistance is small as it is in many practical circuits this method of solution is most simple and direct. It is hoped that this presentation will give an impetus to the use of the method in dealing with this type of circuit.

Increase of Torsional Stiffness of a Prismatical Bar Due to Axial Tension*

M. A. Biot
Columbia University, New York, New York
(Received March 22, 1939)

The author's theory of elasticity of the second order is being applied to calculate the increase of torsional stiffness of a prismatical bar when an axial tension is initially imposed upon it. It is found that the classical shear stress distribution is not affected by the axial stress. However, an increase of torsional stiffness is produced due to the fact that the boundary condition over the cross section contains not only the shearing stress but also the product of the axial stress by the rotations. This increase of torsional stiffness turns out to be proportional to the polar moment of inertia of the cross section with respect to its center of gravity.

BEFORE treating the special problem of torsion of a bar under an initial axial stress we shall first summarize the results of the general theory of elasticity for the small deformations of a body under initial stress.[1]

We denote by

$$\begin{matrix} S_{11} & S_{12} & S_{13} \\ S_{21} & S_{22} & S_{23} \\ S_{31} & S_{32} & S_{33}, \end{matrix} \quad (1)$$

the initial state of stress in an elastic body. These components of stress are symmetric $S_{\mu\nu}=S_{\nu\mu}$ and they must satisfy the equilibrium conditions

$$\begin{aligned} \partial S_{11}/\partial x+\partial S_{12}/\partial y+\partial S_{13}/\partial z&=0, \\ \partial S_{21}/\partial x+\partial S_{22}/\partial y+\partial S_{23}/\partial z&=0, \\ \partial S_{31}/\partial x+\partial S_{32}/\partial y+\partial S_{33}/\partial z&=0. \end{aligned} \quad (2)$$

We now assume that the material undergoes a small deformation. The deformation is associated with displacements of components uvw, rotations of components,

$$\begin{aligned} \omega_x&=\tfrac{1}{2}(\partial w/\partial y-\partial v/\partial z), \\ \omega_y&=\tfrac{1}{2}(\partial u/\partial z-\partial w/\partial x), \\ \omega_z&=\tfrac{1}{2}(\partial v/\partial x-\partial u/\partial y) \end{aligned} \quad (3)$$

and strain components

$$\begin{aligned} e_{11}&=\partial u/\partial x, \quad e_{12}=e_{21}=\tfrac{1}{2}(\partial v/\partial x+\partial u/\partial y), \\ e_{22}&=\partial v/\partial y, \quad e_{23}=e_{32}=\tfrac{1}{2}(\partial w/\partial y+\partial v/\partial z), \\ e_{33}&=\partial w/\partial z, \quad e_{31}=e_{13}=\tfrac{1}{2}(\partial u/\partial z+\partial w/\partial x). \end{aligned} \quad (4)$$

Because of the small deformation the initial

* Publication assisted by the Ernest Kempton Adams Fund for Physical Research of Columbia University.

[1] M. A. Biot, "Non-Linear theory of elasticity and the linearized case for a body under initial stress," Phil. Mag. **27**, 468 (1939). Also: "Theory of elasticity with large displacements and rotations," Proc. Fifth International Congress for Applied Mechanics (Cambridge, U. S. A. 1938). "Theorie de l'elasticité du second ordre," Ann. Soc. Sci. de Bruxelles (1939).

stresses are modified. We denote the stress increments by:

$$\begin{matrix} s_{11} & s_{12} & s_{13} \\ s_{21} & s_{22} & s_{23} \\ s_{31} & s_{32} & s_{33}. \end{matrix} \tag{5}$$

These symmetric stress components $s_{\mu\nu}=s_{\nu\mu}$ are referred to axes which rotate locally with the material so that they are only functions of the strain. They must satisfy equilibrium conditions which will be different from the classical equations for a material initially in a free unstressed condition.

Equations expressing these conditions rigorously have been derived in the general theory. For example, one of these equations expressing equilibrium conditions in the x-direction reads

$$\begin{aligned} &\frac{\partial s_{11}}{\partial x}+\frac{\partial s_{12}}{\partial y}+\frac{\partial s_{13}}{\partial z}+(S_{11}-S_{22})\frac{\partial \omega_z}{\partial y}-2S_{12}\frac{\partial \omega_z}{\partial x} \\ &+S_{12}\frac{\partial \omega_z}{\partial z}-(S_{11}-S_{33})\frac{\partial \omega_y}{\partial z}-2S_{13}\frac{\partial \omega_y}{\partial x} \\ &-S_{13}\frac{\partial \omega_z}{dy}+S_{23}\left(\frac{\partial \omega_y}{\partial y}-\frac{\partial \omega_z}{\partial z}\right)+\frac{\partial S_{11}}{\partial x}(e_{22}+e_{33}) \\ &+\frac{\partial S_{12}}{\partial y}(e_{33}+e_{11})+\frac{\partial S_{13}}{\partial z}(e_{11}+e_{22}) \\ &-\left(\frac{\partial S_{12}}{\partial x}+\frac{\partial S_{11}}{\partial y}\right)e_{12}-\left(\frac{\partial S_{13}}{\partial y}+\frac{\partial S_{12}}{\partial z}\right)e_{23} \\ &-\left(\frac{\partial S_{11}}{\partial z}+\frac{\partial S_{12}}{\partial x}\right)e_{31}=0. \end{aligned} \tag{6}$$

We have two other similar equations. The boundary conditions can be expressed by means of the increment of force per unit area at the boundary. For example, the x-component of this boundary force increment is

$$\begin{aligned} \Delta f_x=&s_{11}\alpha+s_{12}\beta+s_{13}\gamma+[S_{13}\omega_y-S_{12}\omega_z]\alpha \\ &+[S_{23}\omega_y-S_{22}\omega_z]\beta+[S_{33}\omega_y-S_{23}\omega_z]\gamma \\ &+S_{11}[e_{22}+e_{33}]\alpha+S_{12}[e_{33}+e_{11}]\beta \\ &+S_{31}[e_{11}+e_{22}]\gamma-(S_{12}e_{12}+S_{13}e_{13})\alpha \\ &-(S_{12}e_{23}+S_{11}e_{21})\beta-(S_{11}e_{31}+S_{12}e_{32})\gamma. \end{aligned} \tag{7}$$

In these relations $\alpha\beta\gamma$ are the directional cosines of the normal direction to the boundary before deformation.

In the particular problem that we have here in mind, the torsion of a prismatical part submitted to an axial tension, the above equations are very much simplified. Taking the z axis along the axis of the bar, the initial stresses are (Fig. 1)

$$\begin{matrix} 0 & 0 & 0 \\ 0 & 0 & 0 \\ 0 & 0 & S_{33}, \end{matrix} \tag{8}$$

where $S_{33}=S$ is a constant representing the initial axial tension. The equilibrium equations become

$$\begin{aligned} &\frac{\partial s_{11}}{\partial x}+\frac{\partial s_{12}}{\partial y}+\frac{\partial s_{13}}{\partial z}+S\frac{\partial \omega_y}{\partial z}=0, \\ &\frac{\partial s_{21}}{\partial x}+\frac{\partial s_{22}}{\partial y}+\frac{\partial s_{23}}{\partial z}-S\frac{\partial \omega_x}{\partial z}=0, \\ &\frac{\partial s_{31}}{\partial x}+\frac{\partial s_{32}}{\partial y}+\frac{\partial s_{33}}{\partial z}+S\left(\frac{\partial \omega_y}{\partial x}-\frac{\partial \omega_x}{\partial y}\right)=0 \end{aligned} \tag{9}$$

and the boundary conditions

$$\begin{aligned} \Delta f_x&=s_{11}\alpha+s_{12}\beta+s_{13}\gamma+S\omega_y\gamma, \\ \Delta f_y&=s_{21}\alpha+s_{22}\beta+s_{23}\gamma-S\omega_x\gamma, \\ \Delta f_z&=s_{31}\alpha+s_{32}\beta+s_{33}\gamma+S(e_{11}+e_{22})\gamma \\ &\quad -Se_{13}\alpha-Se_{23}\beta. \end{aligned} \tag{10}$$

No approximations have been introduced in the above equations except the basic one that, the displacements are small. We shall now con-

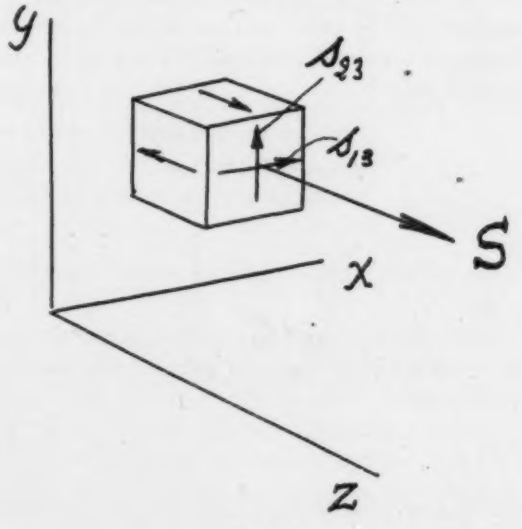

FIG. 1.

sider the relation between the strain and the stress increments $s_{\mu\nu}$. Here of course we have to introduce some approximations and simplifying assumptions as we do not know what these relations are for a material under an initial stress. However we will assume that these relations are the same as for the material in its natural unstressed state and if we assume this state to be isotropic, we may write

$$\begin{aligned} Ee_{11} &= s_{11} - \nu(s_{22}+s_{33}), \\ Ee_{22} &= s_{22} - \nu(s_{11}+s_{33}), \\ Ee_{33} &= s_{33} - \nu(s_{22}+s_{11}), \\ 2Ge_{12} &= s_{12}, \\ 2Ge_{23} &= s_{23}, \\ 2Ge_{31} &= s_{31}. \end{aligned} \tag{11}$$

That this is an approximation is obvious first for a theoretical reason. It was shown by the author[1] that the stress-strain law (11) is in contradiction with the existence of a potential energy and that the error is of the order S/E. Moreover a material which in its natural state is isotropic cannot remain such when it is stretched so that an isotropic stress-strain relation is also an approximation. Again here the error must be of the order S/E.

Keeping these remarks in mind we may solve the problem of torsion by means of Eqs. (9), (11) and the boundary conditions (10). We are going to show that the classical stress distribution of Saint Venant for the torsion of a prismatical bar is also a solution of our problem for the distribution of stress increments $s_{\mu\nu}$. The difference with the classical solution will appear only on the boundary of the cross section in the form of an increase in torsional stiffness. We put as in Saint Venant's solution

$$\begin{aligned} &s_{11}=s_{22}=s_{33}=s_{12}=0 \\ &u=-\theta yz \\ &v=\theta xz \\ &w=w(x,\,y). \end{aligned} \tag{12}$$

We also assume that s_{23} and s_{31} are only functions of x and y.

We deduce $e_{11}=e_{22}=e_{33}=e_{12}=0$, hence the first four relations (11) are satisfied and the two last ones become

$$\begin{aligned} G(\partial w/\partial y+\theta x) &= s_{23} \\ G(-\theta y+\partial w/\partial x) &= s_{31}. \end{aligned} \tag{13}$$

The two first equilibrium Eqs. (9) are also satisfied because

$$\omega_x = w(\partial\omega/\partial y-\theta x), \quad \omega_y = \tfrac{1}{2}(-\theta y-\partial w/\partial x) \tag{14}$$

do not depend on z. The third Eq. (9) becomes

$$\frac{\partial s_{31}}{\partial x}+\frac{\partial s_{32}}{\partial y}-S\left(\frac{\partial^2 w}{\partial x^2}+\frac{\partial^2 w}{\partial y^2}\right)=0. \tag{15}$$

Now from Eq. (13) we deduce

$$G\left(\frac{\partial^2 w}{\partial x^2}+\frac{\partial^2 w}{\partial y^2}\right)=\frac{\partial s_{31}}{\partial x}+\frac{\partial s_{23}}{\partial y}. \tag{16}$$

Hence combining (15) and (16)

$$\partial s_{31}/\partial x+\partial s_{32}/\partial y=0. \tag{17}$$

As we know Eqs. (13) and (17) are the classical equations of Saint Venant's problem of torsion of prismatical bars. This can be immediately verified by introducing a stress function ψ such that $s_{31}=\partial\psi/\partial y$ and $s_{32}=-(\partial\psi/\partial x)$. Then Eq. (17) is satisfied and the elimination of w between Eqs. (13) yields the well-known equation,

$$\partial^2\psi/\partial x^2+\partial^2\psi/\partial y^2=-2G\theta. \tag{18}$$

However, we still have to satisfy the boundary conditions (10). At the surface of the prismatical bar $\gamma=0$. Expressing that this surface is free of forces we find the two first relations (10) to be identically satisfied and the last one becomes

$$0=s_{31}\alpha+s_{32}\beta-Se_{13}\alpha-Se_{23}\beta. \tag{19}$$

Now because

$$2Ge_{13}=s_{13} \quad 2Ge_{23}=s_{23},$$

this condition may be written

$$s_{31}\alpha+s_{32}\beta=0.$$

This is the same boundary condition as in Saint Venant's problem, namely that the shear stress on the cross section be tangent to the contour of the section. Eq. (18) with the boundary conditions (19) determines completely the shear stress $s_{31}s_{32}$ and its distribution over the cross section is therefore the same as in the classical solution of Saint Venant.

We will now calculate the total torque over the cross sections. For this purpose we must use expression (10) for Δf_x and Δf_y with $\gamma=1$, $\alpha=\beta=0$.

We find

$$\Delta f_x=s_{13}+S\omega_y, \quad \Delta f_y=s_{23}-S\omega_x. \tag{20}$$

From Eqs. (13) and (14)

$$\omega_x=\tfrac{1}{2}s_{23}/G-\theta x, \quad \omega_y=-\tfrac{1}{2}s_{31}/G-\theta y, \quad (21)$$

hence the force along x and y acting on the cross section are

$$\begin{aligned}\Delta f_x&=s_{13}(1-S/2G)-S\theta y,\\ \Delta f_y&=s_{23}(1-S/2G)+S\theta x.\end{aligned} \quad (22)$$

The torque is

$$T=(1-S/2G)\int\int(-s_{13}y+s_{23}x)dxdy + S\theta\int\int(x^2+y^2)dxdy, \quad (23)$$

where the double integral is extended to the area of the cross section. The term

$$T_{SV}=\int\int(-s_{13}y+s_{23}x)dxdy \quad (24)$$

represents the torque calculated by the Saint Venant theory in the assumption that the bar is initially in its natural unstressed state. In the second term appears the polar moment of inertia

$$I_0=\int\int(x^2+y^2)dxdy$$

of the cross section with respect to the origin of the coordinates. It depends on the choice of this origin. However the position of this origin is not arbitrary because the forces acting on the cross section are only a pure torque if

$$\int\int\Delta f_x dxdy=\int\int\Delta f_y dxdy=0. \quad (25)$$

Now we know that the Saint Venant shear distribution is a pure torque and therefore if we introduce expression (22) in the condition (25) the latter becomes

$$\int\int ydxdy=\int\int xdxdy=0. \quad (26)$$

Hence the origin must be at the center of gravity of the cross section and

$$I_G=\int\int(x^2+y^2)dxdy$$

is the polar moment of inertia of the cross section with respect to its center of gravity.

The expression for the torque may be written finally

$$T=(1-S/2G)T_{SV}+I_GS\theta. \quad (27)$$

This simple expression has been obtained with the only assumption that the stress-strain relation is the same as the classical Hooke's law for an isotropic medium. As we remarked above this is an approximation which involves an error of the order $S/2G$. Therefore the term $S/2G$ in the factor $(1-S/2G)$ is not significant as it represents a quantity of the order of what we neglected from the start. We write, therefore

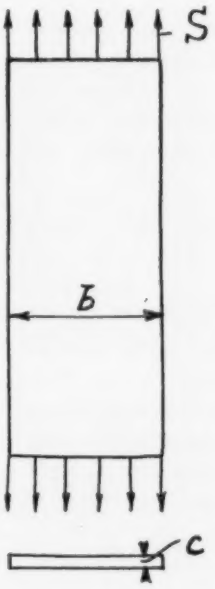

FIG. 2.

$$T=T_{SV}+I_GS\theta. \quad (28)$$

We will now discuss the application of this formula to various cases.

Consider first a circular section. In this case the Saint Venant torque is

$$T_{SV}=GI_G\theta$$

and the total torque is

$$T=I_G\theta(G+S)=GI_G\theta(1+S/G).$$

Here the correction S/G due to the axial stress is of the order of what we neglect in the theory and for this case the correction term loses its physical significance. It would not be so, however, for sections having a low torsional rigidity in their natural state.

Consider for instance the case of a strip of rectangular cross section (Fig. 2). The thickness of the strip being c and the width b (Fig. 2). The Saint Venant torque is

$$T_{SV}=\tfrac{1}{3}bc^3G\theta.$$

The polar moment of inertia

$$I_G=cb^3/12.$$

When the strip is submitted to an axial tension S, applying Eq. (28), the total torque is

$$T=\tfrac{1}{3}bc^3G\theta+\frac{cb^3}{12}S\theta=\tfrac{1}{3}bc^3G\left[1+\frac{1}{4}\left(\frac{b}{c}\right)^2\frac{S}{G}\right]\theta.$$

We see that if the thickness c is small compared to the width, b, the correction $\frac{1}{4}(b/c)^2S/G$ can become very large.

As another example we take the case of a circular thin-walled cylinder split along a generator (Fig. 3), the radius being r and the thickness, c. The Saint Venant's torque is

$$T_{SV}=\tfrac{2}{3}\pi rc^3G\theta$$

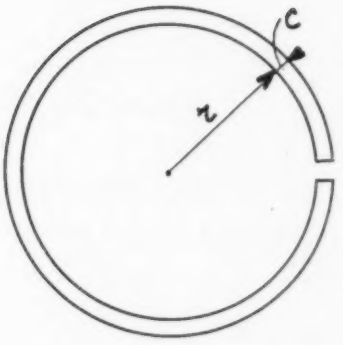

FIG. 3.

and the polar moment of inertia is

$$2\pi r^3c=I_G.$$

The total torque when the cylinder is submitted to an axial tension S is, therefore:

$$T=\tfrac{2}{3}\pi rc^3G\left[1+3\left(\frac{r}{c}\right)^2\frac{S}{G}\right]\theta.$$

The correction in this case is $3(r/c)^2S/G$. If for instance, $S/G=1/1000$ and $r/c=10$, the increase of torsional rigidity is 30 percent.

The Theory of Klystron Oscillations

DAVID L. WEBSTER
Stanford University, Stanford University, California
(Received June 23, 1939)

The principles governing the oscillations in a klystron may be divided into four groups: (1) those of space resonance within each rhumbatron, previously discussed by Hansen; (2) the equations of coupled circuits, with modifications appropriate to space-resonant systems; (3) the kinematics and dynamics of cathode-ray bunching, previously discussed by the author; (4) the constraint on phase relations between the rhumbatrons introduced by the cathode-ray bunches. It is shown here that (4) makes the oscillations assume forms very different from those familiar in free oscillations. These forms are described by general equations and then these equations are applied to three specific problems: maximizing the power output from an oscillator, minimizing the power input for an ideal regenerative amplifier, and finding how stable the frequency is against changes in cathode potential.

I. INTRODUCTION

THE klystron, described in this Journal by R. H. Varian and S. F. Varian,[1] consists essentially of two space-resonant oscillators of one of the types described previously by Hansen[2] and Hansen and Richtmyer[3] and called rhumbatrons, with various accessories which include a

[1] Russell H. Varian and Sigurd F. Varian, "A High Frequency Oscillator and Amplifier," J. App. Phys. **10**, 321 (1939).

[2] W. W. Hansen, "A Type of Electrical Resonator," J. App. Phys. **9**, 654 (1938).

[3] W. W. Hansen and R. D. Richtmyer, "On Resonators Suitable for Klystron Oscillators," J. App. Phys. **10**, 189 (1939).

beam of cathode rays passing through the rhumbatrons and supplying most or all of the power for their oscillations.

Since these rhumbatrons have very low losses, they would continue to oscillate, if the cathode rays were suddenly shut off, with very little damping. With electrical coupling between the rhumbatrons these free oscillations might be superpositions of damped harmonic components in different normal modes of motion, with different frequencies, damping constants, and ratios of the current in one rhumbatron to that in the other. The quantities just mentioned could all be calculated readily enough from various parameters of the individual rhumbatrons and other parts; and since the damping in any mode of motion would be very slow, it might be natural to expect the undamped oscillations, in the presence of the cathode rays, to approximate closely to the damped oscillations in one or another of the normal modes of motion.

In some klystrons a rough experimental survey may give encouragement to this expectation. One does indeed sometimes find two settings of the mechanism for tuning one rhumbatron to the other, to get strong oscillations, in a way suggesting two modes of motion. In such cases, the cathode potentials giving oscillations with the least current form a regular sequence of discrete values; and on testing at these potentials, taken in order, the oscillations are first in one "mode" and then in the other, alternately, in a way suggesting the difference in phase relations between modes for any two coupled oscillators.

On further examination, however, predictions on this basis do not continue to work so well. As a crucial test, one can make a klystron in which the coupling is unsymmetrical, so that in the free oscillations of one mode one rhumbatron would oscillate n times as strongly as the other. Then in the other mode, their ratio would not be n, but $1/n$. In an actual case of this type, however, with $n=4$, experiment showed no such difference in character of the oscillations as a change in this ratio from 4 to $\frac{1}{4}$. Instead, the ratio was obviously about the same for both modes. Evidently the oscillations maintained by cathode rays are very far from resembling free oscillations.

The explanation of this result lies in a principle of phase relations. In free oscillations each normal mode of motion is characterized by its own phase relations, among which is a definite phase difference between the electric fields of the two rhumbatrons. In oscillations maintained by cathode rays, on the other hand, the time of transit of an electron in the center of a bunch, from the first rhumbatron, or "buncher," to the second, or "catcher," imposes a constraint on the phase difference of their electric fields in a manner quite independent of the laws of free oscillations. With this in mind, one might expect the klystron to oscillate "best" (whatever that may mean) when these two causes of phase relations agree on what to cause. Even this expectation, however, turns out to be unreliable: Klystron oscillations do not always resemble free oscillations, and under some of the best practical conditions they may depart widely therefrom.

The purpose of the present paper, therefore, is to develop the theory of klystron oscillations, so as to show what laws really do govern them. In this discussion it will be assumed that the reader is familiar with the ideas and terminology introduced by the Varians[1] and Hansen[2] in the papers referred to above, and also with the principles of the bunching of electrons in the cathode-ray beam of a klystron, discussed in a recent paper by the author.[4]

II. Practical Problems

While it is desirable to formulate the theory of these oscillations so as to cover all cases, there are two problems of such special importance in practice as to merit attention from the beginning. One of these is on the maximum power output and maximum efficiency of an oscillator; the other relates to the amplifier.

In the oscillator, as noted by the Varians,[1] the "catcher" will catch the most power from the cathode-ray beam if it satisfies simultaneously three requirements. First, its maximum electric field must be strong enough to take all the kinetic energy from an electron and not so strong as to waste energy by throwing electrons backward. Second, the catcher must be placed along the beam at the point where the electrons

[4] David L. Webster, "Cathode-Ray Bunching," J. App. Phys. **10**, 501 (1939).

are in bunches of a certain best form, as defined by the author;[4] or practically, since the catcher is not readily moved, the buncher must exert forces on the electrons of the right strength to place the best form of bunching where the catcher is. Third, the catcher must oscillate in the right phase, so that its maximum retarding field occurs while the center of a bunch is passing through it. One of the chief problems of klystron oscillation theory, therefore, is how to satisfy these three conditions all at once.

Turning to the other chief problem, on the amplifier, the author has discussed previously[4] the problem of obtaining the maximum gain in a simple, nonregenerative amplifier, where there is no transfer of power between the rhumbatrons except by the cathode rays. Introducing regeneration, however, means also introducing phase-determining factors of the same sorts as in the oscillator, and therefore coming under the present theory. With regeneration, the gain can be increased indefinitely by simply tuning nearer and nearer to a condition of spontaneous oscillation. A problem of special importance for the design of sealed-off tubes, is how to obtain very high gain with the least heating of the tube, that is, with the least power input. Practically, since the best operating potentials are rather sharply defined, this means, how to minimize the current required at such a potential to be just on the edge of the range for spontaneous oscillation.

III. Assumptions, Fundamental Principles, and Notation

The results of the previous paper on bunching[4] will be assumed valid here, thereby restricting this theory by the assumptions of that paper, of which two deserve repetition. One of these is that the distances through the rhumbatrons along the cathode rays are short enough to justify treating each electron as if the time average of the field encountered by it equaled the space average at the instant when it passed the center of the field. This assumption could be somewhat wrong without much change in the forms of the equations, since the ratio of these averages is nearly the same for all electrons unless it is very far from unity, and it could easily be allowed for by a constant factor applied to each field strength. The other assumption to be repeated is that the buncher voltage is so much smaller than either the cathode or catcher voltage as to be negligible in some of the equations. This condition is fulfilled whenever the times of transit of electrons from the buncher to the catcher are many cycles, but in some klystrons, notably some powerful oscillators with transit times near two cycles, it is far enough from fulfillment to make many of the equations notably less exact. In such a case, for example, one cannot expect the catcher to run at a peak voltage almost equal to the catcher voltage without turning any electrons back and thereby losing their help.

In the notation of that paper, the cathode-ray currents were denoted by i, speeds by v, and line integrals of electric fields by V. The space between the cathode and buncher was designated by subscript 0, with v_0 the speed of an electron at the end of that space. Subscript 1 denoted the buncher, with v_1 the change of speed of an electron most strongly accelerated there, and subscript 2 denoted the catcher.

The bunching occurring in the distance s between the centers of the rhumbatron fields changed i from its d.c. value i_0 to a pulsating current i_2, of which the first harmonic had a peak value to be called here i_2', and

$$i_2' = 2i_0 J_1(r), \tag{1}$$

where J_1 is Bessel's function of the first order and first kind, and

$$r = s\omega v_1 / v_0^2, \tag{2}$$

and ω is 2π times the frequency. At least, i_2 had this value in the absence of appreciable "de-bunching" of the electrons by their mutual repulsion; but with de-bunching, approximately,

$$i_2' = 2i_0 J_1(r) \frac{\sin hs}{hs}, \tag{3}$$

where h depended on the current density and v_0.

In this paper, as in parts of that one, time will be measured from a peak of this harmonic, that is, from an instant when the center of a bunch passes the center of the field of the catcher. Using complex exponentials here instead of the cosines used there, this leaves i_2' real. The line integrals V_1 and V_2, of the electric fields of the

rhumbatrons (not p.d.'s), then become complex; and with the same exponential time factor for them as for i_2', their angles of lag, treating them both as retarding fields, will be called ϕ_1 and ϕ_2, respectively.

In these terms, with no de-bunching and with $|V_1| \ll |V_2|$, the power output is

$$P_2 = i_0 |V_2| J_1(r) \cos \phi_2, \tag{4}$$

whereas the input is

$$P_2 = i_0 V_0. \tag{5}$$

The fundamental principle about phases, mentioned in the introduction to this paper, can be deduced from a statement by the Varians[1] or from its mathematical equivalent in the paper on bunching,[4] that if an electron is to find itself in the center of a bunch it must pass the center of the buncher just as the field there is changing from retarding to accelerating. For the bunch reaching the center of the catcher at $t=0$, this means that this central electron must have passed the center of the buncher when

$$\omega t - \phi_1 = (\pi/2) - 2\pi n, \tag{6}$$

where n is some integer. Since its speed was not changed in the buncher, this t is $-s/v_0$, so the transit angle of the center of a bunch is

$$\tau = s\omega/v_0 \tag{7}$$

and the principle can be expressed in angles only, as

$$\tau + \phi_1 = 2\pi n - (\pi/2). \tag{8}$$

Both of these angles τ and ϕ_1 depend on ω, and ϕ_1 depends also on the constants of the rhumbatrons and coupling loop or capacitance and any other circuits coupled to them, but obviously not on any field strength or current or other function of time. This equation, therefore, determines ω in terms of v_0 and these constants, and therefore is fundamental to the whole theory of the klystron.

As will be proved later, the stability of the frequency against slight changes in cathode potential v_0 depends also on this equation. If V_0 is increased slightly, so is v_0, thereby diminishing τ; but this can be balanced by an equal increase in ϕ_1; and if the frequency is reasonably near resonance for either rhumbatron, this increase in ϕ_1 is obtained through an increase in ω which is relatively very small as compared with the increase in V_0. This makes the frequency very stable.

To determine ϕ_1 as a function of ω and the constants, as well as for other problems, it will be convenient now to formulate the equations for currents, etc. in terms of linear circuits as nearly analogous to the rhumbatrons as their laws permit. As noted by Hansen[2] and discussed in more detail by Hansen and Richtmyer[3] any definitions adopted for the constants of such circuits must be arbitrarily chosen from among several possibilities. While such choices for different purposes may be different, for the present purpose there is a good basis for choice in the fact that one of the essential purposes of the rhumbatrons is to have work done by or on the electrons passing through their electric fields.

The line integral of the field along the axis of either rhumbatron is not a difference of potential, because the field in general is not a gradient of any potential, so its peak value as a function of time will be referred to only as the "voltage," V. In terms of it, the capacitance C will then be defined to make the energy of the rhumbatron $\frac{1}{2}CV^2$. Then the peak value of a certain q will be defined as CV, and a current I as the time derivative of q. By these definitions, q is not equal to the peak value of the total quantity of charge of either sign actually existing within the rhumbatron. Instead q is less, because much of the actual charge is on the ends of lines of force along which the line integrals of the field strength are less than V; and similarly I is less than the peak value of the current crossing the boundary between the negative and positive charges.

The self-inductance L will be defined so as to make $\frac{1}{2}LI^2$ equal the total energy, thus making L exceed its more obvious definition as much as I^2 seems deficient. The series resistance R will be defined similarly to make $\frac{1}{2}RI^2$ equal the average rate of loss of energy, including losses by ohmic resistance and radiation, and in the case of the buncher also by power used for bunching.[4*]

* *Note added in proof.*—This system of definitions is identical in results, though not in logical order, with one of the three alternative systems proposed by Hansen and Richtmyer (reference 3); namely, the one resulting from their Eq. (2). Their starting point is a quantity not used in this paper; namely, the shunt impedance at resonance. In their notation this is called R, but in the notation of the present paper it is L/CR.

Since the transfer of energy from one rhumbatron to the other is usually made by a loop of wire (though it can be made electrostatically), there must be a definition of the mutual inductance M between each rhumbatron and the loop. Since the current densities in all parts of the rhumbatron are almost exactly synchronous, the current crossing a belt around the rhumbatron at the loop will be in phase with I even though not equal to I. So M will be defined so as to represent the e.m.f. induced in the loop by the rhumbatron as $-j\omega MIe^{j\omega t}$. This system of notation can be seen better as a whole in Fig. 1, in which the cross sections are copied from the Varians' Fig. 5. In addition to the symbols already defined, this figure shows the self-inductance of the loop L_3, and its current I_3. The resistance of the loop is negligible, as is also the capacitance between the straight part of the loop and its surrounding conduit. In some of the later models this conduit is only a hole in a thick diaphragm, further reducing this capacitance, but there is no difficulty in keeping it negligible so long as the loop is not so long as to approximate a quarter-wave line.

The directions for positive values of voltages and their associated pairs of charges and currents have already been defined and these definitions are collected in the signs and arrows in Fig. 1.

In the absence of any cathode rays, the free oscillations of such a system would obviously be governed by the equations:

$$Z_1I_1+j\omega M_1I_3=0, \tag{9}$$

$$j\omega M_1I_1+j\omega L_3I_3+j\omega M_2I_2=0, \tag{10}$$

$$+j\omega M_2I_3+Z_2I_2=0, \tag{11}$$

where
$$Z_1=R_1+j\left(\omega L_1-\frac{1}{\omega C_1}\right) \tag{12}$$

and
$$Z_2=R_2+j\left(\omega L_2-\frac{1}{\omega C_2}\right). \tag{13}$$

In introducing the cathode rays into these equations it must be noted that it makes no appreciable difference whether they are allowed to pass through the catcher or caught on a plate replacing its exit grid, because their current i_2, or its first harmonic i_2', is very small in comparison with the conduction current I_2. What

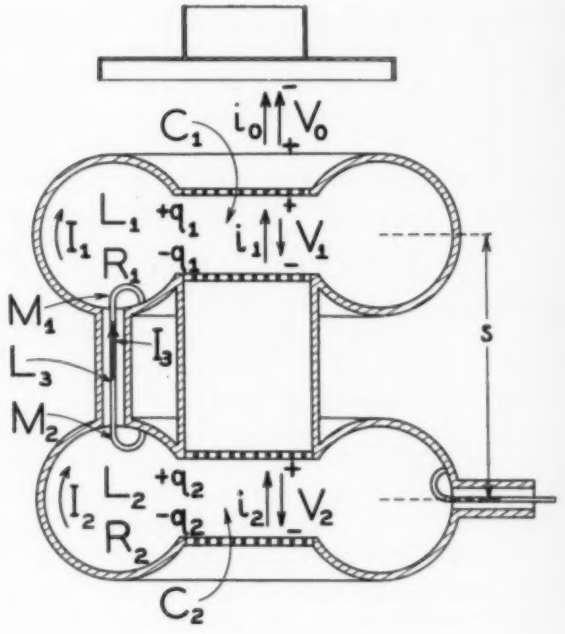

FIG. 1.

really counts is not their current, but the energy they lose or gain. Since the field against which any one of them is moving at any time is nearly the same as for an electron on the axis, where its line integral is $V_2e^{j\omega t}$, and since C_2 is defined here in terms of V_2 and the stored energy, the energy relations are analogous to those of the condenser shown in Fig. 2. So the only change they make in Eqs. (9)–(11) is to change (11) to

$$+j\omega M_2I_3+Z_2I_2+\frac{i_2'}{j\omega C_2}=0. \tag{14}$$

Whether or not they are caught, therefore, this last term in Eq. (14) is the e.m.f. due to their electric field, and they cause little or no error in the equation

$$V_2=I_2/j\omega C_2, \tag{15}$$

and of course, none at all in

$$V_1=I_1/j\omega C_1. \tag{16}$$

For reasons to appear in the solution of these equations some additions to the notation will be

$$L_1'=L_1-(M_1^2/L_3), \tag{17}$$

$$X_1'=\omega L_1'-(1/\omega C_1), \tag{18}$$

$$Z_1'=R_1+jX_1' \tag{19}$$

and similar equations with subscript 2, and

$$M = M_1 M_2 / L_3 \tag{20}$$

and

$$Z_2'' = Z_2' + \frac{\omega^2 M^2}{Z_1'}. \tag{21}$$

IV. General Equations for the Oscillations

Neglecting transients, the general solution for the voltages is

$$V_2 = \frac{i_2'}{\omega^2 C_2^2 Z_2''} \tag{22}$$

and

$$V_1 = j\frac{C_2 \omega M}{C_1 Z_1'} V_2 = j\frac{M i_2'}{\omega C_1 C_2 Z_1' Z_2''}. \tag{23}$$

i_2', however, involves V_1, since Eq. (1) may be rewritten as

$$i_2' = 2 i_0 J_1\left(\frac{\tau |V_1|}{2V_0}\right). \tag{24}$$

So it is possible to solve these equations explicitly for the d.c. cathode-ray current i_0 required to raise V_2 or V_1 to any specified value, but not in general for the V_2 or V_1 given by any specified i_0.

Equation (4), for the power output, now takes the form

$$P_2 = i_0 |V_2| J_1\left(\frac{\tau |V_1|}{2V_0}\right) \cos \phi_2 \tag{25}$$

with

$$\phi_2 = \text{phase angle of } Z_2''. \tag{26}$$

Equation (8), for the frequency or transit angle, becomes

$$\tau + \phi_{12} = 2\pi n \tag{27}$$

with

$$\phi_{12} = \text{phase angle of } Z_1' Z_2''. \tag{28}$$

V. Maximizing the Power Output

The three conditions of Section II for maximizing the power output of an oscillator can be expressed now as requiring special values of certain factors in Eq. (4) or (25), to be denoted by a subscript m, namely

$$|V_2| = |V_{2m}| = V_0, \tag{29}$$

$$r = r_m = 1.84, \tag{30}$$

$$\phi_2 = 0. \tag{31}$$

By Eqs. (30), (29), (23) and (18),

$$X_{1m}' = \pm(\sigma^2 \omega_m^2 M^2 - R_1^2)^{\frac{1}{2}}, \tag{32}$$

where

$$\sigma = \frac{\tau_m C_2}{2 r_m C_1}; \tag{33}$$

and Eqs. (31) and (26) require Z_2'' to be real, resulting in

$$X_{2m}' = X_{1m}'/\sigma^2. \tag{34}$$

Since there is no $\pm$ sign in this equation, the two rhumbatrons must be detuned from the operating frequency in the same direction, but by different amounts; and by Eq. (32) that may be either direction.

In either case, Z_2'' must be

$$Z_{2m}'' = R_2 + (R_1/\sigma^2) \tag{35}$$

and i_0 must be

$$i_{0m} = \frac{V_{0m} \omega_m^2 C_2^2}{2 J_1(r_m)} \{R_2 + (R_1/\sigma^2)\}. \tag{36}$$

V_{0m} and ω_m can be found through τ_m, which is given by Eq. (27) as

$$\tau_m = 2\pi n \mp \sec^{-1}(M/M_0), \tag{37}$$

the upper sign of the $\mp$ going with that of the $\pm$ in Eq. (32) and the subscript 0 this time not indicating the cathode but the value of M which reduces X_1' and X_2' to zero and is the minimum M with which it is possible to make r reach r_m. By Eq. (32), this is

$$M_0 = \frac{R_1}{\sigma \omega_m} = \frac{2 r_m C_1 R_1}{\tau_m \omega_m C_2}. \tag{38}$$

The τ_m and ω_m in Eq. (38) mean that Eq. (37) is not the explicit solution for τ_m which it appears

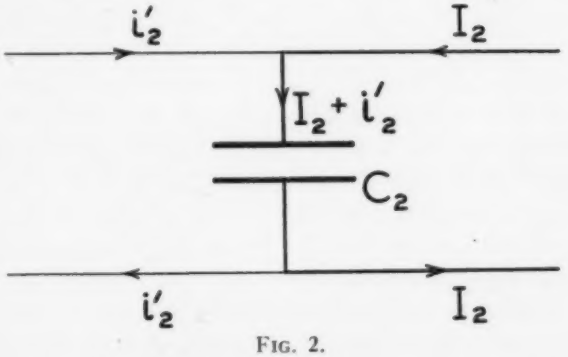

Fig. 2.

to be at first sight; but an approximate value can be found by substituting the resonant frequency of either rhumbatron for ω_m in Eq. (38) and then solving (38) and (37) by trial and error.

Then

$$eV_{0m}=\tfrac{1}{2}mv_{0m}^2=\tfrac{1}{2}m\left(\frac{s\omega_m}{\tau_m}\right)^2, \qquad (39)$$

giving similar approximations for V_{0m} and v_{0m}; and finally, an approximate value for the difference between ω_m and the resonant frequency of either rhumbatron can be found by means of Eq. (32) or (34).

By Eq. (25) the maximum P_2 is

$$P_{2m}=i_{0m}V_{0m}J_1(r_m)=0.58i_{0m}V_{0m}. \qquad (40)$$

Eq. (36) transforms this to

$$P_{2m}=\tfrac{1}{2}V_{0m}^2\omega_m^2C_2^2\{R_2+(R_1/\sigma^2)\}, \qquad (41)$$

which could easily be guessed and therefore serves as a check against mistakes.

With given resistances, this power output can evidently be obtained whenever $|V_2|=V_0$, whether or not the klystron satisfies the other conditions, $r=r_m$ and $\phi_2=0$, stated at the beginning of this section; but with fixed resistances it is difficult to exceed this power very much, because whenever $|V_2|$ exceeds V_0 there is so much loss of power to the cathode rays turned backward in the catcher. Furthermore it can be shown that with $|V_2|=V_0$ any other values of r and ϕ_2 require higher values of the direct cathode-ray current i_0, thereby increasing the power input. So the three conditions for maximizing the power output with fixed resistances also maximize the efficiency.

If greater power output is desired, there are two ways to obtain it: either choose a higher one of the best voltages given by Eq. (39), with a smaller one of the best values of the transit angle, or else increase the resistances. In practice it seems usually best to base the choice of voltage on considerations of space charge and convenience for any reasons external to the klystron, and then increase R_2 by increasing the coupling from the catcher to the antenna or other load or making other changes in the load as needed. These changes should be made subject to the three conditions, Eqs. (29), (30) and (31), so as to keep the maximum efficiency.

The equations of this section explain well some of the phenomena mentioned in Section I, where it was noted that one sometimes observes two modes of motion suggestive of those of free oscillations. When V_0 is raised steadily the two modes appear alternately as required by Eqs. (39) and (37); they can be distinguished from one another by the tuning, as required by Eqs. (32) and (34); and pairs of oscillations merge together when M is reduced, with appropriate changes in the best voltages V_{0m}, as required by Eqs. (39), (37) and (38); and with further reduction in M it becomes impossible to get the full power output P_{2m}, as required by Eq. (38).

The contrast between these modes of motion and free oscillations can be seen in the definition of the critical coupling reactance $\omega_m M_0$, in Eq. (38), which has no relation to the value $(R_1R_2)^{\frac{1}{2}}$ for free oscillations. Experimentally also, it is easily seen by making $C_1=C_2$ and $R_1=R_2$, so that in free oscillations V_1/V_2 would be M_1/M_2 in one mode and $-M_2/M_1$ in the other. If these ratios actually occurred, and M_1/M_2 was made right to maximize P_2 is one mode it would often be impossible to come near maximizing it in the other mode; but actually it is about equally easy in either mode. Moreover, if the coupling loop is made to slide so as to interchange the values of M_1 and M_2 during operation, the oscillation goes on just as well after the change as before, provided there is a slight change of tuning as required by the M_1 and M_2 in L_1' and L_2', respectively, as defined in Eq. (17).

A difference which can be observed between the two modes occurs with low values of n because of the difference in V_{0m}. If an incandescent lamp is placed near the antenna so as to be lit by current caused in it by the electric field, and $n=2$ and $M=2M_0$ or more, the lamp can easily be seen to glow brighter with the mode with the higher V_{0m}, as required by Eq. (41).

These equations cannot pretend to great accuracy, because of their approximations, some of which are noted at the beginning of Section III, but evidently they cover the main points, and the principles underlying them are essentially correct.

VI. Minimizing the Power Input

Turning to the other practical problem of Section II, that of minimizing the power input of a high gain regenerative amplifier, we find another series of best operating cathode voltages, different from those of the oscillator, so the problem becomes one of minimizing the cathode-ray current at one of the best voltages. Since the highest practicable gain is obtained by having the klystron just on the point of starting to oscillate spontaneously, the cathode-ray current needed for this gain with any given setting of the tuning mechanism and cathode voltage is almost the i_0 given by the general equations (22) to (25), of Section IV when V_2, V_1, i_2' and P_2 are all zero. Such a value of i_0 will be denoted by i_{00} and called the "starting current." So i_{00} is a function of V_0, ω, and whichever circuit parameters L_1, L_2, C_1 or C_2 are used for tuning, and as such it can be minimized. Values so obtained will be called i_{000}, V_{00}, ω_0, L_{10}, etc.

If the klystron is oscillating spontaneously and i_0 is reduced to approach i_{00}, not only P_2 but V_2, V_1, r, i_2' and the I's all approach zero. So $2J_1(r)\rightarrow r$ and i_2' can be eliminated between Eqs. (23) and (24). Then

$$i_0\rightarrow i_{00}=2\frac{v_0V_0}{s}\frac{C_1C_2}{M}|Z_1'Z_2''|. \qquad (42)$$

The fact that this i_{00} is proportional to $V_0^{\frac{1}{2}}$, like a current limited by space charge, may be significant in some forms of amplifier in removing any considerations about space-charge from the choice of a working value of V_0.

To minimize i_{00} means now almost the same as minimizing $|Z_1'Z_2''|$ by proper tuning and choice of V_0, so the problem will be treated in that way. The results depend on the relation of ω_0M to $(R_1R_2)^{\frac{1}{2}}$ as shown by Table I. Here again, as in the oscillator with maximum power, there are two modes of motion whenever M exceeds a definite value, but its present critical value is the same as for free oscillations and so quite different from M_0 in Eq. (38). This critical M does not make the amplifier oscillations like free ones, however, as may be seen from the fact that with $C_1=C_2$ and $R_1=R_2$ the value of V_{10}/V_{20} has no more relation to M_1/M_2 or $-M_2/M_1$ than it had in the oscillator.

Table I.

Quantity	Value if $\omega_0^2M^2>R_1R_2$	Value if $\omega_0^2M^2<R_1R_2$
X_{10}'	$\pm\{\omega_0^2M^2(R_1/R_2)-R_1^2\}^{\frac{1}{2}}$	0
X_{20}'	$\pm\{\omega_0^2M^2(R_2/R_1)-R_2^2\}^{\frac{1}{2}}$	0
$\lvert Z_1'Z_2''\rvert_0$	$2\omega_0M(R_1R_2)^{\frac{1}{2}}$	$\omega_0^2M^2+R_1R_2$
i_{000}	$4\frac{v_0V_0}{s}\omega_0C_1C_2(R_1R_2)^{\frac{1}{2}}$	$2\frac{v_0V_0}{s}\frac{C_1C_2}{M}(\omega_0^2M^2+R_1R_2)$
ϕ_{120}	$\pm\sec^{-1}\{\omega_0M/(R_1R_2)^{\frac{1}{2}}\}$	0
τ_0	$2\pi n\mp\sec^{-1}\{\omega_0M/(R_1R_2)^{\frac{1}{2}}\}$	$2\pi n$
V_{00}	$\frac{m}{2e}\left(\frac{s\omega}{\tau_0}\right)^2$	$\frac{m}{2e}\left(\frac{s\omega}{\tau_0}\right)^2$
Z_{20}''	$2R_2$	$R_2+\frac{\omega_0M^2}{R_1}$
ϕ_{220}	0	0
$\lvert Z_{10}'\rvert$	$\omega_0M(R_1/R_2)^{\frac{1}{2}}$	R_1
ϕ_{10}	$\pm\sec^{-1}\omega_0M/(R_1R_2)^{\frac{1}{2}}-\frac{\pi}{2}$	$-\frac{\pi}{2}$
$\lvert\frac{V_{10}}{V_{20}}\rvert$	$\frac{C_2}{C_1}\left(\frac{R_2}{R_1}\right)^{\frac{1}{2}}$	$\frac{C_2}{C_1}\frac{\omega_0M}{R_1}$

Contrasting the amplifier with the oscillator, the formulas for X_{10}' and X_{20}' are seen to be symmetrical, whereas Eqs. (32) and (34) for X_{1m}' and X_{2m}' were not, and there are similar contrasts dependent on this one. Nevertheless if ω_mM_0 is in any way made to equal $(R_1R_2)^{\frac{1}{2}}$, the formulas for the two cases become identical throughout. This is not likely to happen often. With similar rhumbatrons, making $C_2=C_1$, it never happens in the oscillator, where $\omega_mM_0<R_1$ and $R_1<R_2$; but it may happen in an amplifier if the antenna coupled into the buncher has enough radiation resistance to make $R_1\gg R_2$.

The especially important quantity i_{000} is seen in Table I to be independent of M in a tightly coupled amplifier, whereas it increases with any loosening of the coupling below the critical value. Since the resistances are not easily calculated, this means that the easiest way to make an amplifier operate is to make the coupling amply sufficient and then tune it to minimize i_{00}. This procedure results, of course, in two modes of motion, giving an impression that they are a general rule of operation of a klystron. The possibility of operating it with only one mode was indeed found first only by this mathematical analysis. It was then confirmed experimentally by William T. Cooke, by a study of starting currents with a variable coupling loop.

Cooke's experiments confirmed also the mutual approach and coalescence of the values of V_0 for the two modes of motion as M decreased to a critical value, the constancy of i_{000} with tight coupling, and the increase in i_{000} as the coupling is loosened beyond the critical value. These changes were of course not exactly as predicted, because of the approximations in the theory, but the correctness of the equations as first approximations was clearly confirmed.

VII. Frequency Stability

The frequency of oscillation is naturally affected by any changes in dimensions due to heating or other causes, as is well shown by the practical use of such changes for tuning. For stability such changes evidently must be prevented. Further requirements for stability appear in the frequency-determining equation, Eq. (27), where ω is connected not only with the constants of the rhumbatrons and the distance between them but also with v_0 and so with V_0.

The stability of frequency against changes in V_0 will therefore be defined as

$$S=\frac{d\ln V_0}{d\ln \omega}, \tag{43}$$

and it can be found simply by differentiating Eq. (27) to be

$$S=2\left(1+\tau^{-1}\frac{d\phi_{12}}{d\ln\omega}\right). \tag{44}$$

Neglecting the 1 in this equation and approximating $dX_1'/d\omega$ as $2L_1'$ and $dX_2'/d\omega$ as $2L_2'$ and defining

$$Q_1'=\frac{L_1'\omega}{R_1} \quad \text{and} \quad Q_2'=\frac{L_2'\omega}{R_2}, \tag{45}$$

the oscillator running at maximum power and efficiency has

$$S=\frac{4}{\tau_m}\cdot\frac{Q_1'\dfrac{M_0^2}{M^2}\left\{1+\dfrac{\omega_m^2(M^2-M_0^2)}{R_1R_2}\right\}+Q_2'}{1+\dfrac{\omega_m^2M_0^2}{R_1R_2}}. \tag{46}$$

As M increases from M_0 to infinity the numerator of this second fraction decreases from

$$Q_1'+Q_2' \quad \text{to} \quad Q_1'\frac{\omega_m^2M_0^2}{R_1R_2}+Q_2'. \tag{47}$$

With similar rhumbatrons, the radiation resistance makes $R_2>R_1$ and $Q_2'<Q_1'$; and Eq. (38) makes $R_1>\omega_mM_0$. So this decrease in S may be very considerable, and most of it occurs between $M=M_0$ and $M=2M_0$. So from the viewpoint of frequency stability it is best to keep M down to or near M_0.

In the amplifier, using Eq. (44) in the same way, with tight coupling

$$S=\frac{2(Q_1'+Q_2')}{\tau_0}, \tag{48}$$

while with loose coupling

$$S=\frac{4(Q_1'+Q_2')}{\tau_0\left(1+\dfrac{\omega_0^2M^2}{R_1R_2}\right)}. \tag{49}$$

For frequency stability, therefore, there would be some advantage in loose coupling, though never by more than a factor of 2 in S. Such an advantage is not likely often to outweigh the advantage of critical or tight coupling in minimizing the power input. If i_0 can be held sufficiently constant it might be best to use coupling just barely over the critical value, so as to bring the best voltages for the two modes of motion very nearly but not quite together, since this makes the starting current nearly constant over a long range of cathode potential.

The Atomphysical Interpretation of Lichtenberg Figures and Their Application to the Study of Gas Discharge Phenomena

F. H. Merrill and A. von Hippel
Electrical Engineering Department, Massachusetts Institute of Technology, Cambridge, Massachusetts

The extremely finely detailed drawing in Lichtenberg figures offers an unusually clear record of the early stages of discharge phenomena. The interpretation of these records in terms of electronic ionization, space charge, plasma formation, and neutralization of charges is presented in this paper. After giving a short summary of our present knowledge about gas breakdown, the "normal" history of a Lichtenberg discharge is established by a study in nitrogen between five millimeters of mercury and thirty atmospheres of pressure. It progresses in three stages—the primary figure, spark development, and the discharge of negative surface charges. (The "back figure.") Admixture of carbon tetrachloride and experiments in "Freon" up to six atmospheres show the decisive influence of electro-negative components on the development of the phenomena, and reveal the reasons why these new gases are so effective in suppressing corona discharges. Deviations from Paschen's law, recently observed by several workers, can be interpreted in terms of the photographic evidence gained.

GEORG Christoph Lichtenberg, faithful to his maxim of exploring nature with instruments of unusual dimensions, baked a tremendous resin cake for electrostatic experiments (electrophorous). Resin dust settled down on the surface where he had drawn his sparks, forming starlike patterns of peculiar design. The shape and polarity of surface discharges could be developed by dust figures (Fig. 1). Ever since this discovery of 1777,[1] Lichtenberg figures have attracted the interest of the physicist[2] not only because the variety of their forms offers one of the most beautiful spectacles in science but because their characteristics reveal some new aspects of gaseous discharges. The speed of propagation of the figures gives information on the breakdown mechanism and permits the measurement of very short time intervals.[3] Their extension and shape can be used for recording the magnitude and polarity of the transient voltage applied.[4] Finally the extremely fine detail of the figure, especially if recorded on photographic plates (Fig. 2), sets a riddle akin to the hieroglyphics of the Egyptian script. If we can read the signs, we shall know more about the early stages of electric discharges.

The deciphering has not yet progressed very far, and Lichtenberg figures have only rarely been used as witnesses for explaining the development of discharges.[5] Studies of the electrical breakdown in gases by other means reveal the very complex nature of the phenomena involved.[6]

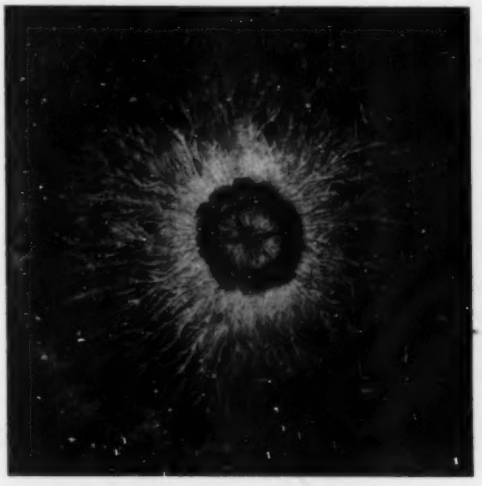

Fig. 1. Lichtenberg's drawing of a dust figure.

[1] G. C. Lichtenberg, Novi. Comment. Gött. Vol. 8, 168, 1777.

[2] See, for example, the excellent review of K. Przibam, *Handbuch der Physik* (1927), Vol. 14, p. 391.

[3] P. O. Pedersen, "On the Lichtenberg Figures," Kgl. Danske Videnskabernes Selskab. Copenhagen, Part I (1919), Part II (1922), Part III (1929). P. Heymens and N. H. Frank, Phys. Rev. **25**, 865 (1925).

[4] See, for instance, T. F. Peters, Elec. World (1924); T. H. Cox and T. W. Legg, Elec. Eng. (1925); M. O. Jørgensen, Inginiorvidenskabelige Skrifter, Copenhagen, 1934.

[5] E. Marx, E. T. Z. 1161 (1930); A. von Hippel, Zeits. f. Physik **80**, 19 (1933); Naturwiss. **22**, 701 (1934).

[6] See, for example: A. von Engel and M. Steenbeck, Elektrische Entladungen II, (1934); A. von Hippel, Ergebnisse d. exakten Nat. **14**, 79 (1935); W. Rogowski, Zeits. f. Physik **100**, 1 (1936); L. B. Loeb, Rev. Mod. Phys. **8**, 267 (1936); L. B. Loeb and A. F. Kip, J. App. Phys. **10**, 142 (1939); R. Strigel, *Elektrische Stossfestigkeit* (Springer, 1939).

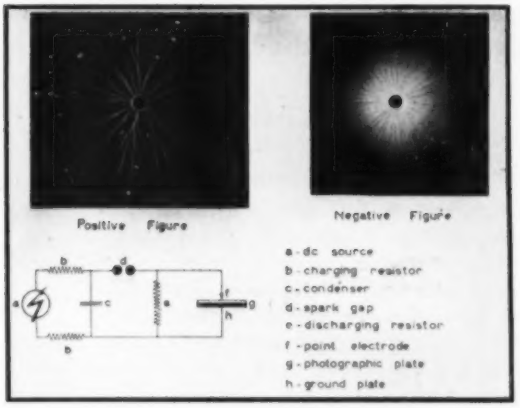

FIG. 2. Lichtenberg figures on photographic plates (positive: 1 atmos. 10 kv, point-ring arrangement; negative: 200 mm, 3 kv, point-plate arrangement).

The unsettled situation demands the application of every method which can give new evidence. The authors therefore undertook an extensive study of the Lichtenberg figures in nitrogen and mixtures of nitrogen and carbon tetrachloride vapor at pressures ranging from a few millimeters to thirty atmospheres. Investigations in Freon (CCl_2F_2) were carried up to six atmospheres. As far as the authors know, no studies have previously been published of figures above atmospheric pressure or in electro-negative gases. The phenomena observed and their discussion on the basis of our present knowledge of the breakdown in gases are reported in this paper.

BREAKDOWN IN GASES

Our present conception of the breakdown mechanism in gases may be summarized as follows:

Primary electrons are required for starting the breakdown process. They may be liberated from the gas, the walls of the chamber, or electrodes by external radiation, or in special cases from the cathode by field emission or thermionic emission.

Free electrons, if not sufficiently accelerated by an electric field, are normally *trapped* (except in the case of rare gases), forming negative ions. They can be re-liberated in intense electric fields by violent collisions of the ions.[7] Therefore, as cloud-chamber pictures directly show,[8] the discharge may use this large indirect supply of electrons at high field strengths if free ones are not available.

Impact ionization by the primary electrons and by the secondaries formed is the next step in the breakdown process, as Townsend demonstrated in his theory of cumulative ionization.[9] This avalanche formation in itself does not result in a permanent destruction of the insulating property of the gas. Only if the discharge becomes self-supporting does it recreate with certainty its initiating electrons. Then breakdown occurs, establishing a new and stable field distribution and discharge form.

Current voltage characteristics alone do not give any decisive evidence about this *regenerative mechanism* for primary electrons but only show the fact of regeneration.[10] Hence additional information had to be sought to decide between the different possibilities proposed. The process of impact ionization by positive ions in the gas had to be discarded as improbable for atom-physical reasons.[11] The next assumption, that positive ions bombarding the cathode release the necessary amount of new electrons, put the whole Townsend theory in a precarious position because apparently the positive ions should have time for traversing the gap before the breakdown is completed.[12] On the other hand, experiments with several different methods[13] showed that instead of the expected times of greater than 10^{-5} second, times of less than 10^{-7} second are

[7] See, for instance, A. M. Cravath, Phys. Rev. **33**, 605 (1929).

[8] E. Flegler and H. Raether, Zeits. f. tech. Physik **16**, 438 (1935); Zeits. f. Physik **103**, 315 (1936). A. M. Cravath and L. B. Loeb, (Physica **6**, 125 (1935)) make this electron supply responsible for the high velocity of propagation of lightning discharges.

[9] J. S. Townsend, *Ionization of Gases by Collision* (1910).

[10] Townsend already pointed out that photoelectric effect or impact ionization by positive ions in the gas or at the cathode would lead to similar formulations. See also L. B. Loeb, J. App. Phys. **10**, 142 (1939).

[11] G. Holst and E. Osterhuis, Physica **1**, 74 (1921); Phil. Mag. **76** 1147 (1923).

[12] W. Rogowski first formulated clearly the difficulties of the situation, Arch. f. Elektrotech. **16**, 496 (1926); Sommerfeld Festschrift, 1929.

[13] P. O. Pedersen, reference 3, W. Rogowski, E. Fleger, and R. Tamm, Arch. f. Elektrotech. **18**, 479 (1927); R. Tamm, Arch. f. Elektrotech. **19**, 235 (1928); J. J. Torok, Trans. A. I. E. E. **47**, 177 (1928); J. W. Beams, J. Frank. Inst. **206**, 809 (1928).

observed at pressures of the order of one atmosphere.[14]

A way out appeared by considering the *positive space charge* left behind by the rapidly migrating electron avalanches. It seemed possible that a fortuitous arrangement of initial electrons in line might allow avalanches to link together over short distances and create a field distortion in steps, accelerating the breakdown.[15] Even more simply it could be shown[16] that a few primary electrons can build up a field distortion by the remaining cloud of positive ions, corresponding to the cathode fall of the final discharge. In this way the breakdown depends only on the speed of the electrons traversing the gap.

Experimental work seemed at first to confirm the last-named mechanism quite generally,[17] but a closer calculation of the retarding action of the positive space charge on its own advancing electron cloud,[18] a consideration of the decrease in ionization if the field distortion becomes too great,[19] and experiments with such new methods as the rotating camera[20] and the Wilson cloud chamber[21] indicated that in a number of cases the breakdown progressed much faster than even the calculated electron velocity (but see, for instance, reference 22).

Two new suggestions have been advanced to overcome this difficulty. Not only the positive space charge but also the negative space charge of the electrons has to be taken into account. While the electrons nearest to the positive-ion cloud slow down, the electrons at the tip of the negative avalanche are speeded up by electrostatic repulsion and projected forward with the high speed observed.[23] On the other hand, a new mechanism may be involved—that of photoelectric liberation of electrons in advance of the electron avalanches by an intense ultraviolet radiation generated through the electron impacts.[24] In this way the electrons need not cross the whole gap, but a number of short avalanches may act together, and also a fast delivery of new electrons from the cathode by photo-effect may be achieved.[25] The existence of the necessary radiation has been established experimentally.[26]

The delivery of new electrons from the cathode may be connected in a complicated way with the starting discharge. Normally the impact of positive ions against the cathode is made responsible for the regeneration of electrons. If the probability γ for this effect would increase very much with field strength, the field distortion by positive space charge could have an important accelerating influence on the further development of the discharge. This assumption[27] has been disproved experimentally[28] but another effect has been discovered[29] creating new primary electrons. Electrons may be emitted by the action of charged surface layers created by the photo-effect of the discharge. Similar effects are known from the "jet-discharge"[30] and from observations on secondary emission.[31]

[14] At low pressures breakdown times consistent with the Townsend theory have been observed. See, for instance, M. Steenbeck, Zeits. f. tech. Physik **10**, 480 (1929); Wiss. Veröff. Siemenskonzern, **9**, 42 (1930). R. Schade, Zeits. f. tech. Physik **17**, 391 (1936); Zeits. f. Physik **104**, 487 (1937).

[15] L. B. Loeb, Science **69**, 509 (1929) and J. Frank. Inst. **210**, 15 (1930).

[16] A. von Hippel and J. Franck, Zeits. f. Physik **57**, 696 (1929).

[17] See, for instance, Steenbeck, Naturwiss. **17**, 981 (1929); Wiss. Veröff. Siemenskonzern **9**, 42 (1930). L. von Hamos, Ann. Phys. **7**, 857 (1930). H. T. White, Phys. Rev. **46**, 90 (1934).

[18] W. O. Schuman, Zeits. f. tech. Physik **11**, 194 (1930). N. Kapzov, Zeits. f. Physik **75**, 380 (1932). J. J. Sämmer, Zeits. f. Physik **81**, 383, 440 (1933).

[19] W. Rogowski, Arch. f. Elektrotech. **24**, 679 (1930).

[20] See review of R. Strigel, *Elektrische Stossfestigkeit*, p. 41, 1939.

[21] H. Kroemer, Arch. f. Elektrotech. **28**, 703 (1934). Snoddy and Bradley, Phys. Rev. **75**, 432 (1934). E. Flegler and A. Raether, reference 8.

[22] R. Holm, Zeits. f. Physik **102**, 138 (1936).

[23] J. Slepian, Elec. World **91**, 761 (1925). R. Strigel, Wiss. Veröff. Siemenskonzern **15**, 1 (1936).

[24] E. Flegler and A. Raether, Zeits. f. tech. Physik **16**, 438 (1935); Zeits. f. Physik **99**, 640 (1936).

[25] A consistent theory of the electric breakdown on a photoelectric basis has been developed by R. Schade, Zeits. f. Physik **111**, 437 (1939); see also S. Werner, Zeits. f. Physik **90**, 384; **92**, 705 (1934).

[26] H. Hertz, Ann. d. Physik **31**, 983 (1887). E. Greiner, Zeits. f. Physik **81**, 543 (1933). W. Christof and W. Hanle, Physik. Zeits. **34**, 641 (1933). A. Cravath, Phys. Rev. **77**, 260 (1935). E. Flegler and A. Raether, reference 8, p. 315 (1936). A. Raether, Zeits. f. Physik **110**, 611 (1938). H. Costa and A. Raether, Naturwiss. **26**, 593 (1938).

[27] W. Fuchs, Zeits. f. Physik **92**, 467 (1934). W. Rogowski and W. Fuchs, Arch. f. Elektrotech. **29**, 362 (1935). W. Rogowski and A. Wallraff, Zeits. f. Physik **102**, 183 (1936).

[28] R. Schade, Zeits. f. Physik **108**, 353 (1938).

[29] H. Paetow, Zeits. f. Physik **111**, 770 (1939).

[30] A. Güntherschulze and H. Fricke, Zeits. f. Physik **86**, 463 (1933). H. Fricke, Zeits. f. Physik **92**, 728 (1934). H. Schnitger, Zeits. f. Physik **96**, 551 (1935).

[31] G. Malter, Phys. Rev. **49**, 478 (1936); **50**, 48 (1936).

Some other aspects should not be overlooked. During the development of a discharge channel the parts first generated may go through a decisive transformation. The high energy input or the sufficiently frequent succession of avalanches may fill the path with electrons which will compensate the space charge of the positive ions, and a plasma of very high conductivity will result. This spark-like structure behaves like a metallic short circuit over the affected part of the gap, and at the head of the progressing spark an increasing overvoltage appears, speeding up the breakdown.[32]

It will be seen that Lichtenberg figures may not only support by new evidence some of the viewpoints mentioned but also reveal several phenomena not hitherto observed.

Apparatus and Procedure

Figure 3 is a photograph of the four-stage impulse generator and pressure tank used in our experiments. The impulse generator delivers an energy of 6 joules at a maximum voltage of 75 kv, and employs the Goodlet modification of the Marx circuit (Fig. 4). Calculations show that it has a wave form of 0.5/28, and that the wave is nonoscillatory by virtue of the 1000-ohm series resistor.

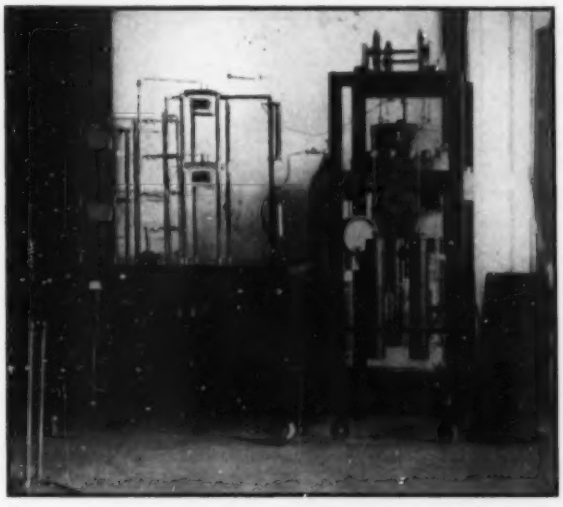

Fig. 3. Four-stage impulse generator and pressure tank.

[32] J. Slepian, Elec. World **91**, 746 (1928). A. von Hippel, Zeits. f. Physik **80**, 33 (1933).

Charging of the impulse generator is done by means of a voltage doubler circuit giving a maximum voltage of 20 kv. With a reversing switch of special design, the output voltage can be made either positive or negative with respect to ground, as desired. By means of bevel gears and insulating rods the four spark gaps of the generator can be adjusted simultaneously and a counter is arranged to record the gap setting. The output voltage of the generator has been calibrated against gap setting, using a 62.5 mm sphere gap.

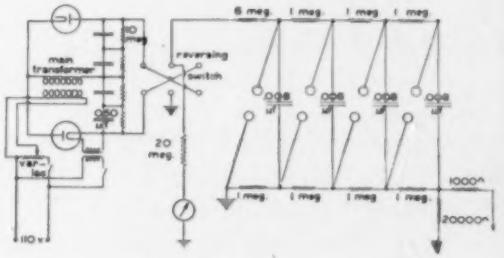

Fig. 4. The impulse generator circuit.

On the right of Fig. 3 is seen the pressure tank in which the discharges are photographed. The tank can be pumped down to a pressure of 10^{-3} mm by means of a mercury diffusion pump in series with a mercury jet pump, which in turn is backed by a mechanical pump. Gas is admitted through a copper U tube which is immersed in a mixture of dry ice and alcohol to freeze out condensable impurities. A thermocouple gauge, a mercury manometer, and a 600-lb. steam gauge are used for pressure measurements. The tank can be isolated from the vacuum system by a ½-inch-diameter globe valve.

Figure 5 shows a cross section of the tank. An octagonal brass plateholder 1 is operated from outside the tank through a valve bonnet 3, and a register 4 is provided to indicate the correct plate position. Each plateholder has a 3¼-inch-diameter hole which is concentric with the high voltage electrode 10. The high voltage insulator 2 is of Pyrex glass; the high voltage electrode slides in a brass fitting at its lower end. A fiber rod 5 connects the electrode 10 to a guided steel rod which carries a roller 6. This roller rides on a cam plate 7 screwed to the

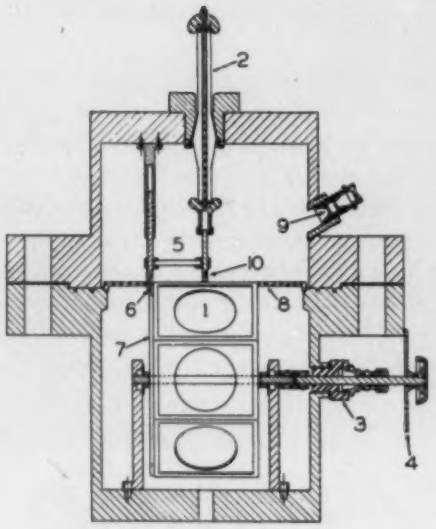

FIG. 5. Cross section of the tank.

plateholder, and is so profiled that as the latter is turned from one position to the next the electrode is lifted from the center of one plate to the center of the next. A steel ground plate 8 is arranged to fit flush with the edge of the plateholder. A quartz window 9 is used for visual observation of the discharges and also for adjusting the electrode.

The "point" electrode on top of the photographic plate is formed by the highly polished flat end of a ¼-inch steel rod. Point and plateholder together make up a point-ring electrode system which can be changed into a point-plane arrangement by slipping a thin metal sheet under the photographic plate. Each system has its own merits: The point-plane system, on account of its higher capacitance and field strength, allows the growth of larger negative figures; the point-ring arrangement with its weaker field distributions gives larger positive branches with more details.

The following procedure is adopted in making a run: Eight plates (Eastman D-C Ortho 9×12 cm, 1.25 mm thick) are loaded into the holder and the tank top is bolted down. The tank is then pumped out until a satisfactory vacuum is obtained, and gas is admitted through the cooled U tube. At the desired pressure the admission valve is closed. The reversing switch is set for the required polarity, the counter is set for the required voltage, and the filament and plate switches in the charging set are closed. The charging voltage is now increased by means of a Variac auto-transformer in the primary of the plate transformer, and when the spark gaps break down the plate switch is opened. The plateholder is then turned to a new position and another figure made at the required voltage and pressure.

The procedure in the case of mixtures of carbon tetrachloride and nitrogen is to place a small open beaker of carbon tetrachloride in the tank after loading, and to pump with a water aspirator, at the same time streaming in nitrogen. After about half an hour the nitrogen inlet valve is closed and the aspirator shut off. Thus the carbon tetrachloride assumes its correct partial pressure at a low total pressure, and between exposures it is necessary to wait only the time required for the thorough diffusion of the carbon-tetrachloride vapor into the nitrogen. After a run with Freon, dry ice is packed round the supply cylinder and the gas recovered from the tank.

THE ORIGIN OF THE FIGURES

When the electric impulse wave strikes the point-plane gap (Fig. 2) a momentary discharge, barely visible to the eye, surrounds the point electrode at the plate surface. Some doubt has arisen as to whether or not the Lichtenberg figure afterwards developed has been created by this feeble light radiation. It is possible, for instance, to create latent discharge figures on plain glass plates by intense impulse waves which even after several days can be made visible by breathing upon the surface. These breath-figures,[23] generated by resistance of the flashed surface to condensation, may be developed permanently with silvering solution, as the authors found. It is therefore necessary to establish experimentally the origin of the photographic pattern.

For this purpose some plates were covered with a clear glyptal coating, thus prohibiting direct contact between the discharge and the emulsion. After dissolving the protecting layer the picture could be developed exactly as before. But if a dye cutting out the effective photo-

[23] J. T. Baker, Phil. Mag. **44**, 752 (1922).

graphic light is added to the glyptal, the picture on the underlying plate is completely suppressed. Hence the authors feel safe in stating that their pictures represent mainly a photographic record of the light emission of the discharge.

The Primary Figures

Starting with low pressure, for both polarities a general haze is recorded, corresponding to the positive column of the glow discharge. Successive avalanches overlap without leaving individual traces.[34] It was possible to photograph single avalanches in this pressure region just below the breakdown voltage by first ionizing the gas with a high frequency discharge and then applying the impulse wave. Sufficient primary electrons were now present for successfully developing several strong avalanches in statistical angular separation, before the discharge died away (Fig. 6). Increasing the pressure to about 50 mm induces the continuous discharge to split up into a discontinuous pattern whose shape is peculiar to the polarity of the electrode. The positive figure presents a system of sharp branches relatively widely spaced, the negative figure consists of broad sectors separated by narrow radial dark lines (compare Fig. 2).

This appearance of a structure becomes understandable by considering the direction and space-charge effect of the electronic impact ionization[35] (Fig. 7).

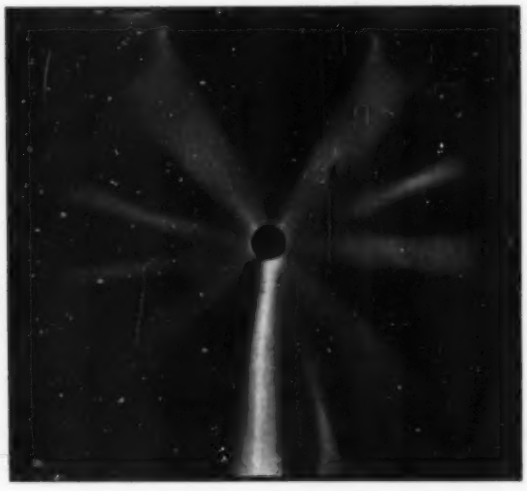

Fig. 6. Single avalanches in N_2 (25 mm, 4.4 kv).

[34] At minimum pressure we could also record a blurred positive-discharge figure of a new type with separated branches; its significance will be studied later.

Primary electrons existing around the positive electrode become accelerated into a field of increasing intensity. In this way they are effectively guided and the electron avalanches disappearing into the anode leave behind radial space charge of positive ions. Near these charged channels the field becomes concentrated and new avalanches strike into these subsidiary channels, lengthening and branching the path. The field in the interspace becomes surrounded by the

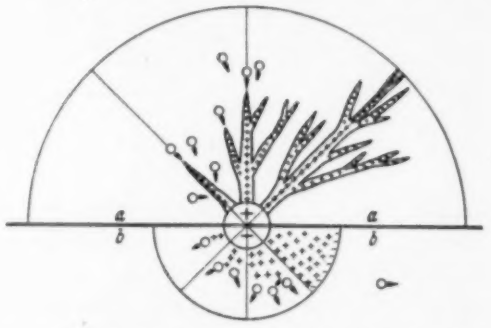

Fig. 7. Generation of the positive (*a*) and of the negative (*b*) Lichtenberg figure. o = electrons.

growing brushes and too weak for effective ionization; hence the avalanche systems stay separate.

Around the negative point electrode the situation is very different. Electrons liberated at or near the cathode are projected into a field of decreasing intensity. The positive space charge left behind weakens the radial field component and creates a tangential one, thus spreading the ionization over a sector. Succeeding avalanches concentrate the field more and more into a steep cathode fall at the cathode, while in the positive figure the cathode fall remains at the tips of the branches. Each sector of the negative figure and each branch of the positive figure owes its existence, in principle, to one primary electron and its successors. The figure attains its final size when the field strength at the boundary has decayed below the value necessary for effective ionization.

This interpretation of the figures can be supported by additional experimental evidence.

[35] A. von Hippel, Zeits. f. Physik **80**, 19 (1933); Ergebnisse der exakten Naturwiss. **14**, 79 (1935).

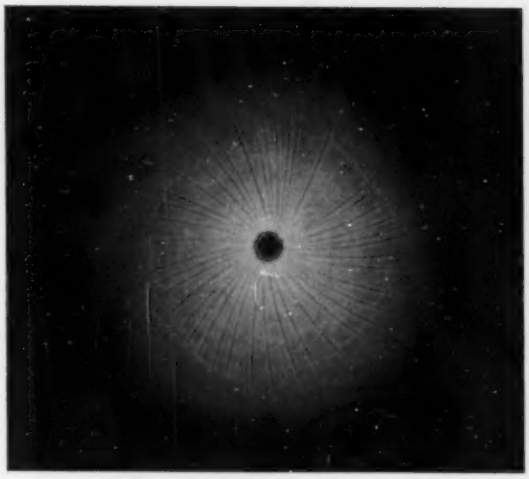

FIG. 8. Bending of the negative figure in a strong magnetic field. (210 mm, 15 kv, 13,800 gauss).

A strong magnetic field perpendicular to the plate surface causes a bending of the pattern, and the observed direction of bending corresponds to the supposition that moving electrons are responsible for the structure development.[36] Bending takes place much more readily in the case of the negative figures, which show clearly an increase of curvature with increasing distance from the center (Fig. 8).[37] Both facts are in agreement with the field distribution claimed above.

While the action of the magnetic field demonstrates the electronic activity in the figures, the influence of electro-negative gases on the discharge can establish the role played by the positive space charge. Addition of carbon-tetrachloride vapor to nitrogen changes the structure of the primary figures completely. Not only does the diameter shrink to a small fraction of its original size but also the fine structure of the positive branches and the sharp subdivision of the negative sectors is lost. (Compare Fig. 9 with Fig. 2; the diameter of the point electrode is $\frac{1}{4}$ in. in all figures unless otherwise stated.) This decisive activity of small admixtures of carbon tetrachloride is easily understood. Electron impact splits the carbon-tetrachloride molecules into two highly electro-negative components, CCl_3 and Cl. Both trap slow electrons, thus hindering the start and quenching the growth of electronic avalanches. The negative ions formed drift slowly through the field like the positive ones, smoothing out the sharp boundaries of the

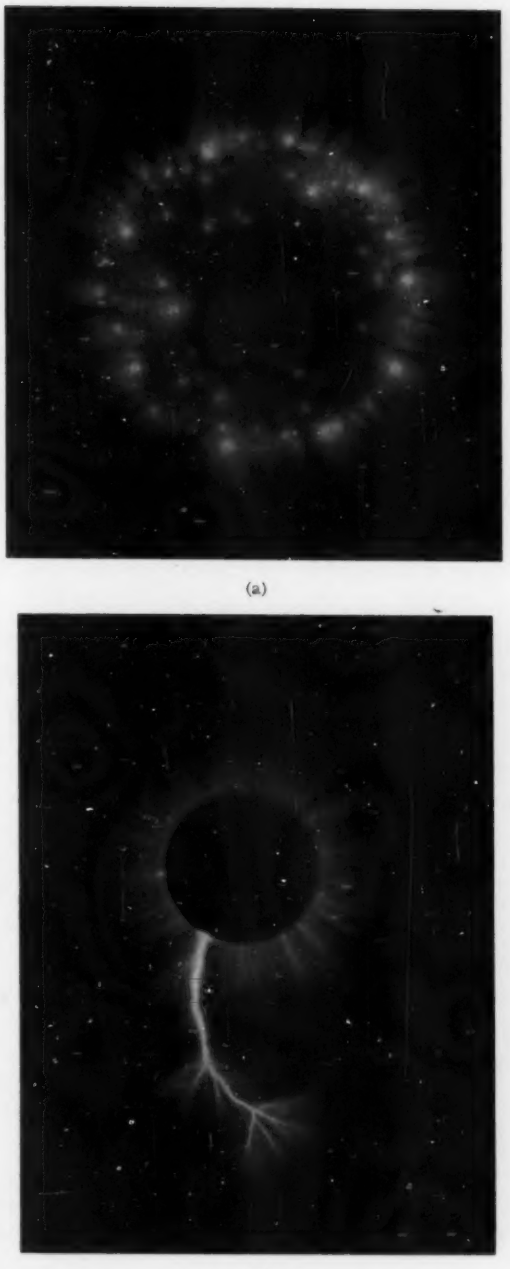

(a)

(b)

FIG. 9. The influence of CCl_4-vapor on size and structure of the primary figures. (*a*) Positive figure in 1 atmos. N_2+sat. pressure CCl_4, 30 kv. (*b*) Negative figure in 227 mm N_2+sat. pressure CCl_4, 3 kv.

[36] C. E. Magnusson, J. A. I. E. E. **49**, 756 (1930); **51**, 117 (1932).

[37] The authors are very much indebted to Professors R. D. Evans and M. S. Livingston for the opportunity to use the magnetic field of the M. I. T. cyclotron for these experiments.

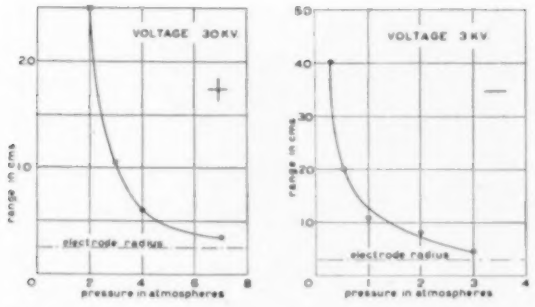

FIG. 10. Two examples of pressure-figure radius relation. (*a*) Positive figure, point-ring arrangement. (*b*) Negative figure, point-plane arrangement.

positive space charge. No sharp negative sectors appear, and instead of far-reaching positive branches only short leaves are formed.

SPARK DEVELOPMENT

Increasing pressure reduces (Fig. 10), increasing voltage increases the size of the figures (Fig. 11), but both parameters can be increased only to certain limits; otherwise a new phenomenon begins to interfere. At the point electrode a narrow, brilliant, and highly conducting[38] discharge path develops; a spark begins to grow.

Primary figures precede and accompany the growing spark and profoundly influence its behavior. The positive spark (Fig. 12) progresses continuously along a tortuous path. The negative spark (Fig. 13) jumps forward along a straight smooth path, stops, and jumps forward at an angle again, traversing its length in a number of steps if the over-voltage is not too high. Spark formation starts at lower pressures and in a

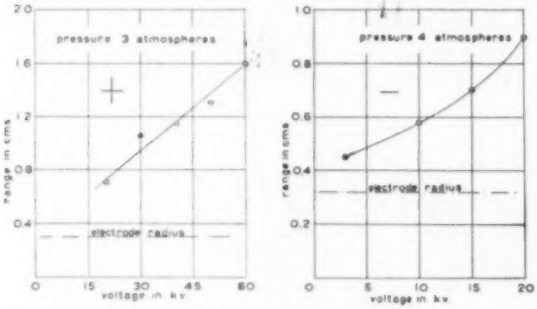

FIG. 11. Two examples of voltage-figure relation. (*a*) Positive figure, point-ring arrangement. (*b*) Negative figure, point-plane arrangement.

[38] M. Toepler, Physik. Zeits. **21**, 706 (1920).

relatively symmetrical fashion in the point-plane arrangement, where the high field strength enhances the ionization. In the point-ring arrangement up to about seven atmospheres nitrogen pressure, only primary figures develop from the positive point, then single spark tracks appear (Fig. 14).

By adding to the space-charge idea (Fig. 7), the assumption that the frequent passage of intense electron avalanches over the same path creates a highly conducting plasma (see p. 876), all the observations described fall into a logical relation with each other. The positive sparks progress by continuously transforming positive branches into plasma (see Fig. 12); therefore they bend back and forth, following the statistical directions of the preceding avalanches. The spark-head is practically at the potential of the point electrode; the process starts only if this initial potential is sufficiently high, but then it proceeds without interruption.

FIG. 12. Development of the positive spark from the primary figure.

At the negative point electrode (Fig. 15) the plasma develops as a result of the steep cathode fall created by the primary figure. The spark track normally starts in the middle of a sector where the highest ionization activity can be expected, and progresses straight forwards, using the high field gradient of the positive space charge for intensified ionization. At the boundary of the primary figure the spark-head stops because here the field gradient has decayed to about its original value. A new primary figure

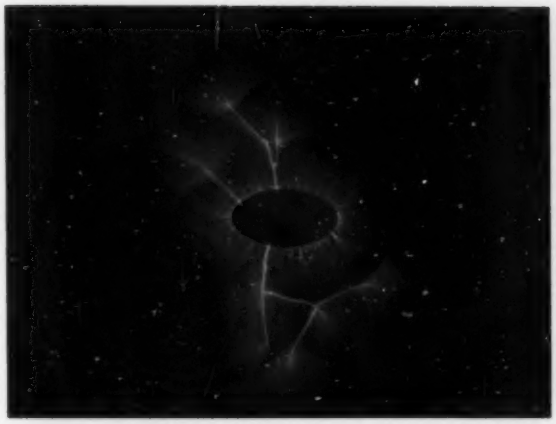

FIG. 13. Negative spark developing in steps (elliptical electrode, 1 atmos., 10 kv).

develops the necessary cathode fall for the next advance. Owing to positive space charge the steepest fall may easily develop at the junction of both figures and cause a sharp break in the spark path.

Up to the highest pressures used (31 atmospheres) positive and negative sparks can be distinguished by their characteristic appearance even if the guiding structure of the primary figures shrinks to very small dimensions (Fig. 16).

THE BACK FIGURE

On the negative plates taken at low pressures (see, for instance, Fig. 2) a ghost-like structure appears behind the sectors. Observed by earlier workers, it had been attributed to circuit oscillations but our system did not oscillate. Closer examination revealed a new and very interesting story.

Increase of pressure sharpens the structure of these "back figures" (Fig. 17); they change from broad foggy trees to sparks traveling preferentially along the outer edges of the negative primary figures (Fig. 18). These sparks of pronounced positive character are soon a dominating factor in the landscape of the surface discharge (Fig. 19), they follow the negative sparks (Fig. 20), and climb like ivy over the negative tree trunks.

All the evidence indicates that the back figures are lightning strokes discharging the negative clouds when the transient voltage

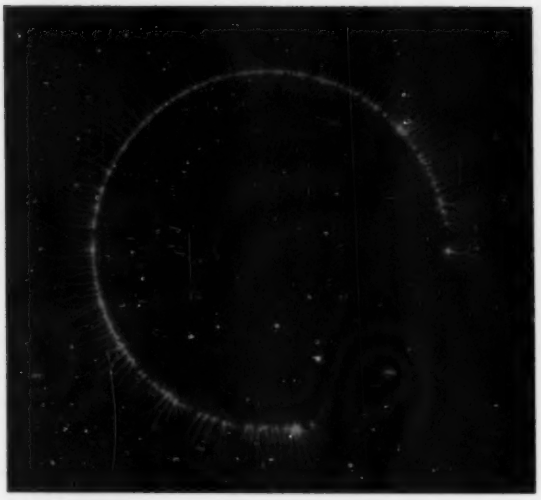

(a)

(b)

FIG. 14. Change from primary figure to single positive spark by increase of pressure. (*a*) 7 atmos., 40 kv; (*b*) 8 atmos., 40 kv.

applied across the electrodes dies away. Fig. 21 schematically describes the situation in terms of surface charge and its removal for a typical case such as Fig. 19. After a rapid building up of the cathode fall by the primary negative figure, a negative spark develops from a preferential point, branches sharply, and covers an appreciable area with a new primary figure. The external voltage starts to fall, and soon the electrode

becomes positive with regard to the negative parts of the cloud. At the point of highest gradient the return flow of electrons starts with sufficiently intense ionization to create a positive spark. Using the large electron supply available in the negative surface charge, the spark grows rapidly and neutralizes the two-dimensional cloud as far as the intensity of the field allows. The final neutralization of the remaining charge is a slow process of local recombination and conduction without the formation of new traces. Lichtenberg figures by powders (see Fig. 1) testify to the long persistence of the surface charges.

If a spark-over occurs, the back figure does not develop extensively from the cathode point, but short branches grow directly at the spark tracks. The exterior field having been removed, recombination between surface charges by ionization takes place wherever the potential difference is sufficient.

The Discharge in Electro-Negative Gases

The usefulness of carbon tetrachloride, Freon (CCl_2F_2), and other gases in suppressing corona discharges has been widely recognized of late on account of the increasing importance of high voltage machinery,[39] but apparently no explanation of the mechanism involved has been given. Here, therefore, we have a good case for proving our statement that Lichtenberg figures are a powerful tool in clearing up discharge phenomena.

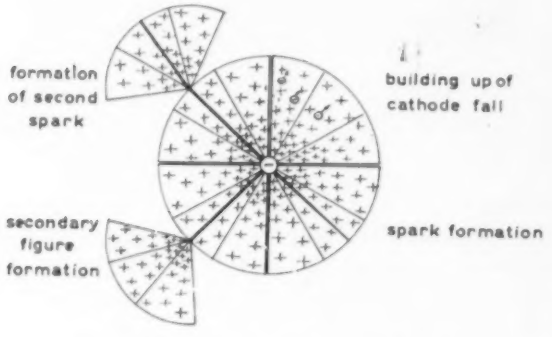

Fig. 15. Growth of the negative spark.

[39] See, for instance: E. E. Charlton and F. S. Cooper, Gen. Elec. Rev. **40**, 438 (1937); M. J. Rodin and R. G. Herb, Phys. Rev. **51**, 508 (1937).

In discussing the primary figures, the action of carbon tetrachloride has already been considered and used for demonstrating the importance of the positive space charge. The electro-negative particles infringe on the discharge mechanism at three different phases: By the capture of primary electrons the starting

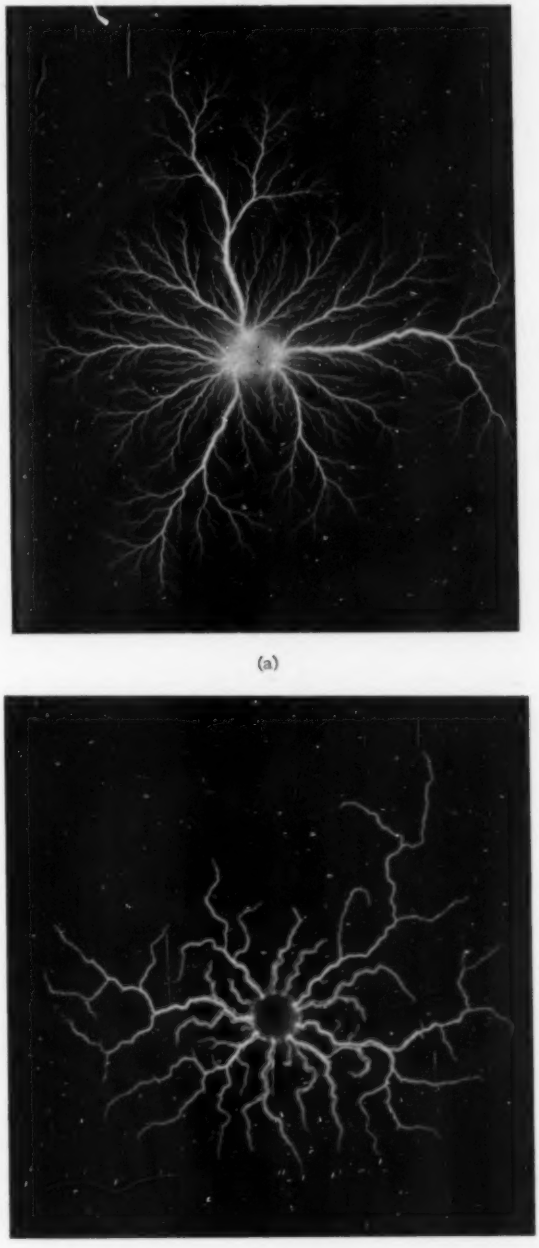

(a)

(b)

Fig. 16. Positive and negative sparks at highest pressure in the point-plate arrangement. (*a*) Positive sparks, 30.3 atmos., 30 kv. (*b*) Negative sparks, 31 atmos., 50 kv.

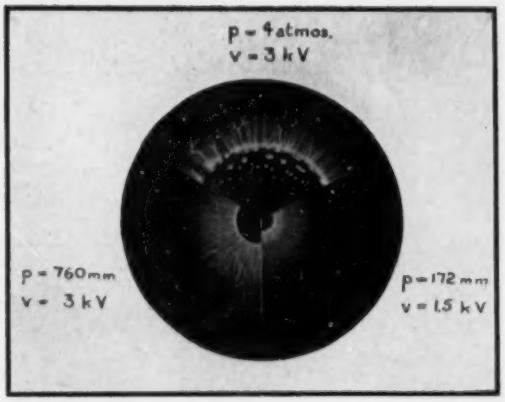

FIG. 17. Sharpening of the back-figure with pressure.

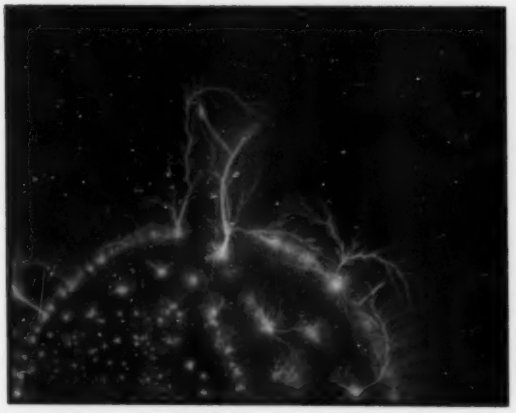

FIG. 19. Negative primary figure, negative spark and back figures forming a landscape (16 atmos., 30 kv).

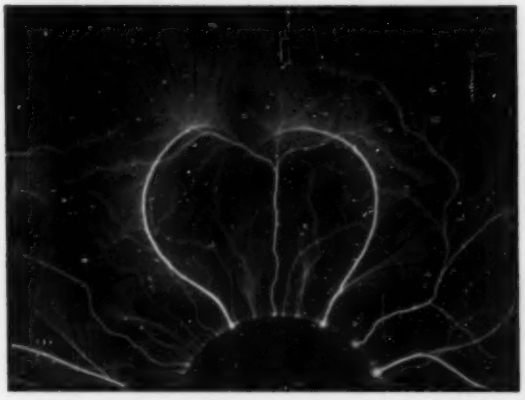

FIG. 18. Negative sparks with primaries and back-figure sparks (11 atmos., 50 kv).

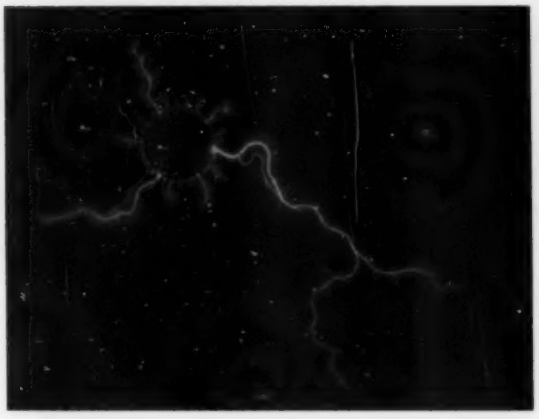

FIG. 20. Negative sparks followed by back-figure sparks (18.5 atmos., 50 kv).

of new avalanches becomes much more difficult, by the trapping of slow secondary electrons the growing of avalanches is badly handicapped, and by formation of negative ionic space charges in addition to positive ones the field is decisively altered. In consequence the primary figures lose structure and shrink tremendously (compare Figs. 9 and 2); the corona discharge is largely suppressed.

The activity of a "suppressor-gas" is not constant. The decomposition of the original molecule into electro-negative components, the trapping of electrons by the decomposition products and the release of electrons from negative ions by violent collisions depend on the character of the gas *and* the experimental conditions. Already a small addition of suppressor gas will have a very strong effect if the electrons make many impacts while being accelerated. Increasing percentages of admixture have in this case less and less effect because the probability that every electron will react approaches unity (Fig. 22). Increase of the field gradient, on the other hand, decreases the number of critical collisions and enhances the probability of liberation for electrons already trapped. The suppressor-gas will only be felt if present in larger amounts, the ionization becomes more violent, plasma develops, and sparks begin to grow (Fig. 23). The observation, that suppressor-gases are more effective against corona than against sparks,[39] is only a consequence of the fact that in the first case the field is lower and therefore more favorable for trapping than in the second.

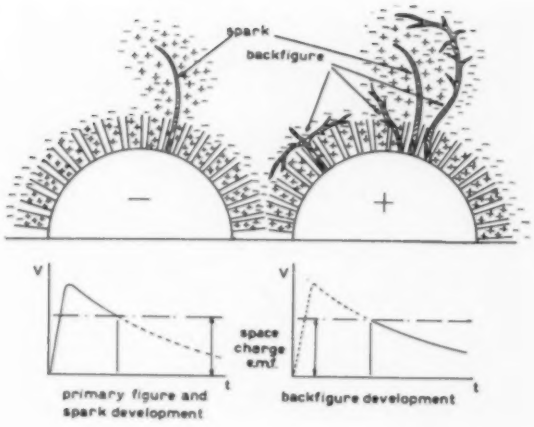

FIG. 21. Development of the back figure.

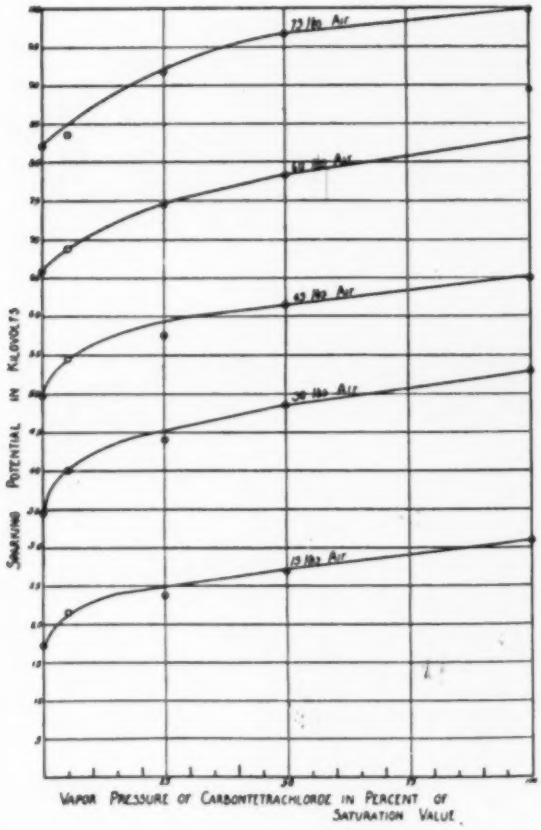

FIG. 22. The influence of CCl_4 vapor on the breakdown strength of air (taken by Rodine and Herb, reference 39).

The growth of sparks is handicapped by the electro-negative gas present, because only in the steepest field zones are free electrons available. Therefore the "stepping" of the negative spark (see Fig. 13) can become much more pronounced

FIG. 23. Negative primary figure, spark development and radial spikes ($1\frac{1}{2}$ atmos. N_2+saturation pressure CCl_4, 3 kv).

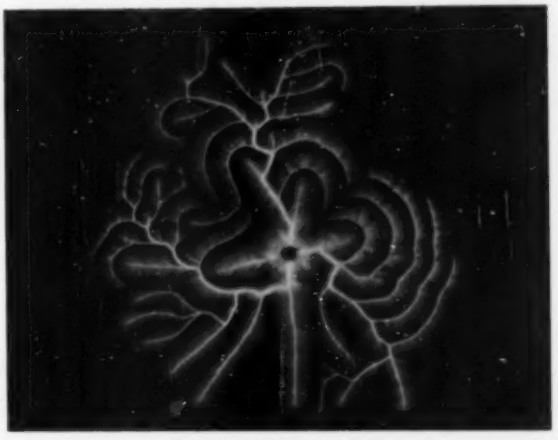

FIG. 24. Pronounced stepping of the negative spark (1 atmos. air +CCl_4 sat. pressure, 4.5 kv, film, electrode 2 mm diameter).

(Fig. 24) and the speed of spark propagation much reduced. But back figures develop as before, marking with their branching the seat of the negative surface charge (see Fig. 23). A comparison with a positive spark structure in Freon (Fig. 25) confirms strikingly the positive character of the back-figure spark.

In Fig. 23 a new phenomenon becomes visible, and Fig. 26 shows a similar effect for the positive discharge—that of the appearance of radial spikes of enhanced ionization. In the case of the negative figure we assume that the negative space charge may become so dense that electrons at the outer boundary are projected outwards, starting new avalanches. In some cases periodic ring structures are formed by periodically revived ionization. These effects disappear if the electronegative gas is highly concentrated. A more detailed study is necessary.

Deviations from Paschen's Law

Paschen's similarity law, stating that the breakdown voltage of a spark gap tested under a gas pressure p with a gap distance d depends only on the product pd, does not hold for high pressures. The breakdown strength increases more slowly than is anticipated and may even pass over a maximum.[40] It is dependent on the surface condition of the electrodes: roughening of one electrode, whether it is positive or negative, reduces the breakdown voltage by approximately the same amount.[41] Self-sustaining discharge currents exist before breakdown, decreasing in magnitude with increasing smoothness of the electrode surfaces (Fig. 27). Both observations indicate the importance of point discharges created at rough spots on the surface for the final breakdown.[41]

We believe that Lichtenberg figures again can reveal the actual phenomenon. For instance, Fig. 28 shows how at preferential points the primary figure changes into a spark discharge and out of this plasma stem electron clouds are erupted into space. On many of our pictures the importance of preferred points for starting a spark of either polarity is demonstrated (see, for instance, Figs. 14 and 16 to 20). The reasons for their development are discussed above.

Very interesting is the observation[41–43] that the breakdown strength and prebreakdown current for a positive point-plane gap suddenly drops decisively if the pressure is increased above a certain critical value (Fig. 29). This fact appar-

[40] J. Goldman and B. Wul, Tech. Phys. U. S. S. R. **1**, 4, 497 (1935); **3**, 16 (1936).

[41] A. H. Howell, Elec. Eng. **58**, 193 (1939).
[42] H. H. Skilling, Elec. Eng. **58**, 161 (1939).
[43] T. Goldman, Tech. Phys. U. S. S. R. **5**, 355 (1938).

Fig. 25. Positive primary figure and sparks in Freon (410 mm CCl_2F_2, 3 kv, point-plane arrangement).

Fig. 26. Positive primary figure and radial spike structure (1 atmos. air+saturation pressure CCl_4, 30 kv).

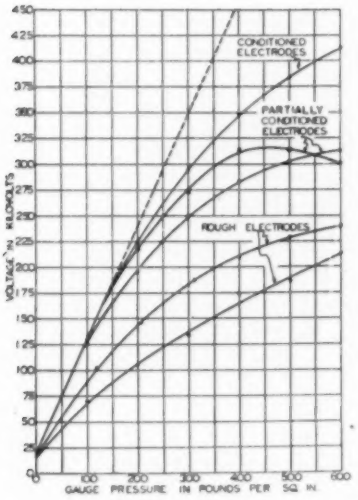

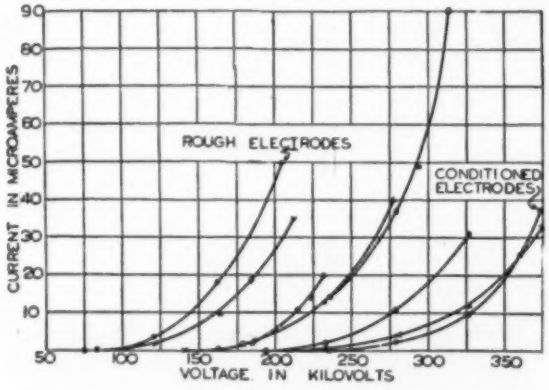

FIG. 27. Effect of electrode conditioning on the breakdown voltage and the current flow between plane electrodes (taken by Howell, reference 41).

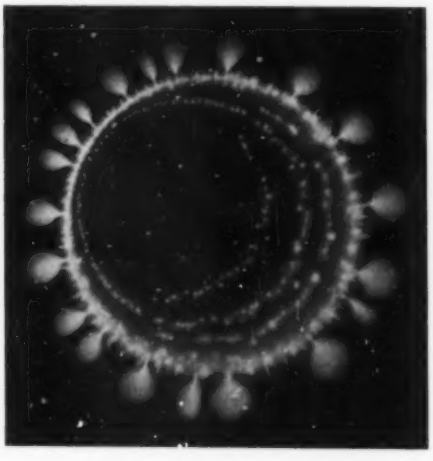

FIG. 28. Electronic eruptions (7 atmos.+saturation pressure CCl_4, 20 kv).

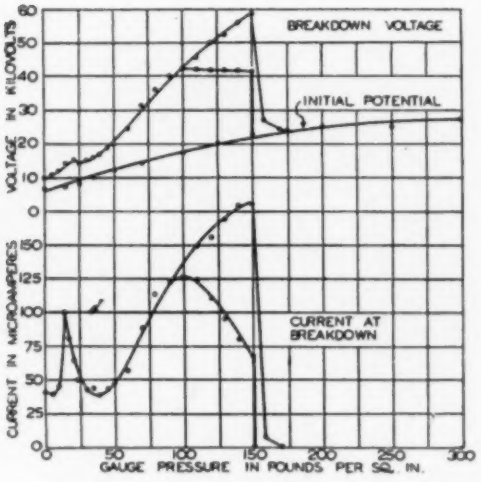

FIG. 29. Voltage and current characteristics for positive point-to-plane electrodes spaced one-fourth inch in air (taken by Howell, reference 41).

ently corresponds to our observation (Fig. 14) that above a critical pressure single positive spark tracks may develop without a preceding primary figure. The ionization density of a single successful avalanche seems to be high enough under these conditions to create the plasma state. Therefore the breakdown voltage in Fig. 29 drops to the initial (offset or starting) potential, and the predischarge current to zero.

CONCLUDING REMARKS

The authors are fully aware that it may be a dangerous undertaking to extrapolate from two-dimensional to three-dimensional discharges. But so far as we see today, the interpretation and use made of Lichtenberg figures in this paper can be justified. There are certainly differences if the importance of photoelectric liberation, the mobility of space charge, and the time of development are at stake. Experiments with impulses of sharply timed duration will give more information about these aspects, and these are planned for the near future.

On the other hand, the authors feel that a discussion of breakdown in gases should not forget that Lichtenberg figures exist and that they reveal in their primary figures phenomena which guide the discharge and which cannot otherwise be photographed. The positive and negative sparks in space are similar in appearance to

surface discharges, as one of us demonstrated a number of years ago[44] (Fig. 30). Therefore even for the stepped leader strokes[45] in thunderstorms the stepping process of the negative spark discussed above should be considered as one possible explanation.

The authors would like to thank Dr. Littleton, of the Corning Glass Works, for the Pyrex insulators used in their apparatus.

[44] A. von Hippel, Zeits. f. Physik **80**, 44 (1933).
[45] B. F. T. Schonland and H. Collins, Proc. Roy. Soc. London **143**, 654 (1933). B. F. T. Schonland, H. Collins, and D. T. Malan, Nature **134**, 177 (1934).

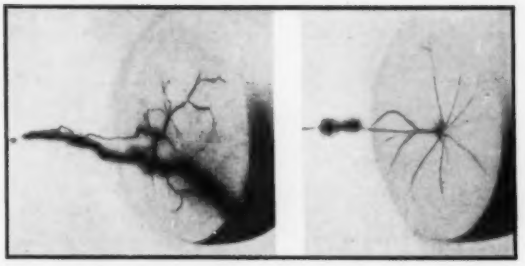

FIG. 30. Discharge between a metal point and a semiconducting plate electrode in air. (*a*) Positive spark striking the negative plate. (*b*) Negative spark striking the positive plate.

A Note on the Elastic Properties of Vinyl Sheeting

S. BATESON
Duplate Safety Glass Company of Canada, Ltd. Oshawa, Ontario, Canada
(Received April 19, 1939)

INTRODUCTION

THE introduction of plasticized vinyl sheeting for use in connection with the manufacture of safety glass has added another member to the rapidly increasing group of synthetic resins which are playing an important role in modern industry.

Vinyl sheeting is prepared by treating a polymerized vinyl acetal resin with a plasticizer, and either calendering or extruding the treated resin into sheet form. The function of the plasticizer is to impart flexibility to the otherwise rigid plastic. A material results which possesses great elasticity, high tensile strength and remarkable recovery upon removal of the load. In addition to these properties vinyl manifests in a marked degree elastic "after effect" or "creep" common in rubber, rayon, nitro-cellulose and other allied materials. In the following procedure the elongation of vinyl sheeting under constant load was observed. The samples selected for test were cut from standard duPont sheeting 0.015 inch thick. This particular product consists of a butyraldehyde replacement resin plasticized with "3GH." The test strips were carefully washed and dried at a temperature of 50°C which is effective in removing residual stress due to rolling.

EXPERIMENTAL METHOD AND RESULTS

A strip of vinyl ½ inch wide and 15 inches long was clamped at one end and allowed to hang freely. A load was applied to the free end of the strip and the elongation observed by means of a scale rigidly attached to the weighted end. The test strip and support were enclosed and maintained at constant temperature.

In Fig. 1 are presented experimental curves showing the elongation of the strip with time under constant load at 20°C. Each curve corresponds to a different load, and indicates that an initial instantaneous elastic stretch accompanies the application of the load. Afterwards the elongation increases slowly. When the load is removed, relaxation takes place accompanied by elastic "after effect." After standing for several hours under no load, the vinyl strip always returned to its original length for a particular temperature.

TABLE I.

W(GRAMS)	S_0	a_1	a_2
27.6	0.082	0.0069	0.0001
47.6	.105	.0222	.0000
67.6	.120	.0320	.0005
97.6	.132	.0573	.0010

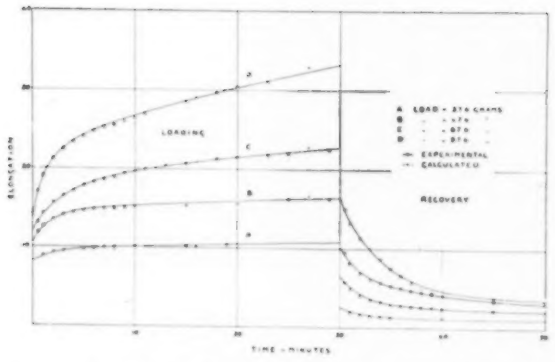

FIG. 1. Elongation and recovery under constant load at 20°C. Calculated values derived from Eq. (1).

The curves in Fig. 2 represent the elongation with time for a load of 27.6 grams at temperatures of 20°, 30°, 40° and 50°C. The initial elongation is greater and a decided increase in creep occurs at 40°C. For higher temperatures recovery was incomplete, indicating that plastic flow existed.

The experimental results of Fig. 1 fit with reasonable accuracy the equation

$$S = S_0 + a_1 t^{\frac{1}{2}} + a_2 t, \qquad (1)$$

where S is the increase in length divided by the original length of the strip and S_0, a_1 and a_2 are constants for a given load. The recovery curves also fit Eq. (1), except that S is now the difference between the elongation at the time of unloading and at any subsequent time t. Eq. (1) is similar to the formula adopted by Filon and Jessop[1] for the increase of strain in nitro-cellulose under constant load. See Table I.

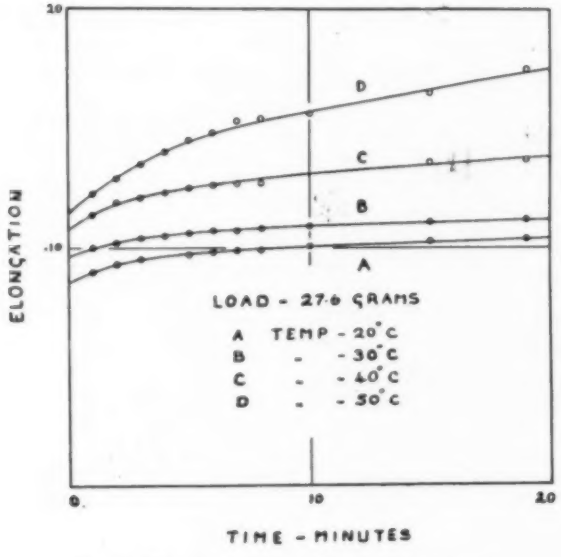

FIG. 2. Elongation at various temperatures.

COMPARISON WITH THEORY

Results similar to those observed in vinyl may be explained in a mechanical way[2, 3] by a model consisting of a system of perfectly elastic springs embedded in a viscous liquid. For higher temperatures, at which the yield point is exceeded and plastic flow takes place, the addition of a plunger, moving in a viscous medium, connected in series with the system affords a rough mechanical analogy.

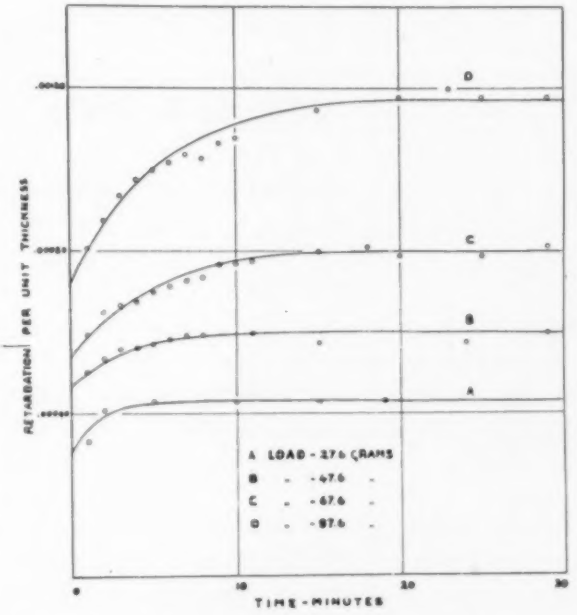

FIG. 3. Retardation under constant load at 20°C. Compare with Fig. 1 for corresponding elongations.

Basically vinyl consists of a series of long chain polymers or micelles which may be oriented at random or grouped about a preferred direction, depending upon treatment of the material. During the process of calendering a degree of orientation is imparted to the micelles. When the material is stretched the micelles tend to orient

[1] Filon and Jessop, Phil. Trans. **A223**, 89–125 (1923).
[2] R. Houwink, *Elasticity, Plasticity and Structure of Matter* (Cambridge University Press), p. 64.
[3] G. W. Scott Blair, *An Introduction to Industrial Rheology* (Blakiston's Son and Company Inc.), p. 94.

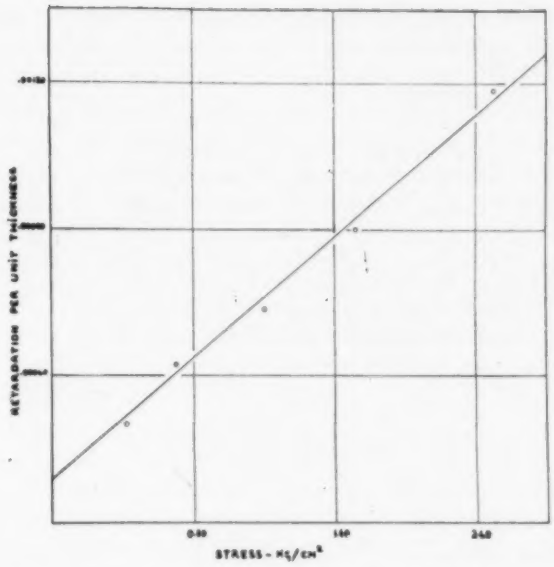

FIG. 4. Stress and retardation at 20°C. Slight residual double-refraction present.

themselves more and more about the direction of stretch. The material when stretched is therefore optically anisotropic and exhibits double refraction. These properties have been studied[4] in a number of careful experiments. Double refraction measurements were also carried out in the present instance for the information they might add to the time-elongation measurements.

MEASUREMENTS OF DOUBLE REFRACTION

Light of wave-length 5890A was polarized at 45° to the axis of elongation and passed through the test strip. The retardation produced upon loading was read by a Babinet compensator, simultaneously with the elongation as read on the scale; the eyepiece and fiduciary mark of the Babinet served the double purpose of sighting telescope and compensator. The resulting observations are presented in Fig. 3.

For a given load the retardation per unit thickness attains a value which is constant within the limits of error, while the extension still continues to increase. At higher temperatures this is even more noticeable, as shown in Table II.

[4] H. W. Farwell, J. App. Phys. **10**, 109 (1939).

TABLE II. *Load—27.6 grams.*

TIME	1 MIN.	4 MIN.	7 MIN.	15 MIN.
$T=50°$ S	0.123	0.140	0.151	0.165
Retardation	.00029	.00030	.00027	.00024
$T=40°$ S	.114	.123	.127	.136
Retardation	.00030	.00032	.00030	.00028
$T=30°$ S	.100	.105	.107	.111
Retardation	.00033	.00033	.00036	.00038
$T=20°$ S	.090	.097	.099	.103
Retardation	.00033	.00043	.00043	.00043

Results such as these suggest that most of the orientation takes place due to the initial elastic extension, and that during the "after effect" further orientation is small.

The proportionality between stress and retardation is illustrated in Fig. 4.

CONCLUSIONS

The specimens of vinyl sheeting examined recover completely upon unloading at temperatures below 50°C. During both extension and recovery, creep is pronounced, the elongation obeying an empirical law of the form $S=S_0+a_1t^{\frac{1}{3}}+a_2t$.

Elongation and birefringence are not strictly proportional but exhibit considerable lag.

Elasticity, creep and birefringence all depend upon the temperature as well as upon the amount of plasticizer present. These properties are also influenced by the viscosity of the polymer from which the acetal resin is derived. Observations of creep and double-refraction in sheeting derived from polymers of different viscosity should prove interesting.

In conclusion it should be noted that the present experiments were confined to strips cut in the direction of extrusion. Enough information is available to indicate different results for test strips cut from the width of the roll.

Piezoelectric *Versus* Mechanical Spring Pressure Gauge

R. Alden Webster
7128 Ninth Street, N. W., Washington, D. C.

That difficulties in the use of various types of pressure gauges warrant meticulous scrutiny in the rendering of an accurate pressure-time curve has advanced each type of gauge for particular work. In powder gas and internal combustion engine gas pressures the spring type and piezoelectric type offer great possibilities with the first a self-contained unit and the latter a charge-collecting device, and with the former following the true curve by an admitted time lag and the latter assumed to be responding instantaneously. Sparse comparative records of the two show the case to be more nearly the reverse of what the popular assumption leads one to believe. Fuller data are needed to determine the comparative lagging characteristics of both types.

DR. A. G. Webster developed a spring-type pressure gauge for use in small arms that had sufficiently high natural frequency to follow pressure curves of powder gases. Many devices have been used for investigating gas pressures as well as hydraulic pressures. At the National Bureau of Standards both the mechanical and the piezoelectric gauges were used for powder gas pressures. It was there that the writer first worked with the Curtis-Duncan mechanical spring gauge for measuring pressures in the chambers of naval guns. Likewise the Eckert-Karcher work with the piezoelectric gauge gave the Army Proving Ground at Aberdeen, Maryland, the start in better understanding of gas pressures in field guns.

All articles written on the piezoelectric gauge speak of the "instantaneous" response of the crystal pile. An article in the April issue[1] of the *Journal of Applied Physics* followed the same idea. The tests the writer has seen done on a comparative basis between these two types do not indicate that the piezoelectric is any more definite in its approach to instantaneous action than the mechanical spring gauge of the Curtis-Duncan type and possibly not as good. Every experimenter agrees there is a time lag in a mechanical system caused by external friction of moving parts, elastic properties of the material, and inertia of moving parts. However, these can be minimized by designing high frequency springs, which naturally have high load, small-displacement characteristics. Offsetting this lag somewhat, the piezoelectric gauge has a much smaller displacement for equal loads, yet it is piston-actuated as are the spring gauges. Here lies a factor that materially affects the two gauges alike, i.e., the starting friction in the initiation of the movement. This is the largest force of friction in the entire course of the plunger, however small or great that motion may be.

Figure 1 is a plot of curves taken on two piezoelectric and one mechanical spring gauge at Aberdeen Proving Ground in collaboration with Doctors Eckert and Karcher.[2] This distinctly indicated on a simultaneous basis that

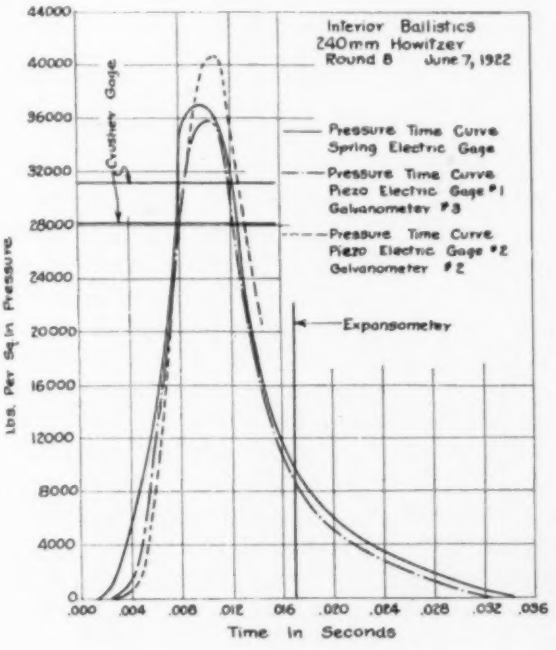

FIG. 1.

[1] "RCA Develops Electric-Engine Indicator Unit," **10**, viii (1939).

[2] Their work is reported by Dr. J. C. Karcher, Nat. Bur. Stand. Sci. Pap. No. 445.

the Curtis-Duncan spring gauge actuated prior to the piezoelectric in the order of a millisecond. This point was discussed with Dr. Eckert at the time, but there was found no practical cause for the condition. It seemed so contrary to all that was claimed by the advocates of the piezoelectric gauge that the idea of its actuality was scoffed at.

The difficulty with which leakage of the electric charge is kept to a negligible amount is cause for some concern for routine use of such a gauge. Possibly this leakage factor is the great cause of the discrepancy noted above. Although it is not an actual time-lag effect, it may very easily show up as such. In this case the peak pressure could be reduced, however. That was not true in the test herein cited, since the average of the two piezoelectric gauge peaks was higher than the Curtis-Duncan. On the other hand, if, because of comparative slowness in calibration, the leakage under calibration should amount to more than that in actual use, where the period of measurement is much shorter, the peak of the curve when interpreted according to that calibration could indicate considerably higher pressures. These conditions would then be misleading in comparative interpretation of simultaneous records of the two types of gauges whether the piezoelectric were either too high or too low.

One great advantage in the mechanical gauge is the fact it is a self-contained unit, calibrated without the characteristics of a recording apparatus entering into the calibration, while the piezoelectric gauge is only a charge producer with the recording apparatus as a part of the gauge. This fact, therefore, militates against accurate calibration in places where leads for conveying the charge have to be extended or passed near interfering inductive circuits. Effects of this condition are noted in the writer's paper on "Piezo-Electric Gauge and Amplifier."[3]

Since there are not enough comparative data for conclusively settling the issue brought up here, it is thought that possibly other experimenters may be induced to further research when opportunity permits. Anyway, healthful and enlightening discussion may prove of tremendous benefit in the realm of pressure-measuring apparatus.

---

[3] J. Frank. Inst. **211**, 607 (1931).

Here and There

Professor Ernest Orlando Lawrence of the University of California was awarded the 1939 Nobel Prize for Physics in recognition of his work in the invention and development of the cyclotron, and of the important results already obtained with the cyclotron, particularly in the field of artificial radioactivity. The award was announced November 9 by the Royal Academy of Sciences at Stockholm, Sweden. Dr. Lawrence, who is thirty-nine years old, is Director of the Radiation Laboratories at the University of California, on whose faculty he has served since 1928.

★

The Battelle Memorial Institute, Industrial and Scientific Research, at Columbus, Ohio, announced the addition to its supervisory staff of Dr. Edward Mack, Jr., who will act as technical advisor in physical chemistry to the sponsored industrial projects and will also correlate the Institute's fundamental work. Dr. Mack comes to Battelle from the University of North Carolina where he has been head of the Department of Chemistry for the past four years.

★

Dean Floyd K. Richtmyer, Dean of the Graduate School of Cornell University, died November 7th in Ithaca, New York. Dr. Richtmyer was a former president of the American Physical Society, of the Optical Society of America and of the American Association of Physics Teachers. He was also Secretary of the Association of American Universities and a former Chairman of the Division of Physical Sciences of the National Research Council. He was a member of numerous important committees and boards including the Governing Board of the American Institute of Physics and the Board of Directors of the National Geographic Society. He had been for many years Editor of the *Review of Scientific Instruments* and of the *Journal of the Optical Society of America*.

Dr. Richtmyer made outstanding contributions to the science of physics through his many researches in the field of x-ray phenomena and received in 1929 The Leavey Medal at the Franklin Institute. He was known also as an author and editor of textbooks in the field of physics. He had served on the faculty of Cornell University since 1906 and in the capacity of Dean of the Graduate School there since 1931.

Dr. Forrest F. Cleveland has been appointed Assistant Professor for the year 1939–40 at the Armour Institute of Technology, Chicago, Illinois. Dr. Cleveland was formerly at Lynchburg College, Lynchburg, Virginia.

★

Dr. Robert S. Shankland, Associate Professor at Case School of Applied Science, has been made acting head of the Department of Physics.

★

Dr. Frank J. Studer has been promoted to the rank of Associate Professor of Physics at Union College, Schenectady, New York, and Dr. Charles V. Strain, formerly of the University of Rochester, has been appointed to the Physics Staff.

★

Dr. Enrico Fermi, Professor of Physics at Columbia University and recipient of the Nobel Prize for Physics in 1938, will give a lecture on "Atomic Disintegration" Wednesday evening, January 24, 1940, in the Engineering Society Building auditorium, New York City. Dr. Fermi will be assisted by Professor Dunning in giving a demonstration after the lecture. This is a part of the program of the Winter Convention of the American Institute of Electrical Engineers. The Edison and Hoover medals will also be presented at the Wednesday evening session.

★

Sigma Pi Sigma, physics honor society, will hold its annual midwinter luncheon in connection with the Christmas meetings of the A.A.A.S. at Ohio State University at 12:30 on Friday, December 29.

★

Calendar of Meetings

December	
1–2	American Physical Society, Chicago, Ill.
4–9	17th Exposition of Chemical Industries, Grand Central Palace, New York, New York.
22–23	American Physical Society, Berkeley, California.
27–29	American Association of Physics Teachers, Columbus, Ohio.
27–Jan. 2	American Association for the Advancement of Science, Columbus, Ohio.
28–29	Sixth Chemical Engineering Symposium, Ann Arbor, Mich.
28–30	American Physical Society, Columbus, Ohio.
28–30	Geological Society of America, Minneapolis, Minn.
January	
15–19	Society of Automotive Engineers, Detroit, Mich.
22–26	American Institute of Electrical Engineers, New York, N. Y.
February	
22–24	American Physical Society, New York, N. Y.
22–24	Optical Society of America, New York, N. Y.
April	
8–12	American Chemical Society, Cincinnati, Ohio.
24–27	Electrochemical Society, Wernersville, Pa.

Contributors to This Issue

Wheeler P. Davey, a graduate of Cornell University, is Research Professor of Physics and Chemistry at the Pennsylvania State College and Consultant for the Radiological Research Institute. He is the author of *A Study of Crystal Structure* and various articles on x-rays and crystal structure.

Photographs and biographical sketches of the following contributors to this issue have already been published:

David L. Webster, page 497, Volume 10, No. 7, 1939.
M. A. Biot, page 36, Volume 9, No. 1, 1938.
John P. Blewett, page 699, Volume 10, No. 10, 1939.
Louis A. Pipes, page 187, Volume 10, No. 3, 1939.

R. Alden Webster received his M.S. from George Washington University in 1928. He has spent 25 years in the service of the United States government, holding positions in the following departments: U. S. Coast Defense Service, War Department, and National Bureau of Standards. Since 1923 he has worked in the Naval Research Laboratory dealing with research and tests on Naval Ordnance.

Sydney Bateson received his B.Sc. and M.Sc. degrees in 1930 and 1932 at Dalhousie University, and his Ph.D. from the University of Toronto in 1936. From 1935 to 1937 he was on the Physics Staff of the University of Toronto and during this time was engaged in research on spectroscopy. Since 1938 he has been research physicist with the Duplate Safety Glass Company of Canada, Limited.

Arthur R. von Hippel was born in Rostock, Germany. In 1924 he received his Ph.D. degree from the University of Goettingen. Dr. von Hippel is now Assistant Professor in the Electrical Engineering Department of the Massachusetts Institute of Technology, where he is in charge of the laboratory for Insulation Research. (His picture appeared on page 815, Volume 8, No. 12, 1937.)

Frederick H. Merrill was graduated from the University of Liverpool in 1923 with the degree of B.Eng. He was awarded a Commonwealth Fund Fellowship, studied at the Massachusetts Institute of Technology, and received his S.M. degree there in 1937. Dr. Merrill returned to England in 1939 and is at present with Imperial Chemical Industries, Ltd.

W. P. Davey

S. Bateson

R. A. Webster

F. H. Merrill

JOURNAL OF APPLIED PHYSICS

(Formerly PHYSICS)

BOARD OF EDITORS

Editor, ELMER HUTCHISSON

Associate Editors

F. BITTER
W. E. FORSYTHE
L. A. JONES
W. F. MEGGERS
B. E. WARREN
J. B. WHITEHEAD
V. K. ZWORYKIN

ADMINISTRATIVE STAFF OF THE AMERICAN INSTITUTE OF PHYSICS

HENRY A. BARTON, *Director*
MADELINE M. MITCHELL, *Publications Manager*
F. K. RICHTMYER, *Chairman, Advertising Committee*

GOVERNING BOARD

JOHN T. TATE, *Chairman*
KARL T. COMPTON
E. C. CRITTENDEN
WHEELER P. DAVEY
FLOYD A. FIRESTONE
HARVEY FLETCHER
ARTHUR C. HARDY
PAUL E. KLOPSTEG
MELVIN MOONEY
FREDERIC PALMER, JR.
R. L. PEEK, JR.
GEORGE B. PEGRAM
W. B. RAYTON
F. K. RICHTMYER
WALLACE WATERFALL

Author Index to Volume 10

References with (L) are to Letters to the Editor

Abbott, Ernest J. Sound measurements in industry—526
Auwärter, M. Rhodium mirrors for scientific purposes—705

Ballard, Stanley S. and Paul L. Gow. Accessories for spectrochemical analysis—556
Barton, Henry A. Advisory council on applied physics of the American Institute of Physics—report of meeting Pittsburgh, March 25, 1939—615
Bateson, S. Note on the elastic properties of vinyl sheeting—887
Berberich, L. J. Electrochemistry of gases and other dielectrics—697 (book review)
Binder, R. C. Motion of cylindrical particles in viscous flow—711
Biot, M. A. Increase of torsional stiffness of a prismatical bar due to axial tension—860
Bitter, F. Magnetische und elektrische eigenschaften des eisens und seiner legierungen—186 (book review)
Blackwood, Oswald. Elementary survey of physics—269 (book review)
Blewett, John P. Properties of oxide-coated cathodes. I—668; II—831
Bozorth, R. M. Modern magnetism—622 (book review)
Brahtz, J. H. A. and J. E. Soehrens. Direct optical measurement of individual principal stresses—242
Breer, Carl. New frontiers for industry—271
Brode, Wallace R. Absorption spectra as applied to molecular identification and analysis—751
Brody, I. and F. Kőrösy. Convection and conduction of heat in gases—584
Bruce, W. A. Thermal distribution and temperature gradient in the arc welding of oil well casing—578

Charlton, E. E., W. F. Westendorp, L. E. Dempster and George Hotaling. New million-volt x-ray outfit—374
Chipman, R. A. Resonance curve method for the absolute measurement of impedance at frequencies of the order 300 mc/second—27
Cobine, J. D., R. B. Power and L. P. Winsor. Reignition of short arcs at high pressures—420
Cohn, Willi M. Note on the quantitative spectrographic analysis of small amounts of rubidium and potassium in biological materials—200
Condon, E. U. Principles of statistical mechanics—691 (book review)
Cork, J. M. Heat engines—697 (book review)

Davey, Wheeler P. X-ray diffraction applied to chemical analysis—820
Dempster, L. E. (see Charlton, E. E.)—374
Dibert, R. M., R. B. Dow and C. E. Fink. Viscosity of Pennsylvania oils at high pressure—113
Dieke, G. H. Molecular emission spectra—780
Dietz, David. Cultural values of physics—86
Dobrin, Milton B. Recreating geological history with models—360
Dornte, Ralph W. Dielectric strength of benzene and heptane—514
Dow, R. B. Introduction to industrial rheology—105 (book review)
—— Text-book on crystal physics—269 (book review)
—— (see Dibert, R. M.)—113
Dunholter, H. and H. Kersten. Electron diffraction study of copper oxides—523

Elbe, Guenther von (see Lewis, Bernard)—344
Elmore, W. C. Electrolytic polishing—724
Engstrom, E. W. Television receiving and reproducing systems—455
Erikson, Henry A. Mobility of positive ions in gases—390 (book review)
—— On understanding physics—104 (book review)
Eskin, S. G. Energy measurements of reigniting a.c. arcs—631
Essig, Sanford F. Structural characteristics of certain silver films—61

Farwell, H. W. Double refraction and change in length of certain plastics—109
Feinberg, R. Simplified calculation of the arbitrary constants of a linear differential equation of the second order with constant coefficients—140(L)
Field, J. E. (see Gehman, S. D.)—564
Fink, C. E. (see Dibert, R. M.)—113
Fonda, Gorton R. Phosphorescence of zinc silicate phosphors—408
Frocht, Max M. Isopachic stress patterns—248

Gehman, S. D. and J. E. Field. X-ray investigation of crystallinity in rubber—564
Gemant, Andrew. Ionic mobility in solid dielectrics—508
Goldmark, Peter C. Problems of television transmission—447
Goudsmit, S. A. Nobel prize goes to Enrico Fermi—14
Gow, Paul L. (see Ballard, Stanley S.)—556
Greenslade, G. R. Patent tactics and law—698 (book review)
Guillemin, E. A. Tensor analysis of networks—315 (book review)
Gunn, Ross. U. S. naval research laboratory—4
Guth, Eugene. Physics of rubber. I. Its observed elastic and thermoelastic behavior—161

Hansen, W. W. On the resonant frequency of closed concentric lines—38
—— **and R. D. Richtmyer.** On resonators suitable for klystron oscillators—189
Harrison, George R. Compilations of spectroscopic data—760
Hays, Margaret B. Applied physics in the Bureau of Home Economics—537
Headrick, L. B. (see Martin, S. T.)—116
Hetényi, M. Application of hardening resins in three-dimensional photoelastic studies—295
Higgins, George. Fine grain photographic development—18
Hipple, A. von (see Merrill, F. H.)—873
Hoag, J. B. Fundamental electronics and vacuum tubes—390 (book review)
Holzer, R. E. and E. J. Workman. Photographs of unusual discharges occurring during thunderstorms—659
Hoover, Herbert. Appeal for fundamental research—688
Hotaling, George. (see Charlton, E. E.)—374
Huggins, Maurice L. Viscosity of dilute solutions of long-chain molecules. III. The Staudinger viscosity law—700
Hutchisson, Elmer. Deeper understanding needed—207
—— Egg or the chick—141
—— Pure physics begets applied physics—3
—— Question before intelligent individuals—85
—— Research—a national resource—597
—— Research and preparedness—733
—— Shall we kill the goose that lays the golden eggs?—525
—— Symposium on temperature—819
—— Television, a task well begun—425
—— That publication problem, again!—343
—— "World of creative physics"—667

Johnson, R. P. (see Nelson, R. B.)—335

Kenty, Carl. Note on the behavior of high intensity mercury arcs falling freely under gravity—714
Kersten, H. (see Dunholter, H.)—523
King, Ronald. Beam tubes as ultra-high frequency generators—638
Kip, Arthur F. (see Loeb, L. B.)—142
Koller, L. R. Bactericidal effects of ultraviolet radiation produced by low pressure mercury vapor lamps—624
Körösy, F. (see Brody, I.)—584
Kuper, J. B. H. (see Roberts, R. B.)—612

Leverenz, Humboldt W. and Frederick Seitz. Luminescent materials—479
Lewis, Arthur B. Effects of irradiation, humidity and sphere material on the sparkover voltage of the two-centimeter sphere gap—573
Lewis, Bernard and Guenther von Elbe. Physics of flames and explosions of gases—344
Lindsay, R. B. Filtration of sound, II—680
Loeb, Leonard B. and Arthur F. Kip. Electrical discharges in air at atmospheric pressure. The nature of the positive and negative point-to-plane coronas and the mechanism of spark propagation—142
Lyons, W. James. Rate of plastic deformation in lead under compression—651

McIlwain, Knox. Survey of television pick-up devices—432
McKeehan, L. W. Alloys of iron and nickel. Vol. I. Special-purpose alloys—316 (book review)
Mack, Julian Ellis. Photographic chemicals and solutions—622 (book review)
Martin, S. T. and L. B. Headrick. Light output and secondary emission characteristics of luminescent materials—116
Meggers, William F. Spectroscopic apparatus—734
Meloche, C. C. Gas analysis—316 (book review)
Merrill, F. H. and A. von Hippel. Atomphysical interpretation of Lichtenberg figures and their application to the study of gas discharge phenomena—873
Mertz, Pierre. High definition television—443
Mindlin, Raymond D. Review of the photoelastic method of stress analysis I—222; II—273
Morgan, F. (see Muskat, M.)—46, 398
—— **and M. Muskat.** Studies in lubrication. IV. The experimental variation of the coefficient of friction with the strength of the lubricant source for a complete journal bearing—327
Morse, Philip M. Introduction to Bessel functions—497 (book review)
Morton, G. A. (see Ramberg, E. G.)—465
Muskat, M. (see Morgan, F.)—327
—— **and F. Morgan.** Studies in lubrication. III. The theory of the thick film lubrication of a complete journal bearing of finite length with arbitrary positions of the lubricant source—46; V. The theory of the thick film lubrication of flooded journal bearings and bearings with circumferential grooves—398

Nadai, A. Second report on viscosity and plasticity—817 (book review)
Nelson, R. B., R. P. Johnson and W. B. Nottingham. Luminescence during intermittent electron bombardment—335
Nottingham, Wayne B. Electrical and luminescent properties of phosphors under electron bombardment—73
—— (see Nelson, R. B.)—335

Pekeris, C. L. and L. B. Slichter. Problem of ice formation—135
Pierce, J. R. Limiting current densities in electron beams—715
Pipes, L. A. Operational calculus. I—172; II—258; III—301
—— Matrix theory of oscillatory networks—849

Power, R. B. (see Cobine, J. D.)—420

Quimby, Edith H. Radium protection—604

Ramberg, E. G. and G. A. Morton. Electron optics—465
Ramo, Simon. Synthesis of a high frequency reactance—138
Randall, H. M. Infra-red spectra—observation and uses—768
Richtmyer, R. D. Dielectric resonators—391
—— (see Hansen, W. W.)—189
Roberts, R. B. and Kuper, J. B. H. Uranium and atomic power—612

Sarnoff, David. Probable influences of television on society—426
Sawyer, Ralph A. Qualitative and quantitative chemical analysis by line emission spectra—741
Seitz, Frederick. (see Leverenz, Humboldt W.)—479
Shockley, William. Nature of the metallic state—543
Sidhu, S. S. X-ray study of menthol—83
Slepian, J. Gaseous electrical conductors—105 (book review)
Slichter, L. B. (see Pekeris, C. L.)—135
Soehrens, J. E. (see Brahtz, J. H. A.)—242
Spangenberg, Karl. Moderne-mehrgitter-elektronenroehren II—104 (book review)
Stauffer, L. H. Experimental electronic violin—96
Struve, Otto. Astronomical spectra, modern observation and interpretation—800
Suits, C. G. Current densities, lumen efficiency and brightness in A, N_2, He and H_2 arcs—730
—— Measurements of some arc characteristics at 1000 atmospheres pressure—203
—— Some properties of the hydrogen arc—648
—— Spontaneous fluctuations of voltage—560 (book review)
—— Temperature of high pressure arcs—728

Taylor, Lauriston S. Economic features of x-ray protection—598
Templin, R. S. Stephen Timoshenko. 60th anniversary volume—622 (book review)
Tonks, Lewi. Lack of "sucking" action by the cathode blast of mercury vapor in a pool rectifier—654
Trytten, M. H. Physik fur studierende un technischen hochschule und universitat—186 (book review)

Vaidya, Wm. Letter to the editor—26
Valasek, Joseph. Light—697 (book review)
—— Photography by infrared. Its principles and applications—698 (book review)
—— Refraction of the human eye and methods of estimating the refraction—559 (book review)
—— Survey of crystal optics with emphasis on the parts finding application in photoelasticity—209
Varian, Russell H. and Sigurd F. Varian. High frequency amplifier and oscillator—140(L)
—— **and S. F. Varian.** High frequency oscillator and amplifier—321
Varian, Sigurd F. (see Varian, R. H.)—140(L), 321

Wahlin, H. B. Principles of electricity and magnetism—559 (book review)
Wald, George. Perception of light—561 (book review)
Warga, Mary E. Proceedings of the sixth summer conference on spectroscopy and its applications—818 (book review)
Warren, B. E. Properties of glass—560 (book review)
Weber, Ernst. Electrostatic field produced by a point charge in the axis of a cylinder—663
Webster, David L. Cathode-ray bunching—501
—— Theory of klystron oscillations—864
Webster, R. Alden. Piezoelectric *versus* mechanical spring pressure gauge—890
Weinberg, Alvin M. Nerve conduction with distributed capacitance—128
Weller, R. New method for photoelasticity in three dimensions—266(L)
Westendorp, W. F. (see Charlton, E. E.)—374
Williamson, Chas. Standards of electroacoustics, 1938—186 (book review)
—— Theory and applications of electron tubes—561 (book review)
Wilson, H. A. Modern atomic theory. An elementary introduction—390 (book review)
Winsor, L. P. (see Cobine, J. D.)—420
Workman, E. J. (see Holzer, R. E.)—659

Subject Index for Volume 10

(L) refers to Letters to the Editor

Aberrations in electron optics, (resumé)—183
Absorption spectra as applied to molecular identification and analysis, Wallace R. Brode—751
Accessories for spectrochemical analysis, Stanley S. Ballard and Paul L. Gow—556
Achromatic lenses, Lithium fluoride-quartz, (resumé)—103
Advances in the application of radioactivity for geological age measurements, (resumé)—373
Advisory Council on Applied Physics of the American Institute of Physics, Report of meeting, Henry A. Barton—615
Alloys, Na-K, Phase diagram at high pressures, (resumé)—372
Alloys of iron and nickel. Vol. I. Special-purpose alloys, J. S. Marsh, (review)—316
A.c. arcs, Energy measurements of reigniting, S. G. Eskin—631
Appeal for fundamental research, Herbert Hoover—688
Application of hardening resins in three-dimensional photoelastic studies, M. Hetenyi—295
Applied physics in the Bureau of Home Economics, Margaret B. Hays—537
Arc characteristics at 1000 atmospheres pressure, Measurement of, C. G. Suits—203
Arc welding of oil well casing, Thermal distribution and temperature gradient in, W. A. Bruce—578
Arcs, Current densities, lumen efficiency and brightness in A, N_2, He and H_2, C. G. Suits—730
Arcs, short, Reignition of, at high pressures, J. D. Cobine, R. B. Power, and L. P. Winsor—420
Artificial daylighting, Recent experiments in, (resumé)—101
Astronomical spectra, modern observation and interpretation, Otto Struve—800
Atomic power, Uranium and, R. B. Roberts and J. B. H. Kuper—612
Atomphysical interpretation of Lichtenberg figures and their application to the study of gas discharge phenomena, F. H. Merrill and A. von Hippel, 873
Axial tension, Increase of torsional stiffness of a prismatical bar due to, M. A. Biot, 860

Bactericidal effects of ultraviolet radiation produced by low pressure mercury vapor lamps, L. R. Koller—624
Beam tubes as ultra-high frequency generators, Ronald King—638
Benzene and heptane, Dielectric strength of, Ralph W. Dornte—514
Beta-brass, Study of, in single crystal form, (resumé)—181
Bureau of Home Economics, Applied physics in, Margaret B. Hays—537

Calculus, The operational, Louis A. Pipes, I—172; II—258; III—301
Capture of neutrons by atoms in a crystal, (resumé)—181
Cathode-ray bunching, David L. Webster—501
Cathodes, Properties of oxide-coated, John P. Blewett, I—668; II—831
Chemical analysis by line emission spectra, Ralph A. Sawyer—741
Chemical analysis, X-ray diffraction applied to, Wheeler P. Davey—820
Color mixture, subtractive, and color reproduction, (resumé)—102
Compilations of spectroscopic data, George R. Harrison—760
Concentric lines, On the resonant frequency of closed, W. W. Hansen—38
Convection and conduction of heat in gases, I. Brody and F. Kőrösy—584
Copper oxides, Electron diffraction study of, H. Dunholter and H. Kersten—523
Coronas, Nature of the positive and negative point-to-plane, Leonard B. Loeb and Arthur F. Kip—142
Cosmic rays, intensity of, and earth's magnetic field, (resumé)—182
Crystal optics, A survey of, Joseph Valasek—209
Crystallinity in rubber, X-ray investigation of, S. D. Gehman and J. E. Field—564
Cultural values of physics, David Dietz—86
Current densities, lumen efficiency and brightness in A, N_2, He and H_2 arcs, C. G. Suits—730
Cylindrical particles in viscous flow, Motion of, R. C. Binder—711

Deeper understanding needed, Elmer Hutchisson—207
Dielectric resonators, R. D. Richtmyer—391
Dielectric strength of benzene and heptane, Ralph W. Dornte—514
Dielectrics, solid, Ionic mobility in, Andrew Gemant—508
Diffusion in metals using radioactive indicators, (resumé)—533
Direct optical measurement of individual principal stresses, J. H. A. Brahtz and J. E. Soehrens—242
Discharges occurring during thunderstorms, Photographs of unusual, R. E. Holzer and E. J. Workman—659
Distributed capacitance, Nerve conduction with, Alvin M. Weinberg—128
Double refraction and change in length of certain plastics, H. W. Farwell—109

Earth's crustal deformations, Experimental study of, Milton B. Dobrin—360
Economic features of x-ray protection, Lauriston S. Taylor—598
Effects of irradiation, humidity and sphere material on the sparkover voltage of the two-centimeter sphere gap, Arthur B. Lewis—573
Elastic and thermoelastic behavior, Observed, for rubber, Eugene Guth—161
Elastic properties of vinyl sheeting, S. Bateson—887
Electrical and luminescent properties of phosphors under electron bombardment, Wayne B. Nottingham—73
Electrical discharges in air at atmospheric pressure. The nature of the positive and negative point-to-plane coronas and the mechanism of spark propagation, Leonard B. Loeb and Arthur F. Kip—142
Electrochemistry of Gases and Other Dielectrics, George Glockler and S. C. Lind, (review)—697
Electrolytic polishing, W. C. Elmore—724
Electron beams, Limiting current densities in, J. R. Pierce—715
Electron bombardment, Electrical and luminescent properties of phosphors under, Wayne B. Nottingham—73
Electron bombardment, Luminescence during intermittent, R. B. Nelson, R. P. Johnson and W. B. Nottingham—335
Electron diffraction studies of thin films, (resumé)—609
Electron diffraction study of copper oxides, H. Dunholter and H. Kersten—523
Electron microscope studies of thoriated tungsten, (resumé)—12
Electron optics, E. G. Ramberg and G. A. Morton—465
Electron optics, Aberrations in, (resumé)—183
Electronic conduction in insulating crystals under very high field strength, (resumé)—12

Electronic violin, An experimental, L. H. Stauffer—96
Electrostatic field produced by a point charge in the axis of a cylinder, Ernst Weber—663
Elementary survey of physics, Arthur E. Haas and Ira M. Freeman, (review)—269
Emission spectra, Molecular, G. H. Dieke—780
Energy measurements of reigniting a.c. arcs, S. G. Eskin—631
Experimental electronic violin, L. H. Stauffer—96

Ferromagnetics, Theory of reversible magnetization in, (resumé)—265
Filament, Oxide-coated, (resumé)—534
Filtration of sound. II, R. B. Lindsay—680
Fine grain photographic development, George Higgins—18
Flames and explosions of gases, Physics of, Bernard Lewis and Guenther von Elbe—344
Forces between ions in solution, (resumé)—11
Fundamental electronics and vacuum tubes, A. L. Albert, (review)—390
Further concentration of N^{15}, (resumé)—313

Gas analysis, A. McCulloch, (review)—316
Gas discharge phenomena, Atomphysical interpretation of Lichtenberg figures and their application to the study of, F. H. Merrill and A. von Hippel, 873
Gaseous electrical conductors, E. L. E. Wheatcroft, (review)—105
Gases, Convection and conduction of heat in, I. Brody and F. Kőrösy—584
Gases, Explosions of, Bernard Lewis and Guenther von Elbe—344
Gauge, Piezoelectric *versus* mechanical spring pressure, R. Alden Webster—890
Generators, Beam tubes as ultra-high frequency, Ronold King—638
Generators, Pressure-insulated electrostatic, (resumé)—535
Geological history with models, Milton B. Dobrin—360

Hearing, Mechanism of, (resumé)—494
Heat engines, A. C. Walshaw, (review)—697
Heat in gases, Convection and conduction of, I. Brody and F. Kőrösy—584
Heptane, Dielectric strength of, Ralph W. Dornte—514
High definition television, Pierre Mertz—443
High frequency amplifier and oscillator, Russell H. Varian and Sigurd F. Varian—140(L)
High frequency oscillator and amplifier, Russell H. Varian and Sigurd F. Varian—321
High pressure arcs, Temperature of, C. G. Suits—728
Hydrogen arc, Some properties of the, C. G. Suits—648

Ice formation, Problem of, C. L. Pekeris and L. B. Slichter—135
Impedance at frequencies of the order 300 mc/second, Resonance curve method for the absolute measurement of, R. A. Chipman—27
Increase of torsional stiffness of a prismatical bar due to axial tension, M. A. Biot—860
Infra-red spectra—observation and uses, H. M. Randall—768
Insulating crystals under very high field strength, Electronic conduction in, (resumé)—12
Introduction to Bessel functions, Frank Bowman, (review)—497
Introduction to industrial rheology, G. W. Scott Blair, (review)—105
Ionic mobility in solid dielectrics, Andrew Gemant—508
Ions in solution, Forces between, (resumé)—11
Isopachic stress patterns, Max M. Frocht—248
Isotope separation, New method of, (resumé)—495
Isotopes, Separation of by thermal diffusion, (resumé)—611

Journal bearings, Lubrication of, M. Muskat and F. Morgan—46, 327, 398

Klystron oscillations, Theory of, David L. Webster—864
Klystron oscillators, Resonators suitable for, W. W. Hansen and R. D. Richtmyer—189

Lack of "sucking" action by the cathode blast of mercury vapor in a pool rectifier, Lewi Tonks—654
Lead under compression, Rate of plastic deformation in, W. James Lyons—651
Lenses, Lithium fluoride-quartz achromatic, (resumé)—103
Lichtenberg figures and their application to the study of gas discharge phenomena, Atomphysical interpretation of, F. H. Merrill and A. von Hippel—873
Light, F. Bray, (review)—697
Light output and secondary emission characteristics of luminescent materials, S. T. Martin and L. B. Headrick—116
Limiting current densities in electron beams, J. R. Pierce,—715
Line emission spectra, Qualitative and quantitative chemical analysis by, Ralph A. Sawyer—741
Lithium fluoride-quartz achromatic lenses, (resumé)—103
Lubrication, Studies in, M. Muskat and F. Morgan III—46; IV—327; V—398
Luminescence during intermittent electron bombardment, R. B. Nelson, R. P. Johnson and W. B. Nottingham—335
Luminescent materials, Humboldt W. Leverenz and Frederick Seitz—479
Luminescent materials, Light output and secondary emission characteristics of, S. T. Martin and L. B. Headrick—116

Magnetische und elektrische eigenschaften des eisens und seiner legierungen, O. V. Auwers, (review)—186
Magnetism, Origin of terrestrial, (resumé)—265
Magnetization, reversible, in ferromagnetics, (resumé)—265
Malleable iron, X-ray study of changes that occur during fatiguing, (resumé)—494
Matrix theory of oscillatory networks, Louis A. Pipes, 849
Measurement of some arc characteristics at 1000 atmospheres pressure, C. G. Suits—203
Measurement of reverberation time, (resumé)—372
Mechanism of hearing, (resumé)—494
Menthol, X-ray study of, S. S. Sidhu—83
Mercury arcs, High intensity, falling freely under gravity, Carl Kenty—714
Mercury vapor in a pool rectifier, The lack of "sucking" action by the cathode blast of, Lewi Tonks—654
Mercury vapor lamps, low pressure, Bactericidal effects of ultraviolet radiation produced by, L. R. Koller—624
Metallic state, Nature of the, William Shockley—543
Milky way, Rotation of, (resumé)—182
Mobility of positive ions in gases, A. M. Tyndall, (review)—390
Modern atomic theory. An elementary introduction, J. C. Speakman, (review)—390
Modern magnetism, L. F. Bates, (review)—622
Modern plastics, E. F. Lougee, Editor, (review)—269
Moderne mehrgitter—Elektronenroehren II, M. J. O. Strutt, (review)—104
Molecular emission spectra, G. H. Dieke—780
Molecular identification and analysis, Absorption spectra as applied to, Wallace R. Brode—751
Motion of cylindrical particles in viscous flow, R. C. Binder—711

N^{15}, Further concentration of, (resumé)—313
Natural constants, New presentation of dilemma of, (resumé)—609
Nature of radio fade-out, (resumé)—532
Nature of the metallic state, William Shockley—543
Naval research laboratory, U. S., Ross Gunn—4
Nerve conduction with distributed capacitance, Alvin M. Weinberg—128
Neutrons, capture of, by atoms in a crystal, (resumé)—181

New frontiers for industry, Carl Breer—271
New long-life cathode for thyratrons, (resumé)—534
New method for photoelasticity in three dimensions, R. Weller—266(L)
New method of isotope separation, (resumé)—495
New million-volt x-ray outfit, E. E. Charlton, W. F. Westendorp, L. E. Dempster and George Hotaling—374
New presentation of dilemma of natural constants, (resumé)—609
New studies of the oxide-coated filament, (resumé)—534
Nobel prize goes to Enrico Fermi, S. A. Goudsmit—14
Note on the behavior of high intensity mercury arcs falling freely under gravity, Carl Kenty—714
Note on the elastic properties of vinyl sheeting, S. Bateson—887
Note on the quantitative spectrographic analysis of small amounts of rubidium and potassium in biological materials, Willi M. Cohn—200

Oil well casing, Thermal distribution and temperature gradient in the arc welding of, W. A. Bruce—578
Oils, Pennsylvania, Viscosity of, at high pressure, R. M. Dibert, R. B. Dow, and C. E. Fink—113
On understanding physics, W. H. Watson, (review)—104
Operational calculus, The, Louis A. Pipes; I—172; II—258; III—301
Optical measurement of individual principal stresses, J. H. A. Brahtz and J. E. Soehrens—242
Origin of terrestrial magnetism, (resumé)—265
Oscillator and amplifier, High frequency, Russell H. Varian and Sigurd F. Varian—321
Oscillatory networks, Matrix theory of, Louis A. Pipes—849
Oxide-coated cathodes, Properties of, John P. Blewett—I—688; II—831

Patent tactics and law, Roger Sherman Hoar, (review)—698
Perception of light, The, W. D. Wright, (review)—561
Phase diagram of Na-K alloys at high pressures, (resumé)—372
Phosphorescence of zinc silicate phosphors, Gorton R. Fonda—408
Phosphors, Electrical and luminescent properties of, under electron bombardment, Wayne B. Nottingham—73
Phosphors, Phosphorescence of zinc silicate, Gorton R. Fonda—408
Photoelastic method of stress analysis, Review of, Raymond D. Mindlin; I—222; II—273
Photoelastic studies, Three-dimensional, M. Hetenyi—295
Photoelasticity, Application of crystal optics in, Joseph Valasek—209
Photoelasticity in three dimensions, New method for, R. Weller—266(L)
Photographic chemicals and solutions, J. I. Crabtree and G. E. Matthews, (review)—622
Photographic development, Fine grain, George Higgins—18
Photographic theory, (resumé)—314
Photographs of unusual discharges occurring during thunderstorms, R. E. Holzer and E. J. Workman—659
Photography by infrared. Its principles and applications, Walter Clark (review)—698
Physics of flames and explosions of gases, Bernard Lewis and Guenther von Elbe—344
Physics of rubber. I. Its observed elastic and thermoelastic behavior, Eugene Guth—161
Physik fur studierende un technischen hochschule und universitat, Paul Wessel, (review)—186
Piezoelectric *versus* mechanical spring pressure gauge, R. Alden Webster—890
Plastic deformation in lead under compression, Rate of, W. J. Lyons—651
Plastics, Double refraction and change in length of, H. W. Farwell—109
Point charge in the axis of a cylinder, The electrostatic field produced by, Ernst Weber—663
Potassium in biological materials, Quantitative spectrographic analysis of small amounts of, Willi M. Cohn—200
Principal stresses, Direct optical measurement of individual, J. H. A. Brahtz and J. E. Soehrens—242
Principles of electricity and magnetism, G. P. Harnwell, (review)—559
Principles of statistical mechanics, Richard C. Tolman, (review)—691
Probable influences of television on society, David Sarnoff—426
Problem of ice formation, C. L. Pekeris and L. B. Slichter—135
Problems of television transmission, Peter C. Goldmark—447
Proceedings of the sixth summer conference on spectroscopy and its applications, George R. Harrison, (review)—818
Properties of glass, G. W. Morey, (review)—560
Properties of oxide-coated cathodes, John P. Blewett; I—668; II—831
Pure physics begets applied physics, Elmer Hutchisson—3

Qualitative and quantitative chemical analysis by line emission spectra, Ralph A. Sawyer—741
Question before intelligent individuals, Elmer Hutchisson 85

Radio fade-out, Nature of, (resumé)—532
Radioactive indicators, use in diffusion in metals, (resumé)—533
Radioactivity, Application of, for geological age measurements, (resumé)—373
Radium protection, Edith H. Quimby—604
Rate of plastic deformation in lead under compression, W. James Lyons—651
Reactance, Synthesis of high frequency, Simon Ramo—138
Recent developments in pressure-insulated electrostatic generators, (resumé)—535
Recreating geological history with models, The experimental study of the earth's crustal deformations, Milton B. Dobrin—360
Refraction, double, and change in length of certain plastics, H. W. Farwell—109
Refraction of the human eye and methods of estimating the refraction, James Thorington, (review)—559
Reignition of short arcs at high pressures, J. D. Cobine, R. B. Power, and L. P. Winsor—420
Research—A national resource, Elmer Hutchisson—597
Research, An appeal for fundamental, Herbert Hoover—688
Research and preparedness, Elmer Hutchisson—733
Resins, Application of hardening, M. Hetenyi—295
Resonance curve method for the absolute measurement of impedance at frequencies of the order 300 mc/second, R. A. Chipman—27
Resonant frequency of closed concentric lines, W. W. Hansen—38
Resonators, Dielectric, R. D. Richtmyer—391
Resonators suitable for klystron oscillators, W. W. Hansen and R. D. Richtmyer—189
Reverberation time, Measurement of, (resumé)—372
Reversed speech, (resumé)—533
Review of the photoelastic method of stress analysis, Raymond D. Mindlin; I—222; II—273
Rhodium mirrors for scientific purposes, M. Auwärter—705
Rotation of the milky way, the earth's magnetic field and the intensity of cosmic rays, (resumé)—182
Rubber, Crystallinity in, S. D. Gehman and J. E. Field—564
Rubber, The physics of, Eugene Guth—161
Rubidium and potassium in biological materials, Quantitative spectrographic analysis of, Willi M. Cohn—200

Second report on viscosity and plasticity, (review)—817
Separation of isotopes by thermal diffusion, (resumé)—611
Shall we kill the goose that lays the golden eggs? Elmer Hutchisson—525
Silver films, Structural characteristics of certain, Sanford F. Essig—61
Simplified calculation of the arbitrary constants of a linear differential equation of the second order with constant coefficients, R. Feinberg—140(L)
Some properties of the hydrogen arc, C. G. Suits—648
Sound, Filtration of, in solid media, R. B. Lindsay—680
Sound measurements in industry, Ernest J. Abbott—526
Spark propagation, Mechanism of, Leonard B. Loeb and Arthur F. Kip—142
Sparkover voltage of the two-centimeter sphere gap, Effects of irradiation, humidity and sphere material on, Arthur B. Lewis—573
Spectra, Astronomical, Otto Struve—800
Spectra, infra-red—observation and uses, H. M. Randall—768
Spectrochemical analysis, Accessories for, Stanley S. Ballard and Paul L. Gow—556
Spectrographic analysis of small amounts of rubidium and potassium in biological materials, Willi M. Cohn—200
Spectroscopic apparatus, W. F. Meggers—734
Spectroscopic data, Compilations of, George R. Harrison—760
Speech, Reversed, (resumé)—533
Spontaneous fluctuations of voltage, E. B. Moullin, (review)—560
Spring pressure gauge, Piezoelectric *versus* mechanical, R. Alden Webster—890
Standards on Electroacoustics, 1938, (review)—186
Staudinger viscosity law, Maurice L. Huggins—700
Stephen Timoshenko. 60th Anniversary Volume, (review)—622
Stress analysis, Review of the photoelastic method of, Raymond D. Mindlin; I—222; II—273
Stress patterns, Isopachic, Max M. Frocht—248
Stresses, Direct optical measurement of individual principal, J. H. A. Brahtz and J. E. Soehrens—242
Structure of water, X-ray analysis of, (resumé)—13
Structural characteristics of certain silver films, Sanford F. Essig—61
Studies in lubrication (con't from Volume 9), M. Muskat and F. Morgan; III. The theory of the thick film lubrication of a complete journal bearing of finite length with arbitrary positions of the lubricant source—46; IV. The experimental variation of the coefficient of friction with the strength of the lubricant source for a complete journal bearing—327; V. The theory of the thick film lubrication of flooded journal bearings and bearings with circumferential grooves—398
Study of beta-brass in single crystal form, (resumé)—181
Subtractive color mixture and color reproduction, (resumé)—102
Superstructure in $FeNi_3$, (resumé)—11
Survey of crystal optics, with emphasis on the parts finding application in photoelasticity, Joseph Valasek—209
Survey of television pick-up devices, Knox McIlwain—432
Symposium on temperature, Elmer Hutchisson—819
Symposium on temperature, its measurement and control in science and industry—693
Synthesis of a high frequency reactance, Simon Ramo—138

Television, a task well begun, Elmer Hutchisson—425
Television, High definition, Pierre Mertz—443
Television pick-up devices, Survey of, Knox McIlwain—432
Television, Probable influences of, on society, David Sarnoff—426
Television receiving and reproducing systems, E. W. Engstrom—455
Television transmission, Problems of, Peter C. Goldmark—447
Temperature of high pressure arcs, C. G. Suits—728
Temperature symposium—184
Temperature symposium, its measurement and control in science and industry—693
Temperature, The symposium on, Elmer Hutchisson—819
Tensor analysis of networks, Gabriel Kron, (review)—315
Terrestrial magnetism, Origin of, (resumé)—265
Text-book on crystal physics, A, W. A. Wooster, (review)—269
That publication problem, again! Elmer Hutchisson—343
The egg or the chick?, Elmer Hutchisson—141
"The world of creative physics," Elmer Hutchisson—667
Theory and applications of electron tubes, Herbert J. Reich, (review)—561
Theory of klystron oscillations, David L. Webster—864
Theory of reversible magnetization in ferromagnetics, (resumé)—265
Thermal diffusion, Separation of isotopes by, (resumé)—611
Thermal distribution and temperature gradient in the arc welding of oil well casing, W. A. Bruce—578
Thick film lubrication of a complete journal bearing of finite length with arbitrary positions of the lubricant source, Theory of, M. Muskat and F. Morgan—46
Thin films, Electron diffraction studies of, (resumé)—609
Thoriated tungsten, Electron microscope studies of, (resumé)—12
Thyratrons, New long-life cathode for, (resumé)—534
Torsional stiffness of a prismatical bar due to axial tension, Increase of, M. A. Biot—860

Ultraviolet radiation produced by low pressure mercury vapor lamps, Bactericidal effects of, L. R. Koller—624
U. S. Naval Research Laboratory, Ross Gunn—4
Uranium and atomic power, R. B. Roberts and J. B. H. Kuper—612

Vinyl sheeting, Note on elastic properties of, S. Bateson—887
Violin, An experimental electronic, L. H. Stauffer—96
Viscosity of dilute solutions of long-chain molecules. III. The Staudinger viscosity law, Maurice L. Huggins—700
Viscosity of Pennsylvania oils at high pressure, R. M. Dibert, R. B. Dow, and C. E. Fink—113

X-ray analysis of the structure of water, (resumé)—13
X-ray diffraction applied to chemical analysis, Wheeler P. Davey—820
X-ray investigation of crystallinity in rubber, S. D. Gehman and J. E. Field—564
X-ray outfit, A new million-volt, E. E. Charlton, W. F. Westendorp, L. E. Dempster and George Hotaling—374
X-ray protection, Economic features of, Lauriston S. Taylor—598
X-ray study of changes that occur in malleable iron during fatiguing, (résume)—494
X-ray study of menthol, S. S. Sidhu—83

Zinc silicate phosphors, Phosphorescence of, Gorton R. Fonda—408

Class E Spectroscopic Plates

THIS RECENT ADDITION to the series of *Eastman Spectroscopic Plates* has its highest sensitivity through the region 6000Å. to 7000Å., with a maximum at 6500 Å. Class E sensitizing can be supplied with Types I, II, III, IV, V, and 144 emulsions.

Astronomers have found these plates valuable in the photography of faint red stars, and they have been successfully used by spectroscopists for photographing weak lines in the red region of the spectrum.

Additional information concerning photography in the H-alpha region will be supplied on request.

EASTMAN KODAK COMPANY

Research Laboratories **ROCHESTER, N. Y.**

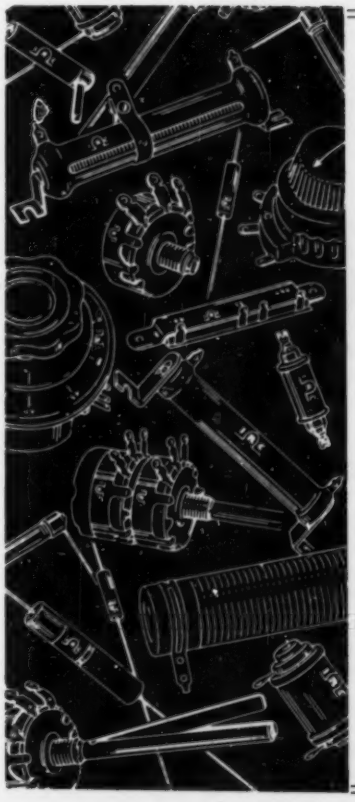

RESISTANCE ENGINEERING DATA BULLETINS

These IRC Resistance Engineering Data Bulletins contain the results of many years of specialized experience in the production of more resistance types for more applications than any other manufacturer in the world. They have been classified and prepared to bring exact needed engineering information to assure selection of the *right* resistor for *any* job. Please ask for them by number.

1. Metallized and Wire Wound Volume Controls and Potentiometers up to 2 watts and 20 meg. resistance.

2. Metallized Type Resistors: Insulated 1/2, 1 and 2 watts; high frequency; high range; high frequency power resistors; high voltage power resistors.

3. Insulated Wire Wound Resistors: Type BW from 1/2 to 1 and 2 watts; Type MW 5 to 20 watts.

4. Power and Precision Wire Wound Resistors: Power types from 10 to 200 watts, fixed and adjustable types, in wide variety of shapes, mountings, etc. Inductive and non-inductive. 14 Precision types to as close as 1/10 of 1% accuracy.

5. Attenuators: Unique new IRC molded motor commutator type 20-step attenuator; also, conventional type 30-step units. Ladder, Potentiometer or Bridge T.

6. Power Rheostats: Quick heat-dissipating all-metal (aluminum) 25 and 50 watt types.

IRC

INTERNATIONAL RESISTANCE CO.

419 N. BROAD ST., PHILADELPHIA, PA.

EPPLEY THERMOPILES *for* RADIANT ENERGY MEASUREMENTS

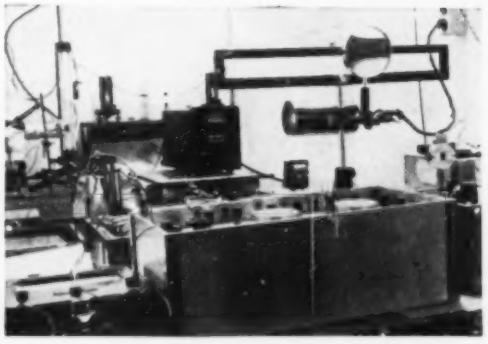

A view of some of the apparatus used for calibrating thermopiles at the Eppley Laboratory, Inc.

Adequate manufacturing, testing and calibrating equipment in the hands of our skilled and experienced technicians insures satisfaction to the users of Eppley Thermopiles.

We are prepared to furnish thermopiles of either bismuth-silver or copper-constantan, mounted in vacuum or air type cases. We also furnish thermopiles and mountings especially designed to meet individual needs. A card will bring you our Bulletin R–3 which contains illustrations, sample curves, complete descriptive matter, prices, references, etc., with regard to Eppley Thermopiles.

EPLAB

THE EPPLEY LABORATORY, INC.
SCIENTIFIC INSTRUMENTS
NEWPORT, R.I.
U. S. A.

"POINTOLITE" *Lamps*

BRILLIANT—CONCENTRATED—STEADY—WHITE

When an evenly distributed field of illumination is needed . . . or a light source of constant intensity . . . or one that will remain in a fixed position . . . use Pointolite Lamps. Let us tell you more about these highly concentrated sources of white light and their various applications.

Bulletin 1530-R lists sizes from 30 to 1000 c.p. for direct current, and 150 c.p. for alternating current, as well as auxiliary control devices. . . . Write for a copy.

JAMES G. BIDDLE CO.
ELECTRICAL INSTRUMENTS
1211-13 ARCH STREET PHILADELPHIA, PA.

STABILIZED A-C VOLTAGE

INPUT 95 130 volts
Instantaneous action
A magnetic unit

OUTPUT
115 volts ±½%
Stabilizes at any load within rating

No moving parts. Nothing to wear out.

RAYTHEON Voltage Stabilizer

APPLICATIONS Broadly it insures stable operation of all precision apparatus obtaining its power from an A.C. source, for example:—

- Insures constant brilliancy from all types of lamps.
- Improves the operation of X-ray equipment.
- Stabilizes all electronic apparatus.

Write for Bulletin 48-71JP.

RAYTHEON MFG. CO. WALTHAM, MASS.

THREE OUTSTANDING NEW BOOKS

MATHEMATICAL METHODS IN ENGINEERING

By Theodore von Kármán, California Institute of Technology, and Maurice A. Biot, Columbia University. 483 pages, 6 x 9. $4.00

The primary objective of this book is to introduce the student to the mathematical treatment of fundamental problems in the engineering sciences. The mathematical methods are presented in connection with their practical applications in the fields of civil, mechanical, aeronautical, and electrical engineering.

INTRODUCTION TO CHEMICAL PHYSICS

By J. C. Slater, Massachusetts Institute of Technology. *International Series in Physics.* 521 pages, 6 x 9. $5.00

In this unified presentation of material common to the fields of both physics and chemistry, the author offers an interesting treatment of thermodynamics and statistical mechanics, including their application to solids, liquids, and gases. There is also a discussion of atomic structure and the resulting interatomic and intermolecular forces, with application to the different types of chemical substances, and to their thermal and mechanical properties.

ELECTRONIC STRUCTURE AND CHEMICAL BINDING

By Oscar Knefler Rice, University of North Carolina. 485 pages, 6 x 9. $5.00

This book is essentially a discussion of the chemical bond as exemplified in inorganic compounds. The early part of the book gives the student a foundation in atomic theory and chemistry; the latter part presents the application of the general principles to particular chemical systems.

Send for copies on approval

McGRAW-HILL BOOK COMPANY, Inc.

330 West 42nd Street **New York, N. Y.**

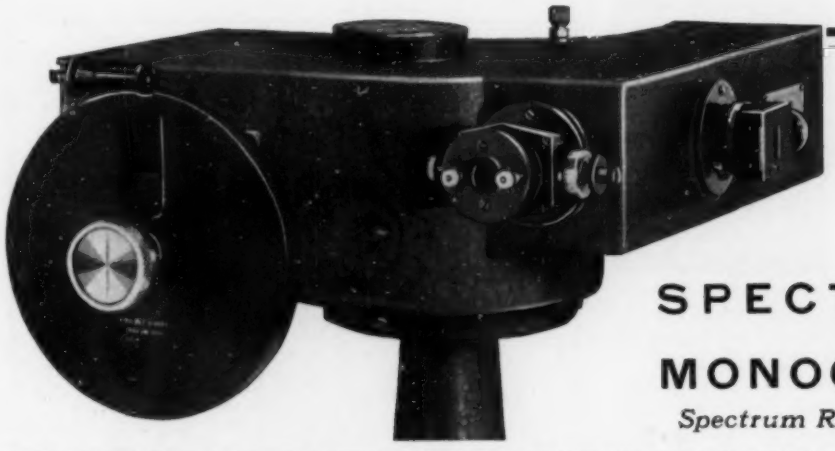

Infra Red.

SPECTROMETER AND MONOCHROMATOR

Spectrum Range .70 Mu to 12.00 Mu

High transmission and great accuracy of setting qualify this constant deviation spectrometer (Wadsworth type) for exacting research. The flat spiral dial has an equivalent scale length of 1.6 meters, with almost equally spaced divisions. Astigmatism and coma found in ordinary parabolic mirrors are eliminated by parabolizing the mirrors about axes lying outside their surfaces. A heating element preserves the rock salt prism. The optical system is almost air tight. Thermopiles and other accessories available.

Write for Catalog L-2 describing this and other Spectroscopic equipment.

Special spectroscopic instruments built to meet your requirements.

THE GAERTNER SCIENTIFIC CORPORATION

1212 WRIGHTWOOD AVENUE, CHICAGO, ILLINOIS, U. S. A.

REPORTS ON
PROGRESS IN PHYSICS
VOLUME V (1938)

445 pages: Illustrated *$5.00 post free* *Bound in cloth*

A COMPREHENSIVE REVIEW

by leading physicists and under the general editorship of Prof. Allan Ferguson

THE CONTENTS INCLUDE CHAPTERS ON

ABSOLUTE ELECTRICAL MEASUREMENTS
PLASTICS IN INDUSTRIAL PHYSICS
AIDS FOR DEFECTIVE HEARING
TEACHING OF PHYSICS IN SCHOOLS
X-RAYS AND γ-RAYS IN MEDICINE
ELECTRIC WAVE FILTERS
THE GEIGER COUNTER
QUANTUM MECHANICS
THE LIQUID STATE
SOFT X-RAY SPECTROSCOPY OF THE SOLID STATE
ATOMIC PHYSICS
SOUND
ASTRONOMY
METEOROLOGY
HEAT
OPTICS
SPECTROSCOPY
ELASTICITY
SURFACE TENSION
VISCOSITY

Orders, with remittance, to

The Physical Society, 1 Lowther Gardens, Exhibition Road, London, S.W.7, England.

Linde

RARE GASES AND MIXTURES

NEON
ARGON
HELIUM
KRYPTON
XENON
MIXTURES

. . . highest purity
. . . for scientific purposes

Linde rare gases are of consistently high purity. They are used in the study of electrical discharges, in rectifying and stroboscopic devices, and in inert atmospheres where heat conduction must be reduced.

Linde rare gases are shipped in spherical glass bulbs, designed to facilitate removal without contamination. Special mixtures for experimental purposes can be supplied upon request.

The Linde Air Products Company
Unit of Union Carbide and Carbon Corporation

30 East 42nd Street UCC **Offices in**
New York, N. Y. **Principal Cities**

The word "Linde" is a trade-mark.

THIS LITTLE GIRL WILL HAVE A HAPPY CHRISTMAS *but*

Tuberculosis is still the greatest killer of youth . . . and takes *fifty per cent more girls* than boys between the ages of 15 and 25!

Two modern aids that help the physician detect tuberculosis in its earliest, *curable* stage are the tuberculin test and the chest X-ray.

Your purchases of Christmas Seals make it possible, not only to teach people that tuberculosis is preventable and curable, but to look for early stages of this dread disease among children who *seem to be* in good health.

So from now 'til Christmas, mail no letter—send no package—unless it is decorated with the Christmas symbol that saves lives!

The National, State and Local Tuberculosis Associations in the United States

BUY CHRISTMAS SEALS

PUBLICATIONS OF THE USSR

JOURNAL OF PHYSICS

Contains articles on historical, experimental and technical physics. Published monthly in English, French and German.

1 year $8.00 6 mos. $4.00

Single Copy $1.00

ACTA PHYSICOCHIMICA URSS

Magazine of original articles on physical chemistry. Published monthly in English, French and German.

1 year $10.00 6 mos. $5.00

Single Copy $1.00

REPORTS OF THE ACADEMY OF SCIENCE OF THE USSR

Published every 10 days, in English, French or German. Theoretical aspects of technical practice in mathematics, physics, natural science.

1 year $15.00 6 mos. $7.50

Single Copy 50c

Subscriptions to be placed with:

BOOKNIGA, Inc., 255 Fifth Avenue, New York, N. Y.

In Chicago: 59 E. Congress St.

OHMITE

Rheostats · Resistors · Tap Switches

For Better Electronic Control

For unfailing dependability—for accurate, trouble-free performance—you can always depend on Ohmite Resistance Units. That's why designers and engineers specify Ohmite Vitreous-Enameled close-control Rheostats, wire-wound Resistors, and high-current Tap Switches *for better electronic control.*

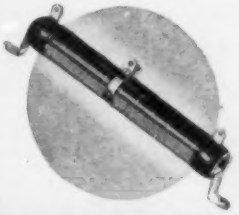

Write Today for Catalog 17

OHMITE MFG. CO.

4889 Flournoy St., Chicago

Be Right with OHMITE

RHEOSTATS · RESISTORS · TAP SWITCHES

IMPROVED "SPOTLIGHT" GALVANOMETERS

Rubicon MULTIPLE REFLECTION galvanometers have recently been improved through a redesign of the optical system. The definition of the line-image is now so sharp that readings can be estimated to .1 of a millimeter division.

These sturdy, self-contained galvanometers are available with sensitivities as high as .0006 microampere per millimeter. The scales, which are 100 mm. long, are remarkably proportional. Send for Bulletin 320.

RUBICON COMPANY

ELECTRICAL INSTRUMENT MAKERS

29 North Sixth Street Philadelphia, Pa.

FINE WIRES

TAYLOR PROCESS

THE TAYLOR PROCESS is a method for making wires from substances which lack ductility. The elements or alloys, because the drawing is done in glass or quartz, are in a very pure state. Lengths of more than a few feet cannot be obtained. The wires may be had with or without the glass insulation. We make Taylor Process wire of Pt, Rh, Au, Ag, Cu, Fe, Zn, Cd, Pb, Sb, Bi, Sn, Se, Te, Tl, Ga, and In, Constantan, Bi-Sn, Cd-Sb (used where large E.M.F. is desired) and many other alloys. Our wires are packed in containers holding one foot and, with few exceptions, the sizes are from one *mm* to one micron. We manufacture, too, fine wire by the Wollaston Method, by extrusion and by bare drawing.

WE ARE SPECIALISTS IN PLATINUM AND CAN SUPPLY IT IN WHATEVER FORM YOU REQUIRE

BAKER & CO., INC.

113 Astor Street, Newark, New Jersey

INDEX TO ADVERTISERS

Name	Page
AJAX ELECTROTHERMIC CORP. — Ajax-Northrup high frequency electric furnaces from laboratory to plant sizes.	iii
BAKER & CO., INC. — Platinum crucibles, dishes, triangles, filter cones, anodes, cathodes, electrodes, platinum tipped crucible tongs, fine wires and bismuth foil.	ix
JAMES G. BIDDLE COMPANY — "Jagabi" Rheostats; Adam Hilger and Kipp & Zonen Optical Instruments; "Pointolite" Lamps; Electrical Testing and Speed-measuring Instruments.	vi
BOOKNIGA, INC.	ix
CENTRAL SCIENTIFIC COMPANY — Manufacturers of Cenco Physical Apparatus and Instruments to meet all requirements of University, College and High School Physics Laboratories. Specializing in high vacuum pumps and development of instruments and apparatus for various sciences.	Cover 4
CLIFFORD MFG. CO. — Hydron metallic bellows for temperature and pressure control devices. Data for engineers.	x
EASTMAN KODAK COMPANY — Purified Organic Chemicals for research purposes; Plates for Photography, Photomicrography, Spectroscopy, Photometry, Astronomy; Wratten Light Filters; Cameras and Films.	v
THE EPPLEY LABORATORY, INC. — Standard Cells, thermopiles, pyrheliometers and temperature bridges.	vi
GAERTNER SCIENTIFIC CORP. — Spectroscopes, Spectrometers, Spectrographs, Spectrophotometers, Heliostats, Measuring Microscopes, Comparators, Cathetometers, Reading Telescopes, Interferometers, Chronographs, Dividing Machines, etc.	vii
GENERAL ELECTRIC VAPOR LAMP CO. — Uviarc lamp for ultraviolet radiation. Sodium Lab-Arc Lamp.	iv
GENERAL RADIO COMPANY — Manufacturers of electronic measuring instruments; vacuum-tube voltmeters, amplifiers and oscillators; wave analyzers, noise meters and analyzers, stroboscopes; laboratory standards of capacitance, inductance and frequency; impedance bridges, decade resistors and condensers; air condensers and variable inductors; rheostats, Variacs, transformers; other laboratory accessories.	Cover 3
G-M LABORATORIES, INC. — Photoelectric Cells; Photoelectric Relays; Slide Wire Rheostats; Galvanometers; Galvanometer Suspensions; Laboratory Stands and Clamps.	ii
INTERNATIONAL RESISTANCE COMPANY — Manufacturers of metallized and wirewound fixed and variable Resistors including high voltage and high frequency types.	v
LEEDS & NORTHRUP COMPANY — Manufacturers of Galvanometers, Resistors, Bridges, Condensers, Inductances, Potentiometers, Testing Sets; Temperature Measuring, Recording and Controlling Apparatus; Instruments for Measuring and Controlling Conductivity of Electrolytes and Hydrogen Ion Concentrations.	i
THE LINDE AIR PRODUCTS CO. — Oxygen, Argon, Helium, Krypton, Neon, Xenon, Rare Gas Mixtures, Nitrogen, Hydrogen, Calcium Carbide, Acetylene, equipment for Oxy-Acetylene welding and cutting.	viii

INDEX—*Continued*

Name	Page
MCGRAW-HILL BOOK CO., INC.	vii
NATIONAL TUBERCULOSIS ASSOCIATION	viii
OHMITE MANUFACTURING CO. — Manufacturers of close control rheostats, fixed and adjustable power resistors, precision and non-inductive resistors, attenuators, tapswitches and R.F. chokes.	ix
PHYSICAL SOCIETY (LONDON)	viii
RAYTHEON MFG. CO. — Voltage stabilizers and regulators. Electrical measurement and control instruments.	vi
RUBICON COMPANY — Galvanometers, electrometers, potentiometers, Wheatstone and Kelvin bridges, resistance boxes, hydrogen ion and conductivity apparatus.	ix

POSITION WANTED

Physicist, high frequency, short wave diathermy, electronics, radium, laboratory and factory experience, trained in physical chemistry and chemistry. Address Box D3–10. Rm. 1502, 175 Fifth Ave., New York, N. Y.

HYDRON

Complete thermal units for self-contained tank regulators and temperature controls. - -

WRITE FOR FREE 44-PAGE ENGINEER'S DATA BOOK

Metallic Bellows

HYDRON Metallic Bellows are used as control elements in temperature-and-pressure-control devices, and for liquid or gas seals of compressors and pumps. We are specialists in the design and production of complete thermostatic and pressure units for temperature and pressure controls. We are, therefore, prepared to extend the fullest co-operation to engineering departments of control manufacturers in the solution of design and engineering problems.

CLIFFORD MANUFACTURING CO.

564 E. FIRST STREET, BOSTON

BOSTON CHICAGO DETROIT LOS ANGELES

PRODUCERS OF BELLOWS EXCLUSIVELY
SERVING AUTOMATIC CONTROL MANUFACTURERS

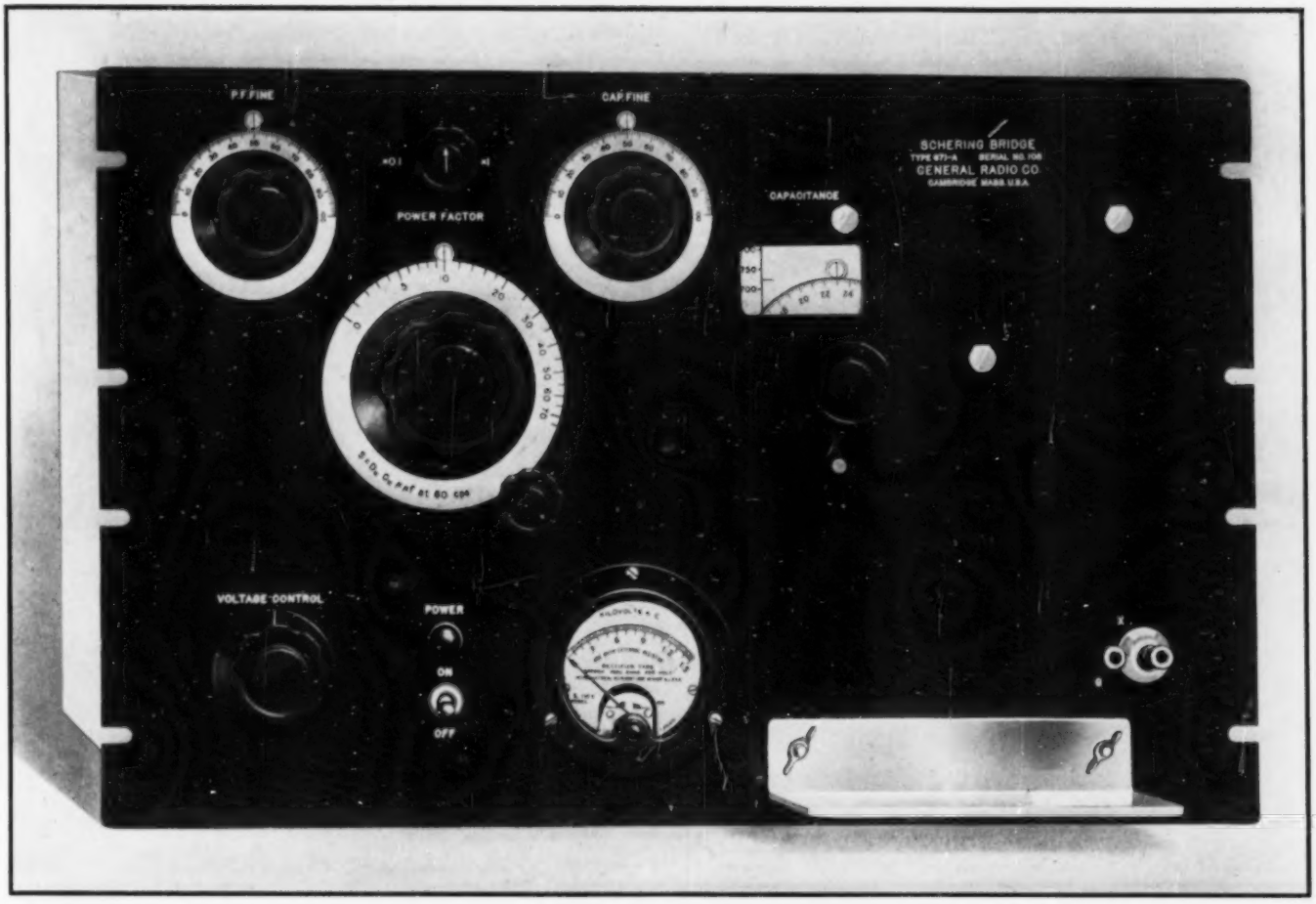

Here's a
New 60-Cycle Schering Bridge

For Testing Materials and Measuring Dielectric Properties from Samples of

INSULATION
CABLES
CERAMICS
PLASTICS
PAPER PRODUCTS
FABRICS

To Determine Moisture Content—Composition—Effects of temperature, humidity and voltage gradient

THIS BRIDGE is very simple to operate and is capable of rapid routine measurements. The 115-volt a-c line is used as the power source. The voltage across the material under measurement can be varied from zero to ten times the line voltage. Input and output transformers are astatically wound and the instrument is electrostatically shielded; external 60-cycle fields do not affect the bridge and the leads. For normal measurements no guard circuits are required. The bridge has a capacitance range from 0 to 1,000 $\mu\mu$f.

TYPE 671-A SCHERING BRIDGE $325.00

• *WRITE FOR BULLETIN 516 FOR COMPLETE INFORMATION*

GENERAL RADIO COMPANY

Cambridge, Massachusetts

BRANCHES: NEW YORK AND LOS ANGELES

MANUFACTURERS of PRECISION ELECTRICAL LABORATORY APPARATUS

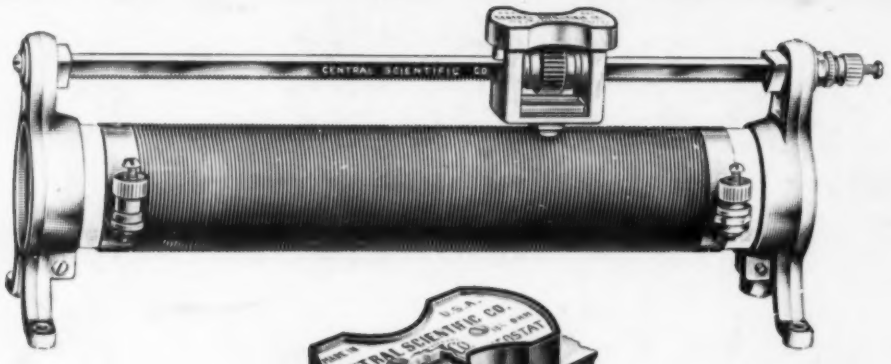

"The Rheostat with the Red Bakelite Insulation"

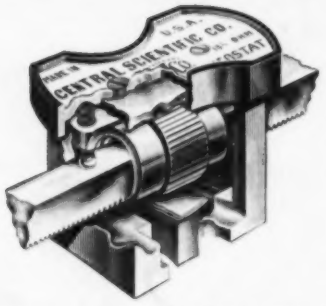

Cutaway View of Slider Showing Details of Mechanism

Wire stays tight in temperature range of normal use

CENCO
PRECISION ADJUSTMENT RHEOSTATS

With Improved Single Sliding Contact

(Pat. No. 1,839,343)

The improved design of the ever popular Cenco Slide-Wire Rheostats. Slider-rod of special shape for perfect electrical contact. End supports of massive design and pleasing appearance. Insulation of Red Bakelite mouldings. Sliding contact of low resistance and long life, contacting at but one point. Micrometer adjustment slider, moves freely under pressure, or moves with slow precision by means of adjusting screw when pressure is released. The knurled adjusting screw advances the contact approximately 1 mm for each quarter turn. Ratings are based on 425 watts dissipation.

No. 82920	E	F	G	H	J	K	L	M
Approx. resistance, ohms	2900	1400	720	360	180	90	44	22
Max. cur. capacity, amps.	.38	.55	.78	1.1	1.6	2.2	3.1	4.4
Each	$7.60	7.60	7.60	7.60	7.60	7.60	7.60	7.60

CENTRAL SCIENTIFIC COMPANY

SCIENTIFIC INSTRUMENTS — TRADE MARK CENCO REG. U.S. PAT. OFF. — LABORATORY APPARATUS

New York • Boston • CHICAGO • Toronto • Los Angeles

LANCASTER PRESS, INC., LANCASTER, PA.